

WATER MOVEMENT IN AN EXPERIMENTAL PLOT
IN THE OUACHITA MOUNTAINS OF
ARKANSAS: THE EFFECT OF
SOIL MACROPORES

By

JOSE DE JESUS NAVAR CHAIDEZ

Bachelor of Science
Instituto Tecnológico Forestal # 1
Durango, Durango, México
1986


Master of Science in Forestry
University of Toronto
Toronto, Ontario
1989

Submitted to the Faculty of the
Graduate College of the
Oklahoma State University
in partial fulfillment of
the requirements for
the degree of
DOCTOR OF PHILOSOPHY
July, 1992

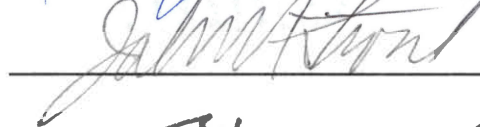
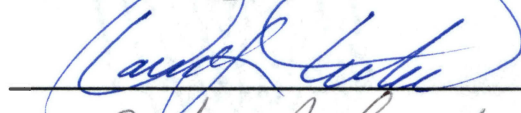
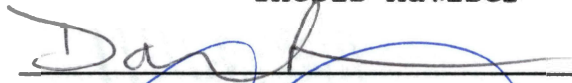
Thesis
1992D
N319W

WATER MOVEMENT IN AN EXPERIMENTAL PLOT
IN THE OUACHITA MOUNTAINS OF
ARKANSAS: THE EFFECT OF
SOIL MACROPORES

Thesis Approved:



Thesis Adviser



Dean of the Graduate College

PREFACE

An experimental forested plot was hydrologically isolated in the Ouachita Mountains of Central Arkansas to study the movement of water under simulated rainfall conditions. It was instrumented with (a) four subsurface flow collectors, (b) three sets of tensiometers, (c) six neutron access tubes, (d) six sentry 200 probes, and (e) a rainfall simulator. Lateral subsurface flow rates, soil water pressure potentials, and soil moisture contents were obtained during seventeen simulated storms for time intervals of 1 to 2 minutes. Due to calibration procedures of the sentry 200 probes and neutron probe, soil moisture contents were not included in this project. The data collected during the course of the study was analyzed to provide evidence of macropore flow based on deviations from potential flow theory. Data analysis, in agreement with field observations, suggested that macropores were actively contributing to subsurface water movement. Lateral macropore space was measured during the installation of the experimental equipment, and estimated from potential flow theory. Macropore and matrix flow were separated with statistical analysis. These findings suggested that modeling water movement should be based on both approaches: potential

flow and kinematic wave theory.

I wish to thank my sponsors, Universidad Autónoma de Nuevo León and Oklahoma State University for providing me with financial support during the course of my doctoral degree. In particular, I want to thank Biólogo, M.Sc. Glafiro Alanís of Facultad de Ciencias Forestales, Universidad Autónoma de Nuevo León and also my major adviser Dr. E. Miller from Oklahoma State University, whose efforts made my graduate studies at Oklahoma State University financially possible.

Special thanks are due to Dr. D. Turton for his technical support during the design of this project and the endless discussions of the data analysis. I am also grateful to M.Sc. Michael Kress for his invaluable help in the field, his technical support and his friendship. Several other people also helped with the field instrumentation and data collection, among them Randal Holeman, Walt Sanders, Boby Baker and Gary Miller.

I would also like to express my gratitude to the other committee members, Dr. Tom Haan and Dr. J.F. Stone, for their questions and comments, which technically enriched this project. Dr. Daniel Storm is also recognized for his willingness to replace Dr. Tom Haan during the defense of the dissertation.

This dissertation would have not been possible without the moral support of many people. My father, mother and

brother, Armando, instilled in me the desire to persevere and accomplish. I know they are still somewhere watching my performance through the course of this life. The rest of my sisters and brothers never had any doubts about my abilities and encouraged me to continue through the rough and smooth times. All of you people deserve my respect and admiration.

Lastly, but not least, my recognition goes to my family. My wife, Martha Graciela, shared and endured my failures, anxieties, stresses and expectations throughout the course of this project. Martha, your patience deserves more than this effort. My sons, César Armando, Carlos Alberto, Luis Fabián, and my daughter, Aida Alejandra, always provided smiles, which kept me going with this endeavor. This dissertation is dedicated to them, because they represent our future.

TABLE OF CONTENTS

Chapter	Page
I. INTRODUCTION.....	1
II. HYPOTHESES AND OBJECTIVES.....	5
Hypothesis.....	5
Objectives.....	6
III. LITERATURE REVIEW.....	8
Physical Processes of Streamflow Generation..	9
Development of Perched Water Tables.....	11
Type of Water Flow.....	12
Non-Potential Water Flow: Macropore Flow.....	13
Type of Soil Macropores.....	14
Controls of Macropore Flow.....	19
Other Far Reaching Processes.....	22
Solute Transport through Soil Macropores.....	23
Approaches to Model Macropore Flow.....	23
Potential Water Flow.....	24
Potential and Non-Potential Flow.....	28
Assessment of Macropores and Macropore Flow from Potential Theory.....	30
Evidence of Macropore Flow from Potential Flow Theory.....	32
IV. COMPARISON BETWEEN TWO ESTIMATES OF SOIL WATER PRESSURE IN AN EXPERIMENTAL PLOT IN ARKANSAS.....	34
Abstract.....	34
Introduction.....	35
Materials and Methods.....	37
Soil Water Potentials.....	37
Field Procedure.....	41
Data Analysis.....	41
Results and Discussion.....	42
References.....	49

Chapter	Page
V. ENERGY RELATIONSHIPS OF AN EXPERIMENTAL PLOT IN THE OUACHITA MOUNTAINS.....	62
Abstract.....	62
Introduction.....	63
Materials and Methods.....	66
The Study Area.....	66
The Experimental Plot.....	67
Subsurface Flow Collectors.....	68
Soil Water Potentials.....	69
Rainfall Simulator.....	70
Field Procedure.....	70
Results and Discussion.....	71
Unsaturated Flow.....	71
More Evidence on Bypassing Unsaturated Flow.....	75
Development of Potential Profiles During Simulated Rainfalls.....	76
Development of Potential Profiles during Desorption of Simulated Rainfalls.....	79
Rates of Soil Water Adsorption.....	80
Rates of Soil Water Desorption.....	81
Flux Density versus Hydraulic Gradient..	82
Conclusions.....	85
References.....	86
VI. MACROPORE AND MATRIX FLOW IN AN EXPERIMENTAL PLOT IN ARKANSAS.....	103
Abstract.....	103
Introduction.....	104
Materials and Methods.....	106
The Study Area.....	106
The Experimental Plot.....	107
Subsurface Flow Collectors.....	108
Soil Water Potentials.....	109
Rainfall Simulator.....	110
Field Procedure.....	111
Determining Macropore Space.....	112
Determining Macropore Flow Rates.....	113
Determining Matrix Flow.....	114
Results and Discussion.....	114
Lateral Macropore Space.....	115
Lateral Macropore Flow.....	117
Lateral Matrix Flow.....	120
Rhodamine Dye Experiments.....	121
Conclusions.....	123
References.....	123

Chapter	Page
LITERATURE CITED.....	139
APPENDIX DATA.....	148

LIST OF TABLES

Table	Page
Chapter IV	
I. Covariance Analysis Procedure for Testing Slopes and Intercepts Homogeneity for the Regression Models between Pressure and Voltage Output for nine Pressure Transducers.....	51
II. The Median Tests for testing the Null Hypothesis of Common Soil Water Pressure Potential between Pressure Transducers and Mercury-Water Columns.....	52
III. The Wilcoxon Test for testing the Null Hypothesis that the Median Difference in Soil Water Potential does not Deviate from Zero.....	53
IV. Regression Parameters between the Estimates of Soil Water Potential.....	54
Chapter V	
I. Soil Description, Textural and Soil Bulk Density Analysis and the Location of Tensiometers and Subsurface Flow Collectors within the Experimental Plot.....	91
II. Large Soil Macropores observed at the lateral face cross sectional Area of the Experimental Plot.....	92
III. Major Characteristics of Simulated Storms.....	93
IV. The Time of Tensiometer Response to Rainfall input for 17 Simulated Storms.....	94

Table	Page
V. The average Mean Sorption and Desorption Rates for nine Tensiometers for 17 Simulated Rainfalls in the Experimental Plot in Arkansas.....	95

Chapter VI

I. Soil Description, Textural and Soil Bulk Density Analysis, and the Location of Tensiometers and Subsurface Flow Collectors within the Experimental Plot.....	128
II. Large Soil Macropores observed at the lateral face cross sectional Area of the Experimental Plot.....	129
III. Some Characteristics of Simulated Rainfalls.....	130
IV. The Parameters of the Covariance Analysis Procedure for testing the homogeneity of Slopes and Intercepts for the Desorption Rates with time.....	131
V. The Reciprocal Regression Equations for Lateral Desorption with Time and Macropore Space in the Experimental Plot in Arkansas....	132

LIST OF FIGURES

Figure	Page
Chapter IV	
1. The Graphical Representation of the Components of a Tensiometer System with a Mercury-Water Manometer and a Pressure Transducer.....	55
2. The Calibration Curves for nine Pressure Transducers.....	56
3. The Development of two Soil Water Potentials (Pressure Transducers and Mercury-Water Manometers for nine Tensiometers for Rainfall 16.....	57
4. The Behavior of the Difference between two Estimates of Soil Water Potential during the Simulation of Rainfall 16.....	58
5. The Correlograms for the Difference between two Estimates of Soil Water Potential during the Simulation of Rainfall 16.....	59
6. The Spectral Density Analysis for the Difference between two Estimates of Soil Water Potential for nine Tensiometers for Rainfall 16.....	60
7. The Linear Relationships between the Mercury-Water Manometer Reading and the Pressure Transducer Reading for nine Tensiometers for Rainfall 16.....	61
Chapter V	
1. The Linear Relationships between Soil Water Potential and the Rates of Lateral Discharge within the Experimental Plot in Arkansas.....	96

Figure	Page
2. The Regression Models for Rainfall Intensity and the Time to Saturation for three Soil Depths at three Locations within the Experimental Plot.....	97
3. The Dependence of the Rainfall Depth to Saturate a Particular Soil Place on Rainfall Intensity.....	98
4. The Development of Vertical Potential Profiles during Sorption Experiments in the Experimental Plot in Arkansas for Rainfall 16.....	99
5. The Development of Vertical Potential Profiles during Sorption Experiments in the Experimental Plot in Arkansas for Rainfall 2.....	100
6. The Development of Vertical Potential Profiles during Desorption Experiments in the Experimental Plot in Arkansas for Rainfall 15.....	101
7. The Relationships between the Hydraulic Gradient and Flux Density for three Soil Horizons for four Simulated Rainfalls of Different Durations and Intensities.....	102

Chapter VI

1. Lateral Desorption Rates of the Experimental Plot in Arkansas after the Simulation of 17 Rainfalls of Different Durations and Intensities.....	133
2. The Dependence of the Lateral Macropore Space on Rainfall Intensity and Soil Water Potential in the Experimental Plot in Arkansas.....	134
3. The Relationships between Rainfall Intensity and Lateral Macropore Flow for 17 Simulated Rainfalls in the Experimental Plot in Arkansas.....	135

Figure	Page
4. The Relationships between Average Soil Water Potential and Lateral Macropore Flow during Desorption Experiments for 17 Simulated Rainfalls in the Experimental Plot in Arkansas.....	136
5. The Non-linear Dependence of Macropore Flow with Macropore Space.....	137

CHAPTER I

INTRODUCTION

The mechanisms of stormflow generation in forested watersheds have been a cause of major concern in the last three decades (Hewlett and Hibbert, 1963; Hewlett and Hibbert, 1967; Whipkey, 1965; Dunne and Black, 1970a, 1970b; Beasley, 1976; Anderson and Burt, 1978; Mosley, 1979, 1982; Beven, 1982; Beven and Germann, 1981; Germann, 1990; Sklash and Farvolden, 1979; Sklash et al. 1986; Pearce et al. 1986). The reasons for this concern are the pollution of streams and lakes, as well as of catastrophes associated to floods and other environmentally-related problems such as: the deterioration of fish habitat, loses of soil nutrients and fertilizers from soils to streams, the movement of acid rain, pesticides and herbicides through soils.

Hewlett and Hibbert (1967) proposed the variable source area concept to explain the dynamic production of stormflow, where rapid subsurface flow is responsible for the temporary development of water tables close to stream channels. Dunne and Black (1970a, 1970b), on the other hand, found saturated overland flow as the major mechanism of stormflow generation in Vermont. Betson and Marius (1969) proposed the mechanism

of partial area concept, where fixed areas on watersheds with unique hydraulic characteristics contribute disproportionately to stormflow generation.

Forested watersheds in the Ouachita Mountains of Arkansas generate stormflow following the variable area source concept through subsurface flow (Turton et al. 1992). This process requires an efficient mechanism of subsurface water movement within soils. Whipkey (1965), Aubertin (1971), Jones (1971), Beasley (1976), Mosley (1979, 1982), Germann (1986, 1990), Germann and Beven (1981), Beven and Germann (1982), observed, suggested, modeled and reported macropores as the rapid mechanism of water movement. Sklash and Farvolden (1979), Sklash et al (1986) and Pearce et al (1986), on the other hand, found that displacement of water, potential flow theory, better explains this process. McDonnel (1990) explained that both macropore flow and potential flow, through the displacement of water concept, are connected through the ground water ridging mechanism, and both are present in forested watersheds in New Zealand.

Stormflow generation was analytically modeled using potential flow theory by the empirically derived law of Darcy (Anderson and Burt, 1978). This approach includes a macroposcopic flow velocity vector, which is the overall average of the microscopic flow velocities over the total soil volume. Darcy's law assumes that water moves because of the differential potential energy at various places within

the soil, that water movement is laminar, and that new water displaces old water (Hillel, 1980a).

Stormflow generation through soil macropores does not obey Darcyan concepts or potential flow theory. Macropore flow, turbulent flow, preferential flow, channelling flow, short circuiting flow, or bypassing flow, indeed, results from water flowing within soil openings larger than 3 mm in diameter, or soil water held under pressures lower than 3.0 cm of water (Luxmoore, 1981; Skopp, 1981; Wilson and Luxmoore, 1986; Germann, 1990a 1990b; Luxmoore et al. 1990). Hence, inertial forces dominate water movement rather than potential energy. Gravity causes water as well as solutes to move far in advance of the dispersed front within the soil system. Macropore flow, hence, has major implications on stormflow generation, as well as on the movement of acid rain, herbicides, pesticides and fertilizers within soils.

Macropore flow is currently a topic of intensive research in all major fields of hydrology and soil science, even though field studies on macropores and their contribution to subsurface flow are lacking. In fact, Germann (1990a), Anderson and Burt (1990) and Sklash (1990) stated the need to establish and provide evidence for the dominance of potential and inertial flow regimes in different environments. This project was designed to provide evidence of the presence and influence of macropores on macropore flow and subsurface flow and consequently,

stormflow flow generation in an experimental plot in the Ouachita Mountains of Arkansas. Bidimensional measurements of the soil water pressure potential, lateral subsurface flow rates and rhodamine dye experiments during simulated rainfall conditions provided this information.

CHAPTER II

HYPOTHESIS AND OBJECTIVES

Hypothesis

The quick response of forested watersheds to rainfall in central Arkansas and southeastern Oklahoma does not include a significant contribution due to Horton overland flow (Turton et al. 1992). Observations of hydrographs from experimental watersheds in the Ouachita Mountains suggest that water moves quickly within the soil down to stream channels. There may be a macropore connection within the soil, which enhances the rate and extent of subsurface flow. Because the measurement of macropores and macropore flow require intensive and detailed experiments, macropore flow can be approached by assessing the deviations of water movement from potential flow theory. Hence:

H_0 = Water movement within forested soils obeys potential energy gradients.

H_a = Water movement within forested soils obeys both potential and macropore flow concepts.

If H_0 is true, then water displacement is the principal mechanism of water movement and soil micropores dominate subsurface flux. If H_a is true, then both bypassing matrix flux by soil macropores and potential flow are responsible

for water movement.

The hypotheses are tested in the following ways.

1. Lateral discharge must occur under a saturated soil matrix and tensiometer response to rainfall input must show a downward trend, since soil water moves via micropores first.
2. The development of hydraulic potentials with soil depth must show a similar trend as the equilibrium potential gradient (see for example Germann and Beven, 1981).
3. Flux density increases with a monotonic increase in the hydraulic gradient.

In order to test H_0 , accurate measurements of soil water pressure potential are needed. Hence, this soil parameter was measured with mercury-water manometers and pressure transducers. I was subsequently interested in testing the following hypotheses:

H_0 = The estimates of soil water pressure between these two devices are not significantly different.

H_a = The estimates of soil water pressure between these two devices are significantly different.

The following objectives should be accomplished to test these hypotheses.

Objectives

1. Determine the contribution of potential flow on vertical and lateral water movement.
 - 1.1. Measure lateral subsurface flow rates at different soil horizons during simulated rainfall conditions.
 - 1.2. Measure soil water potentials in two dimensions within the experimental plot during simulated rainfall conditions with mercury-water manometers and pressure transducers.

2. Estimate macroporosity, and macropore and matrix flow velocities and assess their hydrologic influence on the lateral movement of subsurface water flow.

CHAPTER III

LITERATURE REVIEW

The stormflow response of forested watersheds to precipitation is a two-fold processes: 1) quickflow, rapid flow, or stormflow, which takes a rapid route to the stream channels and 2) baseflow, slowflow or ground water flow, which takes a much slower route to the stream channels. The contribution of these processes to streams is approximately 10 and 24 %, respectively, of the total precipitation for all eastern United States (Woodruff and Hewlett, 1979). The physical causes of quickflow are still debated, whereas baseflow is believed to be produced either by the slow movement of subsurface water or by the slow water release from the groundwater, or both.

The response of undisturbed forested catchments to precipitation is, indeed, rapid (Ward, 1984; Beasley, 1976; Mosley, 1979 and 1982) but rarely is the same among storms (Hewlett and Hibbert, 1967 and Ward, 1984). The causes of the temporal and spatial variations are: differences in rainfall intensity, antecedent soil moisture content, vegetation, soils, slope, topography, aspect, and climate (Dunne and Leopold, 1978 and Anderson and Burt, 1990).

Physical Processes of Streamflow Generation

Horton (1933, 1940) explained that physically the soil surface is capable of absorbing and transmitting some of the rainfall initially falling on it, which sustains groundwater and consequently baseflow in the dry season. When the rate of the soil to adsorbed and/or transmit water is surpassed by rainfall intensity, Horton overland flow is generated, which contributes to quickflow. This physical process takes place in areas where rainfall intensity exceeds the soil infiltration capacity (Dunne and Leopold, 1978 and Anderson and Burt, 1990).

Hursh (1944), Hewlett (1961) and Hewlett and Hibbert (1963 and 1967) observed and suggested that Horton overland flow was the exception rather than the rule in forested, undisturbed lands even when intense rainstorms result in rapid streamflow response. The high soil infiltration capacity was apparently exceeded with storms with large return periods.

These observations required new alternative hypotheses to Horton's, in relation to stormflow generation and quickflow from forested lands. These included flow processes such as: subsurface flow, saturation overland flow, and channel interception. The concept of subsurface stormflow was introduced by Hewlett (1961), Hewlett and Hibbert (1967), and observations made by Weyman (1973) and Anderson

and Burt (1978) supported it. Subsurface stormflow is important in places with steep slopes, deep, highly permeable topsoils, which become less permeable with depth or which overlie impermeable rock (Dunne and Leopold, 1978 and Anderson and Burt, 1990).

Dunne and Black (1970a and 1970b), on the other hand, found that saturation overland flow was the major source of stormflow in northeastern forested watersheds. Dunne and Leopold (1978) and Anderson and Burt (1990) stated that saturation overland flow is important in humid regions with, temperate climates, and deep soils with gentle slopes.

The concepts of subsurface flow and saturation overland flow meet in the variable area source concept. Hewlett and Hibbert (1967) suggested that subsurface flow cause the lower slopes to become saturated, which originates channel expansion during rainfall events and posterior shrinkage. Dunne and Black (1970a 1970b) observed that saturated overland flow was caused close to the stream channels because the elevation of the water table was close to the soil surface. Betson and Marius (1969), on the other hand, proposed the partial area contribution to stormflow generation, where fixed places in the watershed contribute to streamflow generation.

Sklash and Farvolden (1979); Sklash et al. (1986) and Tanaka et al. (1988) raised the question of groundwater as the major contributor to quickflow and baseflow in

watersheds in boreal forests of Canada, New Zealand and temperate forests of Japan.

Development of Perched Water Tables

The rapid response of undisturbed watersheds to precipitation, via subsurface flow or saturated overland flow, results from the development or enhancement of perched, saturated water tables (Hewlett and Hibbert, 1967 and Dunne and Black, 1970a, 1970b). Because forested soils are layered and sloped in nature, soil horizons have differential hydraulic conductivities. Hence shallow perched water tables develop above the soil horizons of lower water transmittance, which also enhance lateral flow on hillslopes (Gaskin et al. 1989 and Anderson and Burt, 1990).

Turner et al. (1987) found that both deep and shallow water tables developed in the Collie River basin in Australia and that the streamflow isotopic composition corresponded to that of the shallow groundwater table. In Japan, Tsukamoto and Ohta (1988) also found two zones of saturation: one immediately below the shallow soil and the other at 1.7 m below the soil surface. It was observed that the lower saturation zone was affected by the storage of water in the upper one. Bren and Turner (1985) observed peak discharges from a springhead, which were reached some days after cessation of rain, while the peak discharges from the flank catchment were reached during or immediately after the

period of rainfall.

Type of Water Flow

The chemical composition of stormflow is of critical importance in determining the flow paths and the conversion of precipitation into stormflow (Sklash and Farvolden, 1979; Sklash et al. 1986 and Sklash, 1990; Jardine et al. 1990). Water stored in the soil, old water, can be displaced by precipitation, new water, to generate stormflow. This approach assumes that if old water dominates stormflow, Darcyan type of water flow, matrix flow, or potential flow dominates water movement.

Sklash and Farvolden (1979), Pearce et al. (1986), Sklash et al. (1986) and Kuyane and Kaihotsu (1988) found that old water composed the major part of the stormflow hydrograph. This phenomenon was explained in terms of the displacement mechanism of old water by new water (Pearce et al. 1986; Sklash et al. 1986; Kennedy et al. 1986), the so called 'piston flow'.

Pearce et al. (1986) measured long term oxygen 18, electrical conductivities and chloride, as a tracer, in the stream and groundwater observing that the mean water residence time was approximately 4 months. Their results also indicated that approximately 3 percent of the storm runoff could be considered new water. Turner et al. (1987) observed that between 60 and 95 percent of the streamflow

generated from the respective rainfall events had originated from antecedent shallow groundwater within the catchment. The low percentage of new water was attributed to channel interception or saturation overland flow or both.

Despite these findings, the spatial variations in the mixing of old and new water, the mechanisms of the water displacement phenomenon, and the mechanisms of short circuit flow remain uncertain. In fact, Sklash et al. (1986) suggested that the findings made by Mosley (1979 and 1982) that subsurface flow takes place very rapidly, via soil macropores, could be thrown into doubt in New Zealand watersheds. His water tracing observations suggested that a displacement mechanism of subsurface water rather than rapid subsurface flow, via macropores, took place in their experiments. On the other hand, Germann (1990) suggested and McDonnell (1990) explained how the groundwater ridge concept affect both macropore and micropore flow and both combine to produce streamflow. This explanation fits well the statements of Beven and Germann, 1981; Germann and Beven, 1981; Beven and Germann, 1982; Germann, 1984; Germann, 1990 and Anderson and Burt, 1990, that subsurface stormflow can be generated by both Darcyan and macropore flow concepts.

Non-Potential Water Flow: Macropore Flow

There is currently a general consensus about the rapid movement of water via soil macropores. Empirical

observations made by Whipkey (1965 and 1967), Aubertin (1971), Jones (1971), Pilgrim et al. (1978), Beasley (1976), Mosley (1979, 1982), Trudgill et al. (1983), Wilson and Luxmoore (1988), Watson and Luxmoore (1988), Luxmoore et al. (1990), Edwards et al. (1988), Edwards et al. (1992) and Jardine et al. (1990) observed and suggested that water moves preferentially via soil macropores causing watersheds to respond rapidly to precipitation. Germann (1986) showed empirically that macropore flow can bypass the entire soil profile of experimental lysimeters, which may cause water tables to rise and enhance subsurface lateral flow.

Type of Soil Macropores

The definition of macropore is at this time arbitrary and is often related more to details of experimental techniques rather than to considerations of flow processes (Beven, 1981; Bouma, 1981 and Skopp, 1981). Aubertin (1971) defined the soil macropore as a large macropore, passageway, channel tunnel or void in the soil through which water usually drains by gravity. Beven and Germann (1982) stated that the word macropore implies structures that permit a type of non-equilibrium channeling flow, therefore flow through a soil would not be described well by a Darcyan approach to water flow through porous media. Skopp (1981) defined macroporosity as that pore space which provides preferential paths of flow so that mixing and transfer

between such pores and remaining pores is limited. Beven and Germann (1982) and Luxmoore et al (1990) presented a review of the size of soil macropores according to several researchers.

In general, volumetric percentages of active macropores or passageways is very small. Bouma et al. (1979) found < 1 % of active (stained) voids estimated by the percentage of surface area. Beven and Germann (1982) pointed out that macropore volume goes from 1 to 4 percent of the soil; although no specifications were made about the type of soil macropore.

Because of the difficulties involved in defining macropores most researchers have grouped soil macropores on a morphological basis as follows:

Macropores Formed by Soil Fauna. Macropores made by animals are usually found close to the soil surface, although in some cases they go also deep into the lower B and C soil horizons. Insects, worms, moles, gophers, and wombats frequently make soil openings. These holes are primarily tubular in shape, but may range in size from less than 1 mm to over 50 mm of diameter (Aubertin, 1971 and Beven and Germann, 1982).

In agricultural fields in Germany, Ehlers (1975) found the number of earthworm channels ranging from 2 to 11 mm in diameter. The number and percentage volume doubled during four years of no tillage practice. The maximum

infiltrability of conducting channels in the untilled soil was computed as more than 1 mm (1 liter per m² min⁻¹), although the volume of channels amounted to only 0.2 percent of the volume. Using fluorescein and pyranine as solute markers, Omoti and Wild (1979) found the population density of earthworm channels to be about 100 per m² with a modal diameter of 2 to 5 mm and a range of 2 to 100 mm. Almost all macropores were continuous to 15 cm long and about 10 percent to 70 cm. The total volume of macropores was only 0.5 percent.

Edwards et al. (1988) found from 5673 to 28966 macropores larger than 0.4 mm of diameter at 30 cm of soil depth in a soil surface of 930.25 cm². Macropores accounted for 1.4 % of the total area. Edwards et al. (1989) observed that flow in earthworm burrows greater than 5 mm in diameter, accounted for 3.9 % of the rainfall movement: 13 times more than their areal distribution. Hammermeister et al. (1982) found large rodent holes in soil pits and water literally poured from these holes in and above the saturated seepage zones. Dye, in fact, passed through the 1-m thick soil in a matter of seconds at these sites.

Macropores Formed by Plant Roots. Decayed roots and living roots are capable of channeling water. Aubertin (1971) pointed out that root channels within the forest soil form a network of relatively large, continuous, interconnected, open or partially filled channels that serve

as pathways for the rapid movement of free water into and through the forest soil horizons. Decayed root holes have been observed to be filled with some soil from soil horizons above, which indicates some kind of subsurface erosion (Gaiser, 1952). In general, decayed roots may comprise up to 35 % of the volume of forest soils and the percent by volume is expected to decrease rapidly with soil depth. Gaiser (1952) measured approximately 9880 vertical root channels per ha, although he pointed out that the estimate was low because not all channels could be discovered by the method used.

Most researchers quoted the importance of roots and root channels on water flow, although there are only a few studies concerning the influence of root channels on the conduction of soil water (Whipkey, 1965; Aubertin, 1971; DeVries and Show, 1978; Beasley, 1976; Pilgrim *et al.* 1978; Mosley, 1979 and 1982). Aubertin (1971) found evidence that in all plots at least one and usually several old roots flowed pipe or faucet-like from a fine textured silt loam forest soil and that the volume of outflow after the beginning of rainfall was normally rapid often with lag times of only 10 to 15 minutes. The volume of outflow per location was frequently high, exceeding 1000 ml min⁻¹.

DeVries and Chow (1978) observed during simulated rainfall that water flow through soil profiles was partitioned between root channels and the soil matrix. The

proportion of flow conducted through channels was at its maximum during the non-steady state phase of the rainfall event, decreasing to a minimum as the steady state was approached. Mosley (1979) observed points of concentrated seepage, usually at the base of the b soil horizon, which drained at rates on the order of 20 l sec^{-1} . Maximum dye tracing travel velocities were up to 300 times greater than the saturated hydraulic conductivity of $0.001 \text{ cm sec}^{-1}$ for the mineral soil studied. In another more intensive study, Mosley (1982) found mean subsurface flow travel velocities of 0.3 cm sec^{-1} and a great deal of variation in velocity (C.V. = 90 %). Hammermeister et al. (1982) found that dye also appeared along living roots after its introduction into the soil indicating flow along the soil root interface.

Cracks and Fissures or Non-Biotic Macropores. Non-biotic macropores are the result of biogeochemical processes acting on the soil horizons. Cracks in clay soils are often the result of shrinkage caused by desiccation (Beven and Germann, 1982). Chemical weathering of bedrock material, in addition to build up of soil water pressures may cause the effect of piping (Jones, 1971).

Jones (1971) and Tanaka et al. (1988) found that macropores caused by soil piping were responsible for the rapid movement of either subsurface water in the vadose zone or groundwater. Tanaka et al. (1988), in a basin in a suburb of Tokyo, observed that most streamflow was comprised of

return flow appearing at the soil surface through decayed stumps and soil pipe outlets at rates similar to those caused by surface flow. In fact, water flow through a large pipe contributed 65 % of groundwater flow issued from stream banks around the main weir. Tsukamoto and Ohta (1988), in an experimental basin of western Tokyo, found the density of pipe networks to be 5.3 m m^{-2} or 6.4 m m^{-3} , with an average diameter of 4.6 cm. Pipes were distributed at various soil depths, although this value changed from season to season. The ratio of pipeflow to total runoff from the soil profile was 85.5 to 99.5 %.

Controls of Macropore Flow

Pore Size. Inertial forces, rather than potential energy gradients, dominate macropore flow. Hence macropore flow is not laminar flow. Several researchers established the boundary between laminar and turbulent flow, which happens in soil openings larger than 3 mm of diameter or pores that drain at soil water tension of 1 cm of water: macropores (Beven and Germann, 1982). Pouiseille's law shows that macropores can transport significant quantities of water, although macropores have to be open to the atmospheric pressures. Soil macropores, however, do not need to extend up to the soil surface to conduct water (Thomas and Phillips, 1979). Water pressures within the range of atmospheric pressure may develop within the soil to enhance

water flow through macropores. Positive pressures must, hence, occur before macropore flow occurs either as a ped, minimum soil structural unit, storage capacity is exceeded leading to outflow (Beven and Germann, 1981) or as a ped infiltration capacity is exceeded (Bouma et al. 1978).

Soil Moisture Content. Macropore flow is dependent on soil moisture content (Steenhuis and Muck, 1988). Rapid drainage was initiated, in lysimeters in Ohio, when the soil was at field capacity (Germann, 1986). However, Thomas and Phillips (1979) pointed out that gravitational flow of water through soil macropores can occur readily in soils that are well below field capacity. Germann (1986), however, demonstrated that antecedent soil moisture in the 0-1.0 m depth range has to be at least greater than 0.3 cm cm^{-3} before rapid drainage occur. Jardine et al. (1990) suggested that macropore flow is somehow independent on soil moisture content because he measured it under an unsaturated soil matrix.

Rainfall Intensity. Macropore flow is also dependent on the rate of rainfall, that is the rate of water supply (Ehlers, 1975 and Omoti and Wild, 1979). Trudgill et al. (1983) observed maximum dye trace output during or just subsequent to high rainfall events equal to or greater than 3 mm h^{-1} lasting for at least 2 hours. Rapid drainage was initiated in lysimeters with rainfall intensities of at

least 10 mm d^{-1} , when the soil was above field capacity (Germann, 1986). Hammermeister et al. (1982) observed by tracer anion movement and soil water pressure measurements that preferential flow occurs through large continuous soil pores during heavy rainfall while the surrounding soil and rock mantle remained unsaturated. This is, in fact, a similar process to the fingering mechanism proposed by Glass et al. (1988), which is discussed below. Edwards et al. (1990) and Edwards et al. (1992) showed that the rate of water input affect the volume and rate of water percolation through preferential places of soil columns.

Soil Hydraulic Conductivity. Mosley (1979) pointed out that the saturated hydraulic conductivity of the soil matrix is not a limiting factor on the ability of soil to generate channel stormflow and reported that dye tracer moved two times faster through soil macropores. Indeed, Germann (1986) pointed out that the hydraulic conductivity of the soil matrix can be ruled out as a direct major hydraulic control because increased drainage occurred within 2 days from the rainfall onset of 98 % of 389 cases regardless of the soil type.

Smettem and Collis-George (1985), on the other hand, demonstrated the influence of the saturated hydraulic conductivity on the steady infiltration rate distribution, which also depended by the soil macropore density. Kneale (1985) calculated that the hydraulic conductivity of arable

soils was affected by macropore channels, which were estimated to be $0.026 \text{ m}^3 \text{ m}^{-3}$ in the topsoil.

Other Far Reaching Processes

Vertical fingering, the breaking of a continuous wetting front, is another mechanism by which wetting fronts advance faster than anticipated by continuum approaches (Glass et al. 1988). This process occurs in coarser porous media that are overlain by finer grained material.

There are also suggestions concerning the pneumatic potential effect on water movement. Heliotis and DeWitt (1987) and Kuyane and Kaihotsu (1988) found that saturated, perched water tables, developed first during rains of high intensity, when the infiltrating water acted as a tightly lid that forced the water table to rise to the level required to compensate for the pressure increase: the Lisse effect. The Lisse effect was supported by Kuyane and Kaihotsu (1988), whose laboratory observations showed a soil moisture decrease immediately below the advancing wetting front. The speculative explanations were that the increase in air pressure below the advancing front or the beginning of the pneumatic potential of entrapped air pushed soil water downwards. Heliotis and DeWitt (1987) proposed a third mechanism, which was caused by the storage response type due to rapid rainfall infiltration and subsequent water table rise.

The conversion of capillary into phreatic water causes a disproportionate increase of the water table, much greater than might be expected given the specific yield of the soil and the magnitude of the rainfall input (Anderson and Burt, 1990). The capillary fringe effect has also been considered as the place where the translation of water occurs. That is, new water entering this zone displaces old water. A possible explanation for this effect is that macropore flow may be actively providing water into the water table.

Solute Transport through Soil Macropores

Water flow through preferential pathways, soil macropores, may result in solute being transported far in advance of the dispersed front of solute within the soil matrix (Beven and Young, 1988). This concept is supported by Richard and Steenhuis (1988) who measured chloride concentrations in a drain tile and showed that while solutes diffused into the micropores, micropore contribution to drainage flow was masked by macropore flow during major flow events. Everts et al. (1989) measured the mobility of 4 tracers with varying levels of soil absorption and found that all of them appeared at the outflow approximately at the same time, which again suggested macropore flow.

Approaches to Model Macropore Flow

Macropore flow is difficult to measure in part because

of the highly variable spatial distribution and the wide range in sizes of macropores. Some approaches to model the effect of macropores on lateral subsurface water movement are based on kinematic wave theory (Germann, 1990a and Germann, 1990b). For flow in vertical soil macropores to lateral hillslope processes Germann (op.cit) proposed:

$$Q = b_1 H^a \sin (\alpha) \quad (1)$$

where

- Q =Volume of water per unit width of slope (m^2sec^1).
 b_1 =Lateral conductance ($m^{2-a} sec^{-1}$).
 H =Height of water table (m).
 α =Slope angle (degrees).

Model 1 is similar to the kinematic wave equation to predict lateral subsurface flow in a soil slab (Beven, 1982).

Potential Water Flow

Water flow in porous media was described by Darcy (1856 in Hillel 1980, 1982) for saturated soils and by Richard's equation (Hillel 1980, 1982) for unsaturated soils. The volume flux density of water through saturated sand columns was modeled as a function of a driving force or hydraulic gradient, and a proportionality factor. The driving force is the change in hydraulic head or total potential per unit length of the flow path. In saturated flow, the gravity gradient is the only driving force and matrix gradients are zero. The proportionality factor is referred to as the hydraulic conductivity.

Potential Energy. Soil water contains significant amounts of energy in different quantities and forms. The two main forms of energy are: kinetic and potential (Hillel, 1980). The potential energy is characterized by the position and internal condition of water in the soil. It is of critical importance in determining the state and movement of water in the soil. Soil water obeys the universal law that all matter moves from where the potential energy is higher to where it is lower and that each parcel of matter tends to equilibrate with its surroundings. The magnitude of the potential energy gradient is in fact the driving force causing flow. Therefore, it is not the absolute amount of potential energy contained in the water which is important in itself, but rather the relative level of that energy in different regions within the soil (Cassel and Klute, 1986).

The potential energy of a parcel of water in the soil is the algebraic sum of all forces acting on that parcel (Hillel, 1980, 1982). It includes matric or pressure potential, gravitational potential, osmotic potential, pneumatic potential and other forces may be possible. The most important sources of energy when considering water flow from a hydrological point of view are: matric or pressure or suction potential and gravitational potential. Generally, osmotic, chemical, or pneumatic potential are considered negligible so the sum of pressure and gravitational potential constitutes the total hydraulic potential.

Measurements of Potential Energy. The determination of soil water pressure potentials in situ provides information critical to an understanding of water storage and transport in soils. Soil water pressure potentials have been measured with tensiometers (Cassel and Klute, 1986) and thermocouple psychrometry (Rawlins and Campbell, 1986). Tensiometers work on the principle that a ceramic cup placed in contact with the surrounding soil attains the same pressure potential as the soil itself. Hence, the measurement of the pressure potential at the ceramic cup or an extension of the ceramic cup can be easily carried out. The components of a tensiometer are discussed in chapter IV.

Soil water tension can be measured with tensiometers in combination with mercury, mercury-water manometers (Cassel and Klute, 1986), and vacuum gauges, as well as, pressure transducers (Anderson and Burt, 1978; Long, 1982; Lowery et al. 1986; Williams, 1987; Dowd and Williams, 1989). The manometer or vacuum gauge system requires intensive labor, and they are a disadvantage when information is needed during rapid changes in soil water potentials. Pressure transducers have the advantage of automated data collection, although they are expensive, in relation to mercury-water manometers or vacuum gauges. The performance of pressure transducers, in relation to mercury-water manometers has been questioned by Trotter (1984). He showed that pressure transducers are not as accurate as mercury-water manometers.

Dowd and Williams (1989), on the other hand, reported that conventional mercury-water manometers are accurate only within 20 cm of water.

Hydraulic Conductivity. The hydraulic conductivity of a soil is a measure of its ability to transmit water (Klute and Dirksen, 1986; Amoozegar and Warrick, 1986). The hydraulic conductivity can be saturated or unsaturated.

Saturated hydraulic conductivity at saturation is maximal because all soil pores are contributing to water movement. It is mathematically defined as the ratio of water flux to the hydraulic gradient or physically described as a function of the soil permeability and fluid characteristics (Hillel, 1980b).

For saturated soils, Darcy's law, in a three dimensional space and allowing for anisotropy, can be written as follows (Hillel, 1980):

$$K_z \frac{\delta^2 H}{\delta z^2} + K_x \frac{\delta^2 H}{\delta x^2} + K_y \frac{\delta^2 H}{\delta y^2} = 0 \quad (2)$$

where

K = The saturated hydraulic conductivity (L T⁻¹)
 H = The Total head (L).
 x,y,z = Three-dimensional space coordinates (L).

As soils become unsaturated, soil water is subject to sub-atmospheric pressure or suction, which is equivalent to a negative pressure. In this case, assuming uniform soils, water tends to be drawn from a zone where the hydration

envelopes surrounding the particles are thicker to where they are thinner, and from a zone where the capillary menisci are less curved to where they are more highly curved. Water flows spontaneously from where matric suction is lower to where matric suction is larger (Hillel, 1980, 1982). As soil becomes drier, larger matric suction, the largest pores drain first and the unsaturated hydraulic conductivity diminishes quickly.

The unsaturated hydraulic conductivity is a function of the matric potential. This relationship is, however, hysteretic. Hysteresis, according to Green *et al.* (1986) is the process by which the soil moisture retention curve changes shape depending on whether the soil is draining or wetting. Darcy's law was extended by Richards (1931) in Hillel (1980) to unsaturated flow as follows:

$$\frac{\delta\theta}{\delta t} = \frac{\delta(D\delta\theta/\delta z)}{\delta z} + \frac{\delta(D\delta\theta/\delta x)}{\delta x} + \frac{\delta(D\delta\theta/\delta y)}{\delta y} \quad (3)$$

where

- D = Diffusivity ($L^2 T^{-1}$).
- θ = Soil moisture content ($L^3 L^{-3}$)
- zxy = Three-dimensional space coordinates (L).
- t = Time (T).

The relation between unsaturated hydraulic conductivity and volumetric wetness $K(\theta)$ or and degree of saturation $K(s)$ is affected by hysteresis to a much lesser degree.

Potential and Non-Potential Flow

In macroporous soils, water flow takes place via both: macropore flow and matrix flow. This is called the two domain flow concept (Beven and Germann, 1982). The two flow processes do not need to be independent of one another. Relatively small soil pores can conduct much water when continuous through the soil. Wilson and Luxmoore (1988) found that although macropore flow constituted 85 % of the ponded flux, the mesopore, 0.011 cm of radius, fluxes were also large, $2 \times 10^{-5} \text{ m sec}^{-1}$, and were considered sufficient to infiltrate rainfall without macropores filling and contributing to water flow.

Infiltration. Infiltration, the entry of water into the soil, reflects a combination of both matrix and macropore flow. It is a function of soil moisture content, rate and duration of water input (Hillel, 1982). Theoretical (Philip, 1957), semi-empirical (Green and Ampt, 1911 in Hillel, 1980) and empirical (Horton, 1940; Kostiaikov, 1932, in Hillel, 1980) infiltration models have been developed.

Philip (1957) introduced an infiltration model based on the form of the Darcy-Richards approach which uses a diffusivity parameter instead of unsaturated hydraulic conductivity. In this approach, the infiltration rate becomes a function of the square root of time (t), the steady state infiltration rate (i_c), and a constant S , the soil sorptivity:

$$i = i_c + (S / 2t^{1/2}) \quad (4)$$

where

- i = Infiltration rate ($L T^{-1}$).
- i_c = Infiltration rate ($L T^{-1}$).
- S = Sorptivity (L).
- t = Time (T).

Notice in equation 4 that, as time increases, i approaches i_c asymptotically. The characterizing constants, i_c and S can be empirically determined.

Assessment of Macropores and Macropore Flow from Potential Theory

Macropores. Watson and Luxmoore (1986) and Wilson and Luxmoore (1988) derived the number of macropores, N , by using Poiseuille's equation,

$$N = 8\mu\delta K_m / \pi p g (r)^4 \quad (5)$$

and the effective total macroporosity is given by:

$$\epsilon_m = N\pi r^2 \quad (6)$$

where

- N = Number of effective macropores per unit area.
- K_m = Macropore flow rate (LT^{-1}).
- μ = The viscosity of water ($ML^{-1} T^{-1}$).
- p = Density of water (ML^{-3}).
- g = Acceleration due to gravity (LT^{-2}).
- r = Pore radii (L).
- ϵ_m = Total effective macroporosity ($L^3 L^{-3}$).

The pore radii is derived from the capillary equation:

$$r = 2\sigma \cos\alpha / pgh \quad (7)$$

where

- σ = Surface tension of water (MT^{-2})
- α = The contact angle between the water and pore wall (assumed 0).
- h = Water pressure (L).

This procedure allows for differential macropore sizes which, according to Poiseuille's law, are of fundamental importance in water movement. This approach is similar to that obtained from the functional relationship between the unsaturated hydraulic conductivity and the soil moisture content, $K(\theta)$. Soils subject to differential pressures show differential water drainage, which corresponds to some pore size. This approach assumes cylindrical pore size.

Macropore Flow. Phillips' model of infiltration, equation 4, is composed of the saturated hydraulic conductivity and sorptivity. Physically the parameter i_c comprises both micropore and macropore flow since sorptivity, S , approaches 0 asymptotically. Micropore flow results from water input into the soil matrix, hence sorptivity, S , must approach a constant final value, rather than a final close to zero value. If sorptivity, S , can be empirically determined as a final constant value, then $i_c - S = \text{macropore flow}$.

The influence of macropores on macropore flow can also be empirically derived by measuring ponded infiltration and matrix infiltration (Watson and Luxmoore, 1986 and Wilson and Luxmoore, 1988). Matrix flow represents the volume flux density of water accounted for by the matrix suction gradient, $\delta H_p / \delta z$, which under saturated conditions is 0. The effect of macropores on water movement results from the subtraction of the water entering the soil under a matrix

suction of < than 0.1KPa from K_s (Germann, 1990a). The matrix suction component may be measured by using the tension infiltrometer reported by Watson and Luxmoore (1986). When water flow is restricted by a tension larger than 14 cm of water suction (i.e. under low rainfall intensities), most water travel via micropores less than 0.011 cm of radius. Hence, sorptivity, S , contributes only to matrix water movement.

Evidence of Macropore Flow from Potential Flow Theory

Sorption or desorption experiments of a soil block must show a unit hydraulic gradient when vertical water movement follows an infiltration-type process. That is a line with a 45° angle with soil depth or 1:1 slope. This approach assumes that water infiltrating is not limiting. Germann and Beven (1981) postulate that deviations from the unit hydraulic potential must be explained by macropore flow.

Mein and Larson (1973) presented a model for determining the ponding time, t_s , at soil surface. The ponding time is the amount of rainfall needed to saturate the soil surface and generate Horton overland flow. The model is based on the solution of the Green-Ampt equation for a given constant rainfall intensity as follows:

$$t_s = \frac{F_s}{r} \quad (8)$$

where

$$F_s = \frac{S_f(m_s - m_i)}{r/(K-1)} \quad (9)$$

where

- F_s = Depth to Saturation (cm).
- S_f = Soil Suction (cm).
- m_s = Soil Moisture at Saturation ($\text{cm}^3 \text{ cm}^{-3}$).
- m_i = Initial Soil Moisture Content ($\text{cm}^3 \text{ cm}^{-3}$).
- r = Rainfall Intensity (cm h^{-1}).
- K = Saturated Hydraulic Conductivity (cm h^{-1}).

Equation 9 show that rainfall intensity is exponentially negative related to F_s . Deviations from this physically based equation shows that macropore flow is considered important on the vertical movement of water.

CHAPTER IV

COMPARISONS BETWEEN TWO ESTIMATES OF SOIL WATER POTENTIAL IN AN EXPERIMENTAL PLOT IN ARKANSAS

José De Jesús Návar*, Edwin L. Miller, and Donald J. Turton¹

Abstract

Accurate measurements of soil water potential are of fundamental importance to soil water storage and transport. This study was conducted to determine whether pressure transducers and conventional mercury-water manometers produce similar measurements of soil water potential. Pressure transducers and mercury-water manometers were connected simultaneously to a tensiometer system. Tensiometers were installed in an experimental forested plot in the Ouachita Mountains of Central Arkansas. Changes in soil water potential were initiated with simulated rainfall. A comparison of the two methods of measurement was made using nonparametric analysis. The difference between both methods of measuring soil water potential was tested for

¹ J. De J. Návar, Dept of Ciencias Forestales, Universidad Autónoma de Nuevo León, Apartado Postal # 136, Linares, N.L. 67700 México; and E.L. Miller and D.J. Turton, Dept of Forestry, Oklahoma State Univ., Stillwater, OK 74078.
*Corresponding Author.

normality, independence, frequency and deviation from zero by using the Shapiro-Wilk, Correlograms, Spectral Density and Wilcoxon tests, respectively. Linear regressions between both estimates of pressure were developed. The results showed that the medians of both measurements of soil water potential were not significantly different from each other ($p=0.05$) for 85 % of the tensiometers tested. The median difference between both methods of measuring soil water potential was different from zero for 41 % of the tensiometers tested. The difference between both measurements of soil water potential was dependent on previous differences with periodicities of approximately 2 and 128 minutes. The periodicities were partially attributed to the differential lag time response between both devices. The slopes for the linear regression equations were between 0.99-1.11 and 1.12-1.25 for 70 % and 30 % of the tensiometers, respectively. Pressure transducers and mercury-water manometers appeared to produce errors, which were not consistent among tensiometers neither among storms.

Key words: Pressure Transducers, Mercury-Water Manometers, Soil Water Potential.

Introduction

Soil water potential is of fundamental importance to soil water storage and transport. It has been measured with tensiometers (Cassel and Klute, 1986) and thermocouple

psychrometry (Rawlins and Campbell, 1986). When tensiometers are used, mercury, mercury-water manometers (Cassel and Klute, 1986), and vacuum gauges, as well as, pressure transducers (Anderson and Burt, 1978; Long, 1982; Lowery et al, 1986; Williams, 1987; Dowd and Williams, 1989) are utilized to show the level of tension present. Manometer and vacuum gauge systems require intensive labor, and are a disadvantage when information is needed during rapid changes in soil water potentials. Currently pressure transducers are becoming more popular because they have the advantage of automatized data collection, although they are more expensive than mercury-water manometers or vacuum gauges. The performance of pressure transducers, in relation to mercury-water manometers has been mathematically questioned by Trotter (1984). He showed that pressure transducers are not capable of matching the measurement accuracy of mercury-water manometers. Dowd and Williams (1989), on the other hand, suggested that conventional mercury-water manometers are accurate only within 20 cm of water. However, there is a lack of information on the performance of both systems of measuring soil water potential connected simultaneously to the same tensiometer system.

This report focuses on the measurement of soil water potentials with both pressure transducers and mercury water manometers connected to a tensiometer system. The tensiometer system was placed in an experimental plot to

measure rapid changes in soil water content during the application of simulated rainfall. The hypothesis was that there would be no significant differences between both estimates of the soil water potential parameter using these devices, and also, that the difference between both methods of measuring soil water potential would be independent and normally distributed.

Materials and Methods

Tensiometers were installed in the soil of an experimental forested plot 6.3 m long by 3.1 m. Three tensiometers each were placed at three soil depths: 20, 50 and 80 cm in the upper, middle and lower part of the plot. The codes for the tensiometers were U20, U50, U80, M20, M50, M80, L20, L50, and L80, respectively. Tensiometers were installed one year in advance of the experiment to allow the soil to heal from the disturbance caused by the installation procedure. The soil texture of the experimental plot ranges from a loamy A horizon at the upper 15-20 cm to a clayey C soil horizon at the lower 70 cm of soil depth. Water movement in the experimental plot was induced by the application of simulated rainfall.

Soil Water Potentials

Soil water potentials were measured with custom-made tensiometers. The construction of the tensiometers followed

the design of Cassel and Klute (1986) with some modifications by the author. Porous ceramic cups with an air entry value of 1020 cm of water were used. The rounded bottom and straight neck top ceramic cups were cemented inside a 1.27 cm internal diameter PVC tube. The inside of the PVC tubes were rasped out to provide a good fit. Contact cement was applied to the inside of the PVC tubes and to the necks of the ceramic cups and the neck of each cup inserted into a tube. Sight tubes were cemented inside the top of the PVC tube. A 0.3175 cm diameter hole was bored into the top part of the PVC tube, immediately below the sight tube. Nylon tubing with the same external diameter provided a water and mercury column from the PVC tube to the mercury reservoir. The mercury reservoir consisted of individual vials with volumes of 4.65 cm³. Pressure transducers were also installed to the top of the sight tubes (Figure 1).

Soil water potentials were measured with the tensiometer, via the pressure transducers and mercury-water manometers.

Pressure transducers. Ten solid state temperature compensated pressure transducers (Sensym 143SC²) for measuring pressures from ± 1055 cm of water, which provide a 5 V output were used in this study. The performance

² Sunnyvale, CA 94089. Note: Use of trade names does not imply endorsement of the product by the authors.

specifications are reported by Sensym (1991). Nine pressure transducers were installed on top of nine tensiometers and the last one was left open to observe voltage changes due to temperature changes.

Each pressure transducer was calibrated as follows. A manifold was built with 11 openings, ten for the pressure transducers and the last one for a mercury manometer. The pressure transducers were connected to a data logger (Campbell 21X). A range of positive and negative pressures were applied to one end of the manifold. The pressures were held constant for periods exceeding two minutes. The pressure from the mercury manometer was recorded during this interval of constant pressure. Forty-one pressure readings within a range of ± 550 cm of water at pressure intervals of approximately 25 cm of water were taken (Figure 2). Applied pressure and voltage output fitted linear regressions with all coefficients of determination, r^2 s, in the range of 0.99 and with a standard deviation due to the regression of the order of 1.7 cm of water. The linear regression of the pressure potential relative to output voltage for pressure transducers is also presented by Long (1982) and Dowd and Williams (1989). The results of covariance analysis showed that both the intercepts and slopes were statistically different (Table I). Hence, linear regression equations were obtained for each pressure transducer to insure the best possible measurements of soil water potential.

Transducer output voltage was converted to pressure potential using:

$$\phi_{pt} = (a + bx) - L_t \quad (1)$$

where

$$\begin{aligned} L_t &= \text{Length of tensiometer, from ceramic cup to the} \\ &\quad \text{opening of the pressure transducer (cm).} \\ x &= \text{Voltage output } (\mu V). \end{aligned}$$

The linear regression, $a+bx$, of equation 1 comes from the transformation of the voltage output to pressure potential.

Mercury-Water Manometers. The estimations of soil water potential with the mercury-water manometers, ϕ_{mw} (cm), were carried out as shown in Figure 1 and calculated using the following relationships:

$$\phi_{mw} = -P_{hg}gh_2 + P_wgh_1 \quad (2)$$

where

$$\begin{aligned} P_{hg} &= \text{Density of mercury (g cm}^{-3}\text{).} \\ P_w &= \text{Density of water (g cm}^{-3}\text{).} \\ g &= \text{Gravitational acceleration (cm sec}^{-1}\text{).} \\ h_1 &= \text{Elevation between ceramic cup and mercury} \\ &\quad \text{column (cm).} \\ h_2 &= \text{Elevation of mercury column (cm).} \end{aligned}$$

The small vials used as mercury reservoir violated the assumption of constant mercury reservoir elevation. Hence, a calibration factor, cf , was calculated using:

$$cf = \frac{A_t}{A_v} h_2 \quad (3)$$

where

$$A_t = \text{Cross sectional area of tubing (cm}^2\text{).}$$

A_v = Cross sectional area of vial (cm^2).

Equation 3 was added to h_2 on the right hand side of equation 2.

Field Procedure

Simulated rainfall was applied at constant intensity to the experimental plot for a time until nearly equilibrium conditions in lateral fluxes and soil water potentials within the experimental plot were attained. Soil water potential was recorded with the data logger from pressure transducers every minute during rainfall simulation and every 10 minutes thereafter. Mercury-Water manometers were manually recorded every 2-3 minutes during simulated rainfall. The human reader took approximately one minute to read all nine tensiometers and readings were recorded 30 seconds in advance for the first and 30 seconds later for the last tensiometers.

Simulated rainfalls were applied 17 times over the period from July 25th to October 10 of 1991. Various rainfall intensities and durations were applied, under different initial soil water potentials. For this report only 3 rain storms were considered: storm 10, 15 and 16 with 1.59, 2.66 and 1.04 cm h^{-1} of rainfall intensity and 3.0, 2.17, and 4.25 hours of duration, respectively.

Data Analysis

The measured soil water potentials from pressure transducers and mercury-water manometers, as well as, the difference between both methods of measurement were analyzed for normality and lognormality by using the Shapiro-Wilk univariate test (SAS, 1987). Because neither of these probability density functions fitted the data, nonparametric analyses were used.

The median test was applied to test the null hypothesis that the two sampled continuous distributions have a common median (Steel and Torrie, 1980). The Wilcoxon rank test was applied to test the null hypothesis that the difference between both methods of measurement has a median of zero (Steel and Torrie, 1980 and SAS, 1987). Friedman's test with a complete randomized block design was also used to test the equality of the median difference among tensiometers and storms (Steel and Torrie op. cit.). The autocorrelation function was used to test the independence of the difference between both methods of measuring soil potential (Wilkinson, 1989). Because the difference was dependent on previous differences, spectral density analysis was used to determine periodicities (Wilkinson, 1989). Linear regression equations between the two methods of measurement of soil water potential were obtained and the slopes were tested for deviations from 1.0 (Haan, 1977).

Results and Discussion

Measured soil water potentials from pressure transducers and mercury-water manometers for 9 tensiometers during and after a 255 minute simulated storm with a rainfall intensity of 1.04 cm h^{-1} are presented in Figure 3. The pre-rainfall soil water potential measured with mercury-water manometers was less than that for the pressure transducer readings for most tensiometers for all simulated storms. As soon as the soil water potentials responded to water inputs, both methods of measurement of pressure followed a similar trend. The peak of soil water potential was also similar for most tensiometers at the peak of the soil water potentials. The decaying soil water potential is also smaller for most mercury-water manometers.

The median test failed to reject the null hypothesis for 85 % of the tensiometers tested ($p = 0.05$) (Table II). This indicated that estimated soil water potential with pressure transducers are not different than the measurements of soil water potential with mercury-water manometers. The tensiometers which produced data resulting in a rejection of H_0 were located at the upper 20 cm of soil depth and three of them belonged to storm # 16.

The Wilcoxon rank test failed to reject the null hypothesis for 59 % of the tensiometers tested ($p = 0.05$) (Table III). These results demonstrate that both systems of measuring soil water potential were biased for 41 % of the tensiometers tested. The deviation from zero mean difference

between the methods of measuring soil water potential was not consistent between tensiometers among rains, except for tensiometers U80 and L20.

The difference between the two methods of measuring soil water potential followed a similar trend as the estimates of soil water potential for each tensiometer (Figure 4). The difference went from a negative to a positive direction. The pressure transducer measurement was larger at the beginning of the storm. The difference decreased as the storm progressed and the mercury-water manometer potential become larger at nearly constant conditions. The trend was reversed at the end of the simulated storm. The maximum difference was attained either before rainfall simulation or at some time after it stopped.

The range in median difference between the two methods of measuring soil water potential was -7.64 to +6.44 cm of water. The randomized complete block design for medians showed that the median difference between both methods of measuring soil water potential were different among tensiometers and among storms ($p = 0.0001$). However, the median sign and magnitude for any particular tensiometer were not consistent through storms.

The difference between the two methods of measuring soil water potential was not independent. The correlograms for this parameter showed a trended time series (Figure 5). The confidence intervals were calculated assuming that the

time series are circular, which is an appropriate assumption for the time series. The serial autocorrelation coefficient follows a different trend for most tensiometers and it demonstrated that the difference between both methods of measuring soil water potentials are dependent on previous differences.

The spectral density analysis (Figure 6) showed that the difference between the two methods of measuring soil potential has an approximate time period of 2 minutes, since the case number represents an interval of time of 2 minutes and the series were truncated to 64 cases. This period represents partially the lag time mercury-water manometers take to respond to soil water potential changes in relation to the lag time of pressure transducers. This value was checked with the physical estimations of Klute and Gardner (1962), whom determined the lag time of gauge response, T_r , by:

$$T_r = (KS_g)^{-1} \quad (4)$$

where

$$\begin{aligned} K &= \text{Cup conductance } (L^2T^{-1}) \\ S_g &= \text{Gauge sensitivity } (L^{-2}) \end{aligned}$$

The cup conductance, for a ceramic cup with an air entry value of 1020 cm of water, at high flow response was empirically measured in the laboratory as $1.31 \times 10^{-3} \text{ cm}^2 \text{ sec}^{-1}$. The sensitivity of the pressure transducer-tensiometer system was approximately $3.00 \times 10^4 \text{ cm}^{-2}$ (Cassel

and Klute, 1986). The sensitivity of the mercury water manometer-tensiometer system was estimated as $8.31 \times 10^2 \text{ cm}^{-2}$. The average lag time of response, T_r , were 0.3 and 1 second for the pressure transducer and mercury-water manometer systems, respectively. The 2-minutes lag time was probably associated to the lag time of reading mercury-water manometers.

There was another set of periodicities at approximately 128 minutes which were probably related to the increase of the difference at the end of the simulated storm or the return of the maximum decrease of soil water potential.

The relationships for both estimates of soil water potential for the same information presented above for storm 16 are presented in Figure 7. The regression coefficients were, in general, larger than 1.00 but smaller than 1.11 for 70 % of the tensiometers. The slopes were significantly different from 1.0. However, most intercepts, 23, were negative, which offset somehow the slope overestimation (Table IV).

This report shows that pressure transducers can match the soil water potential measurements of conventional mercury-water manometers, or vice versa, in agreement with the findings reported by Dowd and Williams (1989) and Lowery et al. (1986). The medians for most estimates between pressure transducers and mercury water manometers are not significantly different. The trends both methods follow are,

in fact, very similar, except for the tails. The maximum reported median difference between both methods of measuring soil water potential, -7.64 or + 6.5 cm of water, is in good agreement with the maximum soil water potential deviation theoretically estimated by Trotter (1984) for pressure transducers and is less than that suggested by Dowd and Williams (1989) for conventional mercury-water manometers. The maximum median difference represents approximately 8 % of the range of soil water potentials, although it was not clear whether the percentage increases with the range of soil water potentials measured.

The median difference between both methods of measuring soil water potential was not consistent among tensiometers neither among storms. The median difference and the sign of the median difference change among storms and among tensiometers.

The magnitude of the difference between both methods of measuring soil water potential is not constant over time. The probable causes of this behavior are varied and should be discussed in detail. Among them are:

- 1). Air bubbles in the water system. Even though the sight tubes and tubing were checked out carefully before the experimental runs and boiled, distilled water was used, some small air bubbles were observed in the highest point of the tubing system of some tensiometers as the storm progressed. Air bubbles affected mostly mercury-water readings because

they were out of the zone of measurement of the pressure transducer.

2). The ability of the person to read precisely the length of the mercury column. This effect caused a stair step on soil water potential readings for mercury-water columns.

3). The pressure transducer measurements were not calibrated for changes in temperature before and after the rainfall was simulated. A reading of a check pressure transducer showed that pressures could change by 1 cm of water when the temperature of the applied water was different than that of the environment.

4). The pressure transducer measurement was not calibrated to account for the differential elevation between the additional water elevation of the mercury-water manometer. Empirical observations showed that this water elevation did not have a significant effect on the pressure transducer reading at zero soil water potential. It may have had an effect at larger soil matric potentials. A plot of the length of the mercury column against the difference between both methods of measuring soil water potential showed no particular trend and a large variation.

5). The pressure transducer readings were not calibrated for the hysteretic loop caused by a change of the systematic increasing or decreasing of soil water potential. This may also account for up to 3 cm of water in the full

range of the pressure transducer measurements.

6). A lag time existed between the reading of some tensiometer and the actual reading of the pressure transducer. This could have affected 4 tensiometers, which were read 30 seconds after the pressure transducer reading. This factor was more important when the rate of soil water potential change was highest.

Air bubbles caused the mercury-water manometer to have a sluggish response to changes in soil water potential. This effect was more important early in simulated storms for some tensiometers, since the periodograms at that time were highly variable and the difference did not follow any particular trend. As the simulated storm progressed, the lag time between both devices become apparent.

The six sources of error discussed above were partially responsible for the slope's deviation from 1.0 between the regression of both soil water potential estimates.

References

- Anderson, M.G., and Burt, T.P. 1978. Automatic monitoring of soil moisture conditions in a hillslope spur and hollow. *Journal of Hydrology* 33:27-36.
- Cassel, D.K., and Klute, A. 1986. Water potential:tensiometry. *In*: A. Klute (Ed.) *Methods of Soil Analysis, Part I*. 2nd ed Agronomy 563-596.
- Dowd, J.F., and Williams, A.G. 1989. Calibration and use of pressure transducers in soil hydrology. *Hydrological Processes* 3:43-49.
- Haan, C.T. 1986. *Statistical Methods in Hydrology*. Fourth Printing. The Iowa State University Press. Ames IO.

- Klute, A., and Gardner, W.R. 1962. Tensiometer response time. *Soil Science* 93:204-207.
- Lowery, B., Datairi, B.C., and Andraski, B.J. 1986. An electrical readout system for tensiometers. *Soil Science Society American Journal* 50:494-496.
- Long, F.L. 1982. A new solid state device for reading tensiometer. *Soil Science* 133:131-132.
- Rawlins, S.L., and Campbell, G.S. A. 1986. Water potential:thermocouple psychrometry. In: A. Klute. (Ed.) *Methods of Soil Analysis. Part I*, 2nd ed. Agronomy 597-618.
- Steel, R.G.D., and Torrie, J.H. 1980. *Principles and Procedures of Statistics: A Biometrical Approach* 2nd ed. McGraw-Hill. New York.
- SAS/STAT Guide for Personal Computers. 1987. Version 6 Edition. SAS Institute Inc. Cary, N.C.
- SENSYM: Solid-State Sensor Handbook. 1991. Sunnyvale, CA.
- Trotter, C.M. 1984. Errors in reading tensiometer vacuum with pressure transducers. *Soil Science American Journal* 50:494-496.
- Williams, T.H.L. 1978. An automatic scanning and recording tensiometer system. *Journal of Hydrology* 39:175-183.
- Wilkinson, L. SYSTAT: The System for Statistics. 1989. Evanston, IL: SYSTAT, Inc.

TABLE I

COVARIANCE ANALYSIS PROCEDURE FOR TESTING SLOPES AND INTERCEPTS
HOMOGENEITY FOR THE REGRESSION MODELS BETWEEN PRESSURE
AND VOLTAGE OUTPUT FOR NINE PRESSURE TRANSDUCERS

Dependent Variable: Pressure (cm)

Source	DF	Sum of Squares	Mean Square	F Value	Pr > F
Model	17	30914726.29	1818513.31	57280.90	0.00001
Error	351	11143.30	31.75		
Corrected Tot	368	30925869.59			

R-Square	C.V. (%)	Root MSE	Y Mean
0.999640	4.94	5.634473	-113.85388

Dependent Variable: Pressure (cm)

Source	DF	Type I SS	Mean Square	F Value	Pr > F
MODEL	1	30896805.78	30896805.78	99999.99	0.00001
INTERCEPT	8	17358.75	2169.84	68.35	0.00010
SLOPE	8	561.76	70.22	2.21	0.02610

TABLE II

THE MEDIAN TEST FOR TESTING THE NULL HYPOTHESIS OF COMMON
SOIL WATER PRESSURE POTENTIAL BETWEEN PRESSURE
TRANSDUCERS AND MERCURY-WATER COLUMNS

TENSIO- METER CODE	STORM 16		STORM 10		STORM 15	
	χ^2	$P > \chi^2$	χ^2	$P > \chi^2$	χ^2	$P > \chi^2$
U20	105.34	0.0001	0.7837	0.3749	0.6215	0.4305
U50	0.02	0.8849	0.0314	0.8591	0.6215	0.4305
U80	0.13	0.7226	0.1260	0.7226	0.6215	0.4305
M20	22.90	0.0001	0.7873	0.3749	0.0388	0.8438
M50	0.02	0.8849	0.2834	0.5945	0.0388	0.8438
M80	3.17	0.0850	0.1260	0.1260	0.6215	0.4305
L20	11.16	0.0008	2.5613	0.1095	15.5480	0.0001
L50	0.52	0.4693	0.1261	0.7226	2.4862	0.1149
L80	1.03	0.3101	0.7874	0.3479	0.0388	0.8438

TABLE III
 THE WILCOXON TEST FOR TESTING THE NULL HYPOTHESIS
 THAT THE MEDIAN DIFFERENCE IN SOIL WATER
 PRESSURE POTENTIAL DOES NOT
 DEVIATE FROM ZERO

TENSIO- METER CODE	STORM 16		STORM 10		STORM 15	
	χ^2	$P > \chi^2$	χ^2	$P > \chi^2$	χ^2	$P > \chi^2$
U20	51.44	0.0001	0.34	0.5611	0.670	0.4123
U50	3.32	0.0687	0.02	0.8796	0.100	0.7551
U80	7.07	0.0078	7.08	0.0078	6.780	0.0092
M20	22.33	0.0001	16.00	0.0001	0.240	0.6211
M50	0.45	0.5040	4.56	0.0328	0.570	0.4517
M80	2.02	0.1558	2.52	0.1121	1.430	0.2300
L20	15.47	0.0001	8.83	0.0030	11.100	0.0009
L50	1.24	0.2669	1.69	0.1939	8.250	0.0040
L80	0.08	0.7750	1.06	0.3028	0.000	0.9678

TABLE IV
THE REGRESSION PARAMETERS BETWEEN THE ESTIMATES OF SOIL WATER
PRESSURE POTENTIAL

TENSIO- METER	STORM 16			STORM 10			STORM 15		
	r ²	a (cm)	b	r ²	a (cm)	b	r ²	a (cm)	b
U20	0.98	4.90	1.09	0.94	-1.15	1.07	0.88	-1.01	0.96
U50	0.99	2.32	1.19	0.98	-1.49	1.21	0.91	-3.25	1.15
U80	0.99	-8.17	1.07	0.99	-8.23	1.07	0.99	-10.2	1.13
M20	0.99	4.76	1.10	0.96	7.88	1.25	0.97	-0.74	1.19
M50	0.98	-2.20	1.07	0.99	-6.46	1.11	0.98	-6.22	1.25
M80	0.98	-0.27	1.08	0.98	-4.36	1.15	0.99	-2.29	1.11
L20	0.99	-4.68	1.00	0.94	-3.13	1.02	0.96	-6.37	1.10
L50	0.97	-1.38	0.99	0.95	-2.70	1.00	0.96	-7.17	1.07
L80	0.98	-2.09	1.09	0.98	-6.34	1.10	0.98	-9.66	1.14

Note: The estimate of soil water pressure potential with pressure transducers was the dependent variable.

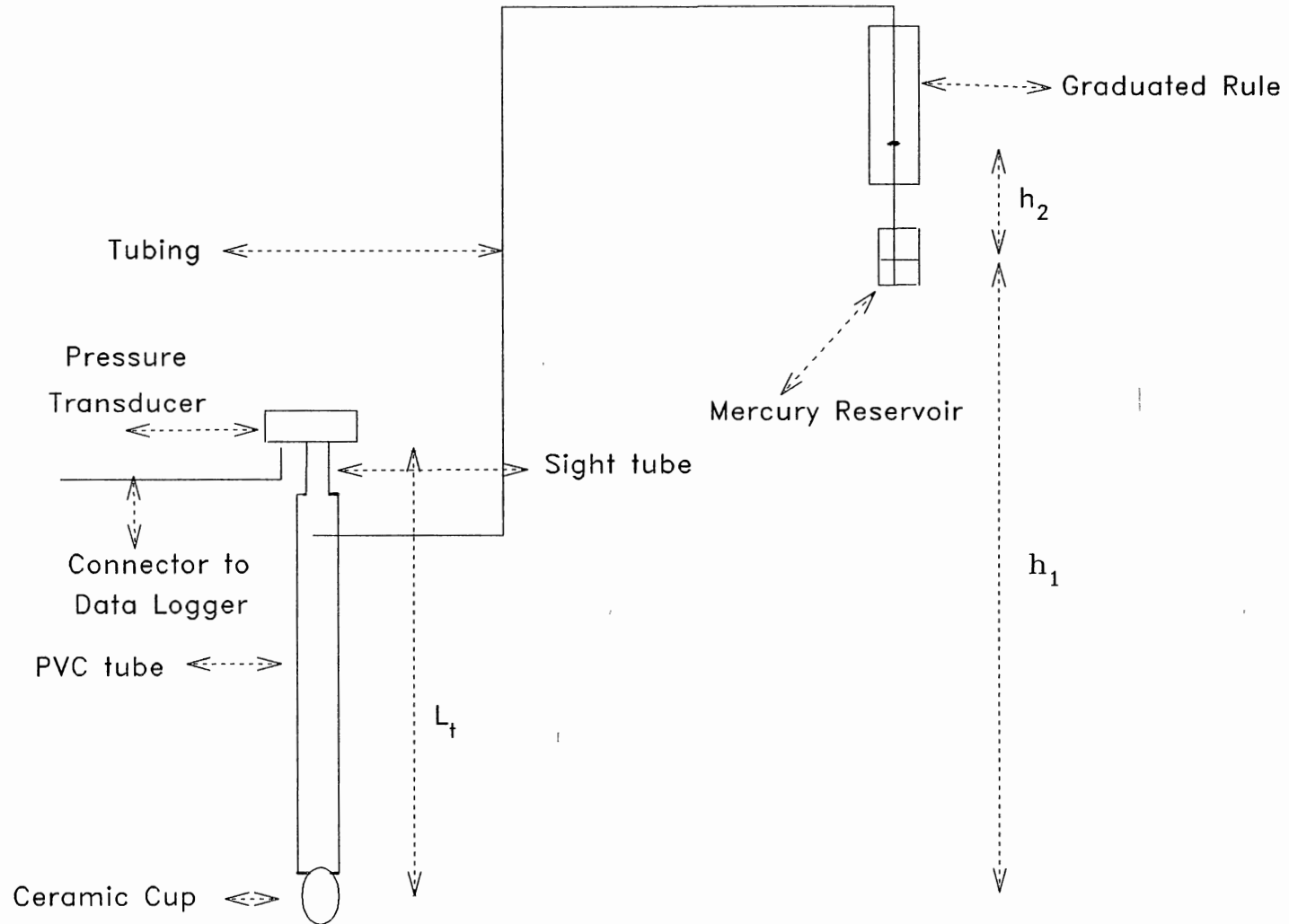


Figure 1. The Graphical Representation of the Components of a Tensiometer System with a Mercury–Water Manometer and a Pressure Transducer.

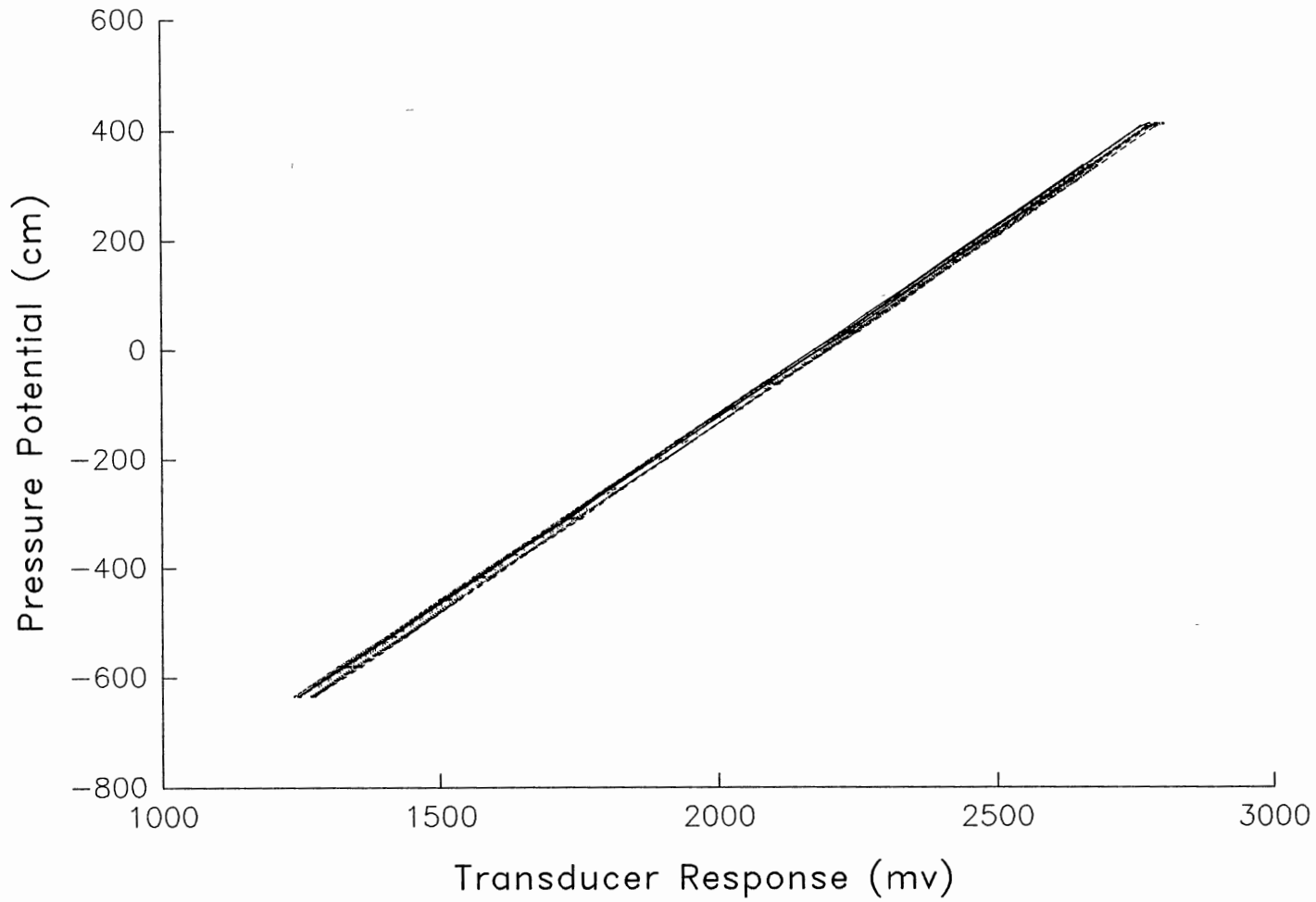


Figure 2. The Calibration Curves for nine Pressure Transducers (n=41 for each Pressure Transducer)

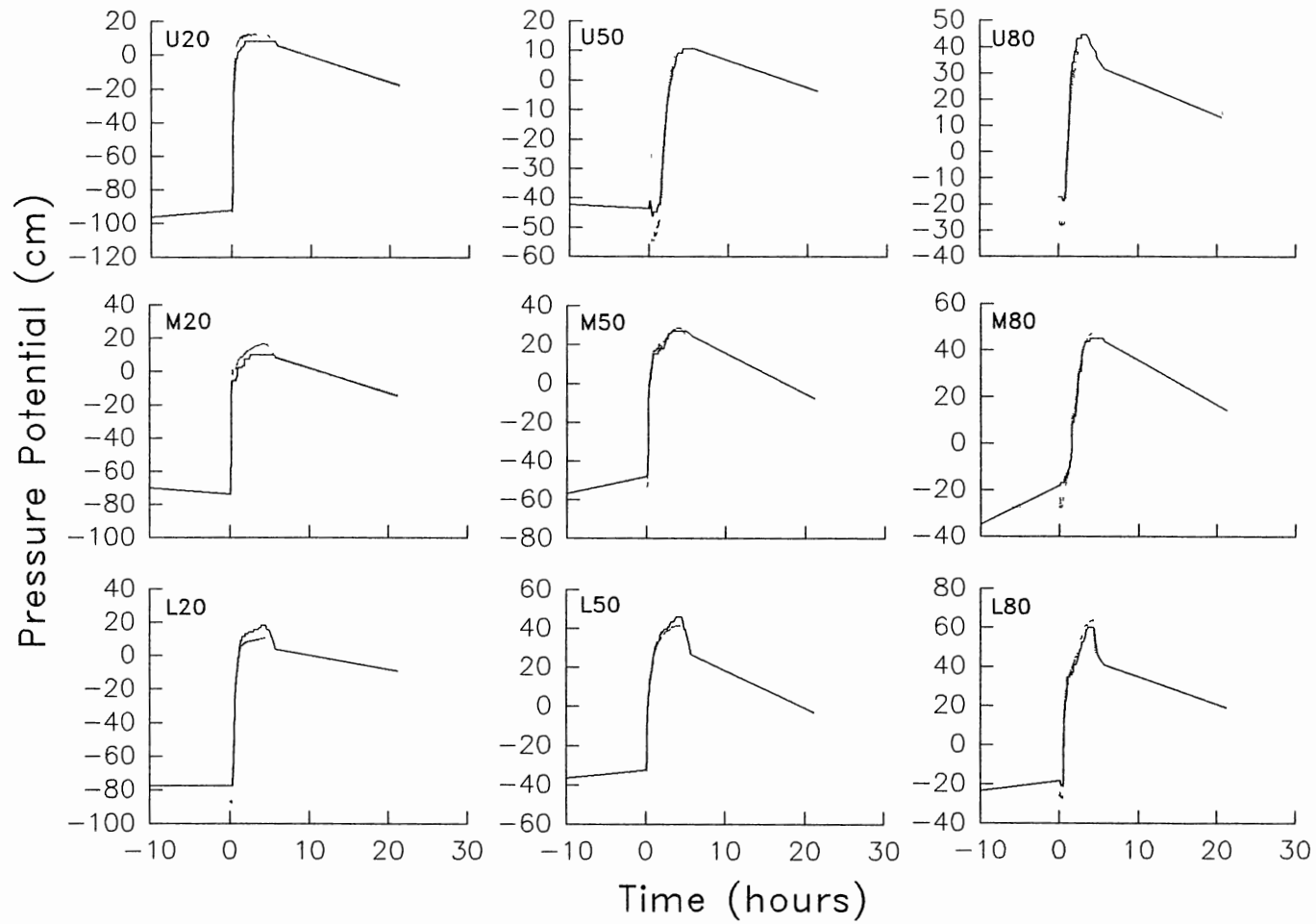


Figure 3. The Development of Soil Water Potential (—Pressure Transducers Mercury-Water Manometers) for nine Tensiometers for Rainfall 16.

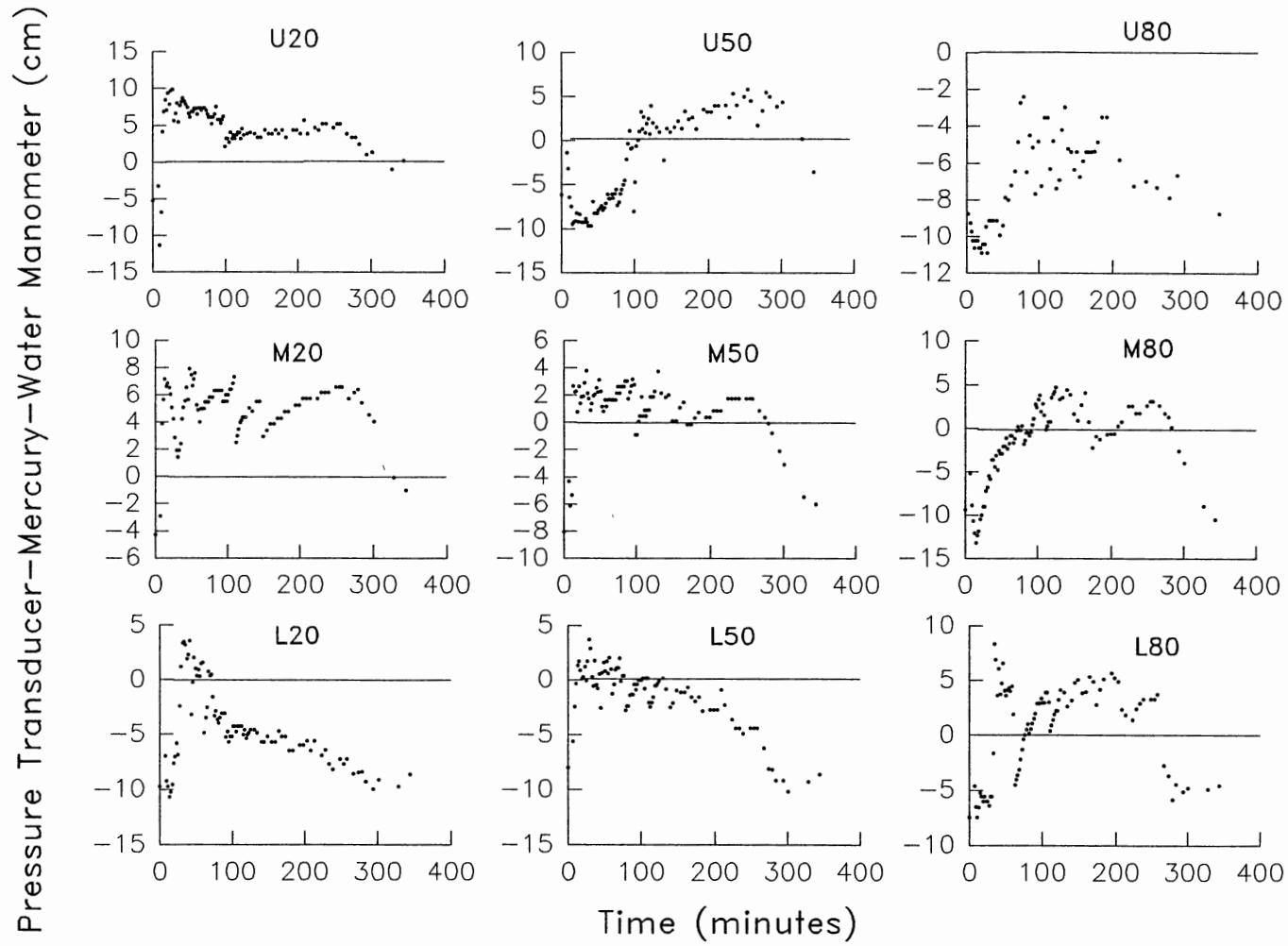


Figure 4. The Behavior of the Difference between two Estimates of Soil Water Potential during the Simulation of Rainfall 16.

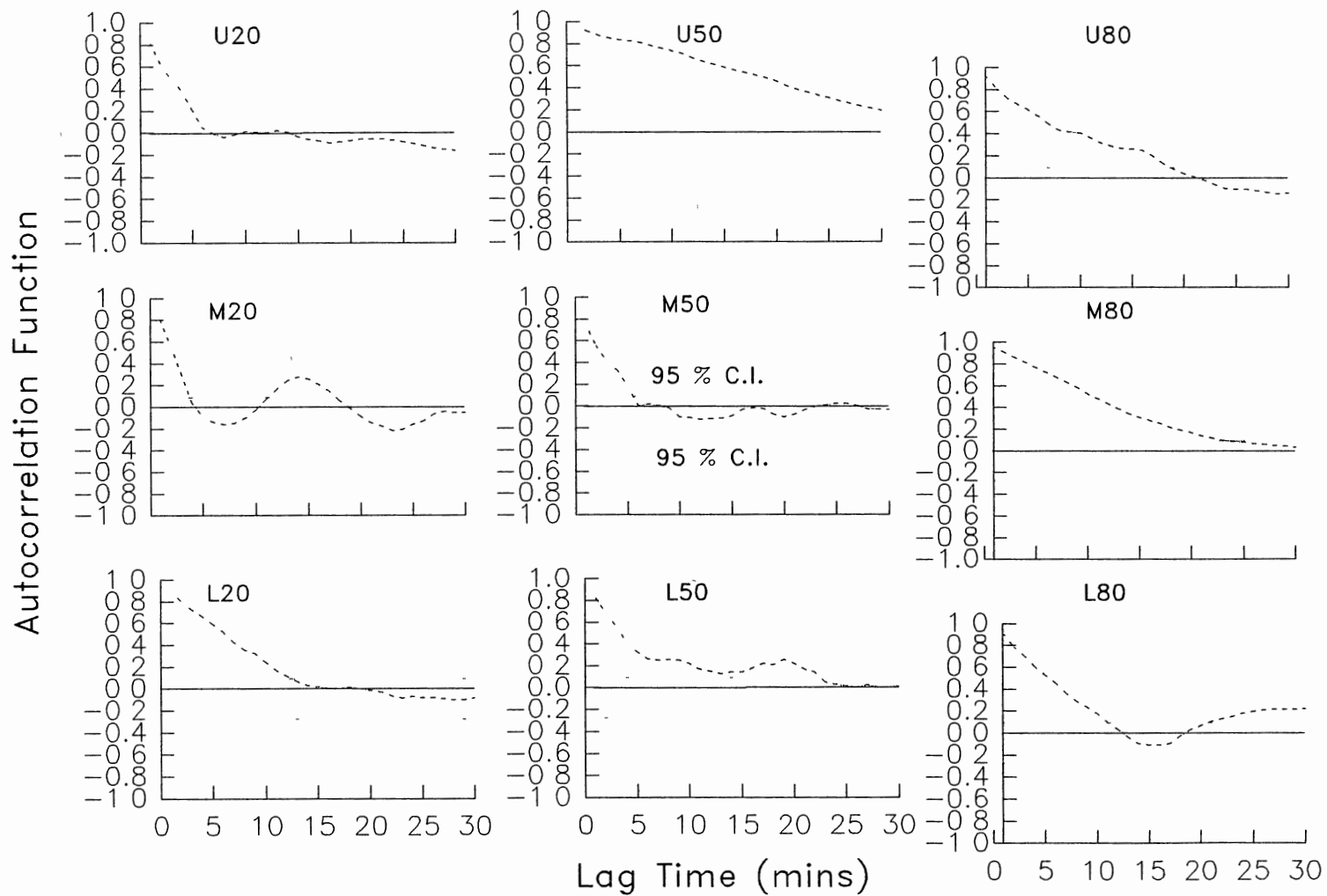


Figure 5. The Correlograms for the Difference between two Estimates of Soil Water Potential during the Simulation of Rainfall 16.

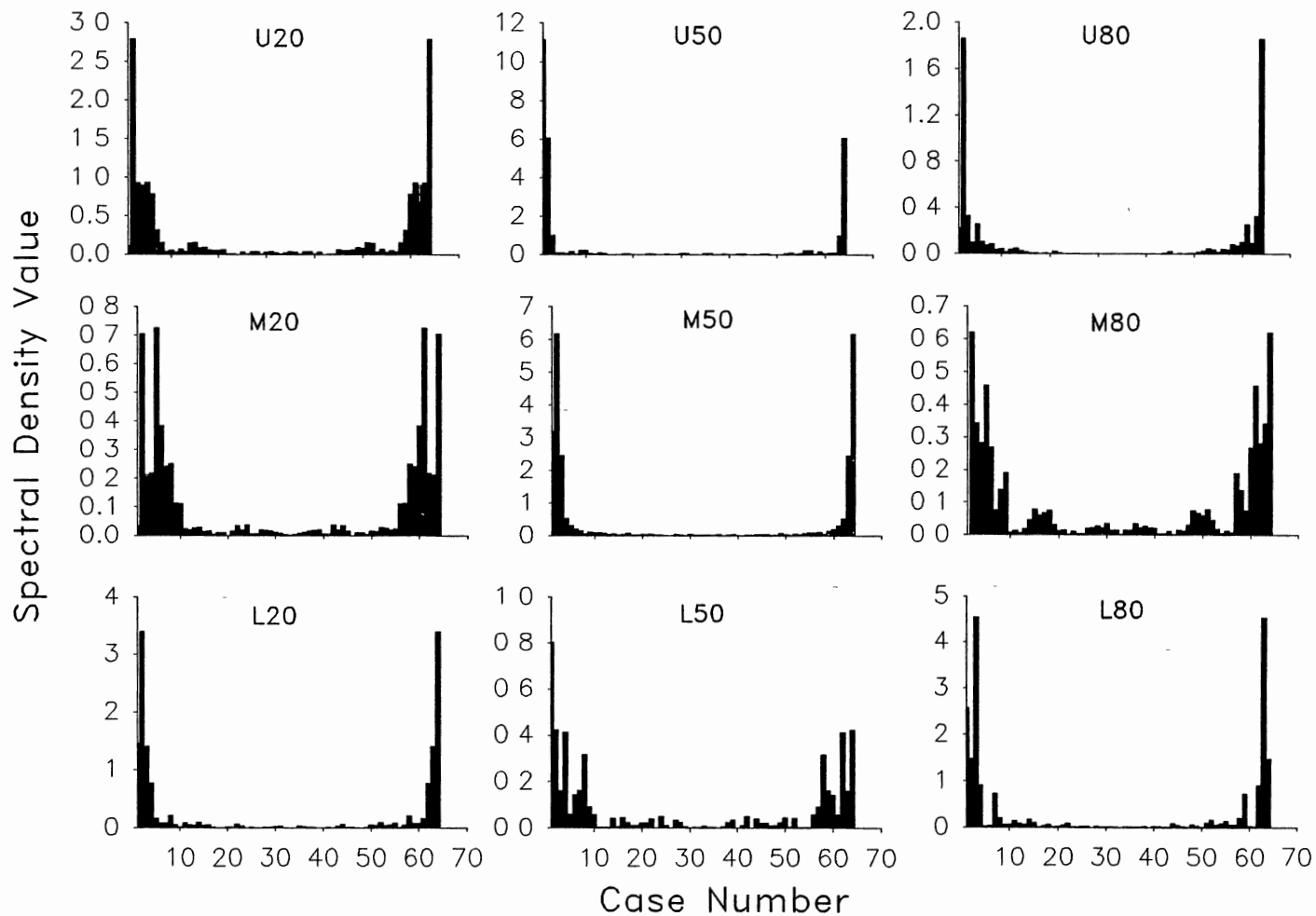


Figure 6. The Spectral Density Analysis for the Difference between two Estimates of Soil Water Potential for nine Tensiometers for Rainfall 16. A Case Number Represents a 2-minute Interval (The Series were Truncated to 64 Cases).

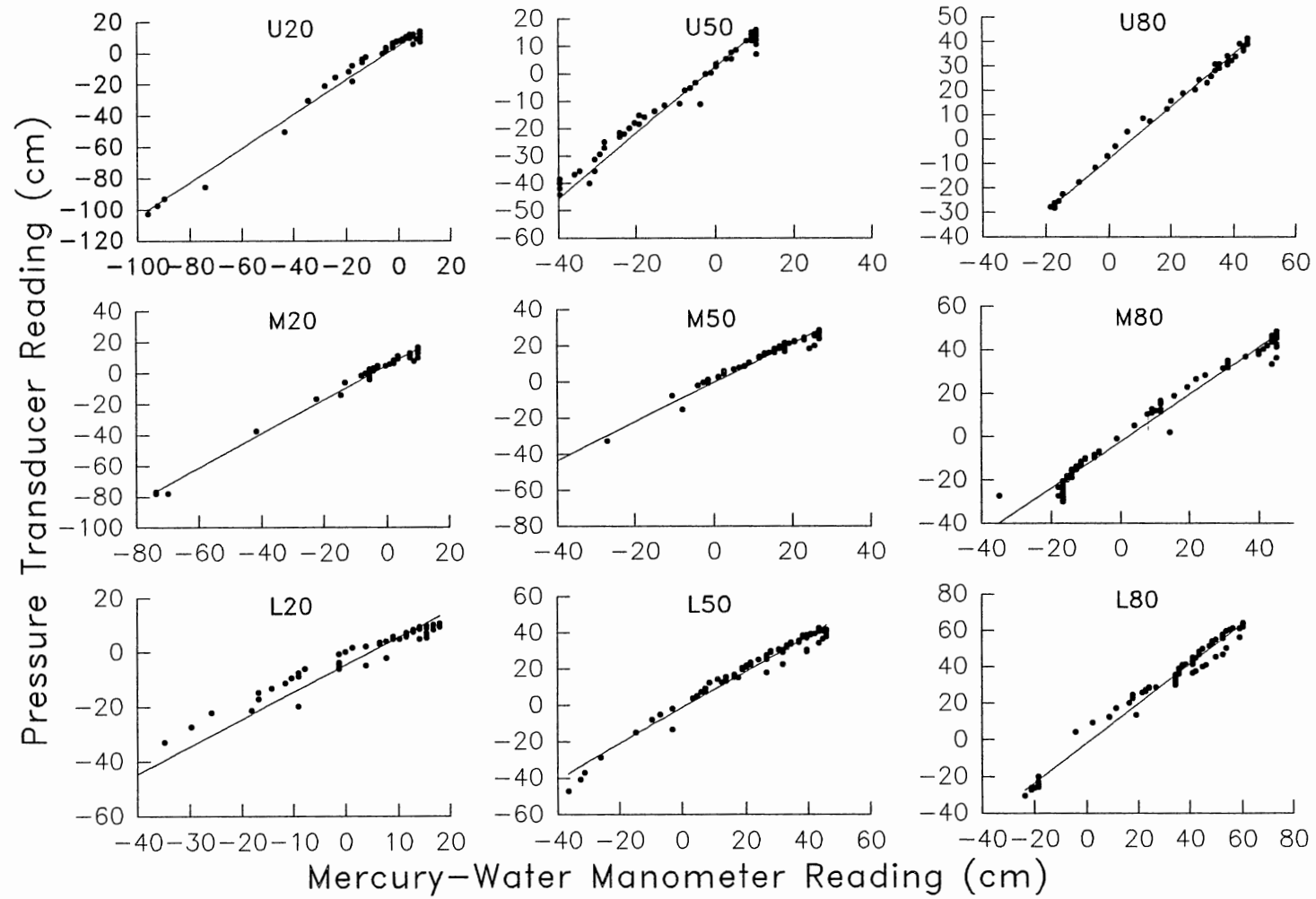


Figure 7. The Linear Relationships between the Mercury-Water Manometer Reading and the Pressure Transducer Reading for nine Tensiometers for Rainfall 16.

CHAPTER V

ENERGY RELATIONSHIPS OF AN EXPERIMENTAL PLOT IN THE OUACHITA MOUNTAINS

José De J. Návar*, Edwin L. Miller, and Donald J. Turton³

Abstract

Lateral water flux and soil water potentials were measured in an experimental forested plot in the Ouachita Mountains of Arkansas during and after simulated rainfall. Lateral water flux was measured from four depths and soil water potentials were measured at three depths in the experimental plot. Rainfall was applied 17 times during the period of July 17 to October 10 of 1991 under soil water potentials of less than 100 cm of water of suction. Soil water potentials showed irregular development of the wetting and desorption fronts in both the lateral and vertical directions of the plot. Soil sorption and desorption rates were spatially variable. The relationships between lateral

³ J. De J. Návar, Dept of Ciencias Forestales, Universidad Autónoma de Nuevo León, Apartado Postal # 136, Linares, N.L. 67700; and E.L. Miller and D.J. Turton, Dept of Forestry, Oklahoma State Univ., Stillwater, OK 74078. *Corresponding Author.

flux density and lateral hydraulic gradients were not linear. Unsaturated flow occurred both vertically and laterally in the experimental plot. Perched water tables developed upward from the bottom of the studied soil depths. These findings in addition to visual observations of the lateral discharge during simulated rainfalls demonstrated that bypassing flow, which deviates from potential flow theory, was actively contributing to water movement in the experimental plot. These observations strongly suggest potential flow theory does not generally apply to the soils studied.

Key Words: Potential Flow, Bypassing Flow, Subsurface Flow.

Introduction

Water movement has been analytically modeled by the empirically derived law of Darcy for saturated soils (Anderson and Burt, 1978), as well as, Richards equation for unsaturated soils (Hillel 1980, 1982). Richard's equation and Darcy's law are based on potential flow theory. The assumptions of potential flow theory are: 1) soil water flow is driven by a potential gradient, 2) water moves in the direction of a decreasing potential, 3) the rate of water flux is proportional to the potential gradient, and 4) soil water flow is laminar (Hillel, 1980, 1982). Richard's equation and Darcy's law also assume that soils are homogeneous and isotropic (Bouma, 1990, and Kung, 1990a,

1990b).

Forest soils of the Ouachita Mountains have been shown to be nonhomogeneous and anisotropic, with stones, roots, root channels, and worm burrows, which may be critical to soil water flow. The authors observed macropore flow from root, insect and rodent channels during and after natural rainfalls on the U.S. Forest Service Experimental Watershed 11 and in adjacent road cuts. Miller et al. (1988) and Turton et al. (1992) suggested that the rapid generation of stormflow on small watersheds, via subsurface flow, in the Ouachita Mountains, was probably associated with macropore flow.

Macropore flow does not behave according to the assumptions of potential flow theory. Field observations and analytical evidence have demonstrated that water (Whipkey, 1965; Jones, 1971; Aubertin, 1971; Beasley, 1976; Pilgrim et al. 1978; Mosley, 1979, 1982; Beven and Germann, 1981; Germann, 1986, 1990a, 1990b; McDonnell, 1990; Andreini and Steenhuis, 1990; Booltink and Bouma, 1991 and Edwards et al. 1992) and solutes (Bouma et al. 1979; Pearce et al. 1986; Beven and Young, 1988; Richard and Steenhuis, 1988; Mulholland et al. 1990; Jardine et al. 1990; Andreini and Steenhuis, 1990 and Edwards et al. 1992) can move farther and more rapidly than would be predicted by potential flow theory. Therefore, current physical models of subsurface water movement generally include a dual mode of water flow:

matrix flow and macropore flow (Beven and Germann, 1981).

Germann (1990b) and Sklash (1990) stated the need to establish the mode of subsurface water movement. Although macropore flow is difficult to measure, Ehlers (1975), Mosley (1979, 1982), Edwards et al. (1988, 1989, 1990, 1992), Andreini and Steenhuis (1990), and Booltink and Bouma (1991) assessed the relative importance of macropore flow on soil columns and field blocks.

The measurement of soil water potentials in macroporous soils during rainfall can provide evidence of the mode and the relative importance of macropore flow. However, few studies have dealt with the energy relationships of macroporous soils. DeVries and Chow (1978), Germann and Beven (1981), Jardine et al. (1990), and Booltink and Bouma (1991), studied the development of soil water potentials of soil columns and field soil blocks. But the suitability of applying potential flow theory to subsurface water movement in macroporous forest soils require further study.

This paper focusses on reporting the soil water energy relationships of a soil block during and after simulated rainfall conditions and also tests several hypotheses based on potential flow theory.

The hypotheses tested were:

- 1). Lateral subsurface flow must occur under a saturated soil matrix, because potential flow theory predicts that soil moisture moves first via micropores.

2). The changes of potential profiles during rainfall as sorption occurs or after rainfall as desorption occurs must follow the equilibrium pressure gradient⁴. If macropores contribute to water movement, irregular potential profiles may occur.

3). Flux density increases with a monotonic increase of the hydraulic gradient as predicted by Darcy's law.

Materials and Methods

The Study Area

An experimental plot was established 35 miles north of Hot Springs, Arkansas, on the U.S Forest Service Alum Creek Experimental Forest in the Ouachita Mountains of Arkansas. The mountains were formed as a result of the Ouachita Orogeny, in the Late Paleozoic Era. Sedimentary rocks (sandstones, shales, limestones and conglomerates) were folded and faulted in the east-west orientation, due to northerly compressive forces (USDA Forest Service, 1964). The soils on the Alum Creek experimental watersheds are classified by the USDA Forest Service as the Alemance associations (Typic Hapludults). DeWit and Steinbrenner (1981) classified the soil as the Sandlick Series. The general soil slope for the experimental plot was 16 %. The soil description of the area, textural and bulk density

⁴ Equilibrium pressure gradient, EPG.

analyses and the location of tensiometers and subsurface flow collectors are reported in Table I.

The vegetation of the Alum Creek Watersheds is classified as an association of Loblolly- Shortleaf pine, Pinus taeda-Pinus echinata and hardwoods, Quercus alba, Quercus rubra, Cornus florida, Acer rubrum, Carya spp and Nyssa silvatica.

The climate of the area is temperate-humid with an annual average temperature of 74.3° F; ranging from 52.7° F in January and 93.2° F in August. The mean annual precipitation is 1250 mm of which 33 % occurs during April through June. The wettest month of the year is April with 153 mm and the driest is October with 90 mm. There is no well defined dry season, however summer precipitation is highly variable and high rates of summer evapotranspiration cause frequent soil moisture deficits.

The Experimental Plot

An experimental plot 6.3 m in length by 2.05 m in width, with a 0.5 m buffer strip zone on each side, was hydrologically isolated by digging a trench down to the C soil horizon (0.90 to 1.1 meters). The side and upslope walls were sealed with polyethylene sheets, while the lower wall was left uncovered for sample collection and observations during the simulated rainfalls. Perforated pipes were layed at the bottom of the upper and two side

trenches and covered with 35 cm of gravel to allow drainage around the experimental plot. The remainder of the trench was filled with the original soil to provide support to the experimental block. The site was cleared of all shrubby and large trees.

The experimental plot was instrumented with three sets of tensiometers, four subsurface flow collectors, and six neutron probe access tubes. A rainfall simulator was constructed to supply rainfall to the plot and the buffer area. A tarp was also set up at approximately 1.80 m height to prevent direct throughfall from natural rainfall into the experimental plot.

Subsurface Flow Collectors

The system to measure subsurface flow at the lower open cross sectional area, 13630 cm^3 , of the experimental plot was constructed as described by Turton et al. (1992). The subsurface collection system consisted of four troughs placed at 14, 26, 44 and 67 cm of soil depth. The first trough collected water from the Litter, A and E soil horizons, 2680 cm^2 , the second and third troughs from the B1, 2375 cm^2 and B2, 3870 cm^2 , soil horizons, and the last one from the interface between the B and C soil horizons, 4710 cm^2 . To avoid soil crumbling from the open lateral face, galvanized wire screen was used. Before the installation of the subsurface flow collection system, the

largest lateral soil macropores were mapped (Table II).

Troughs were constructed by cutting 0.11 X 2.1 m PVC drain pipe lengthwise. Polyethylene sheeting was inserted horizontally into the soil to approximately 5 cm to direct collected subsurface flow from the soil horizon into the troughs. Flow collected from each through was drained into a recording individual tipping bucket. A data logger recorded the number and time of tips for each tipping bucket.

Soil Water Potentials

Soil water potential was measured with pressure transducers and mercury-water manometers connected to custom-made tensiometers. The tensiometers were constructed following the design of Cassel and Klute (1986). Eighteen tensiometers were installed in the fall of 1990 on the experimental plot: one year in advance of the experiments to allow the soil to settle from any installation disturbance. Tensiometers were installed at three soil depths, 20, 50 and 80 cm, in the upper, middle and lower part of the experimental plot. Nine tensiometers were fitted with pressure transducers, which were coded as follows: U20, U50, U80; M20, M50, M80; and L20, L50, and L80 for the upper, middle and lower part of the experimental block at 20, 50 and 80 cm of soil depth, respectively. Tensiometers without pressure transducers were installed to insure having at

least one operational unit at each location. Calibration and performance of the pressure transducers and mercury-water manometers are reported elsewhere (Navar, 1992).

Rainfall Simulator

A rainfall simulator was built to generate rainfall movement on the experimental plot. It consisted of a rectangular frame made of 1.905 cm in diameter PVC pipe with spraying nozzles placed underneath. The industrial spraying nozzles (Lechler from Jackson and Associates⁵) produced a full cone axial spray pattern. The number and type of nozzles varied according to a specific rainfall intensity. The rainfall simulator was suspended by ropes and swung back and forth to insure even distribution of rainfall. A water reservoir consisting of a plastic tank with a 5000 liter capacity was located upslope from the simulator to provide gravity feed of water. The system was capable of delivering water through a 3.81 cm PVC pipe at a pressure of approximately 700 cm of water. A pressure gauge with a manual valve was installed between the lower part of the 3.81 cm PVC pipe and the rainfall simulator to maintain constant rainfall.

Field Procedure

⁵ P.O. Box 551585, Dallas, TX 75355-1585. Note: use of trade names does not imply endorsement of the product by the authors.

Simulated rainfall was applied to the experimental plot for 17 storms ranging in depth and duration from 8.26 to 4.04 cm and 0.82 to 4.25 hours, respectively (Table III). Individual rainfalls continued until changes in the rates of outflow and soil water potentials become negligible. Soil water potentials from pressure transducers and the rates from subsurface flow collectors were recorded at one minute intervals during simulated rainfall and for a 2-hour period after rainfall was stopped. After 2-hours, data were recorded at 10 minute intervals. Mercury-water manometers readings were taken every two to three minutes during rainfall. Rainfall input was measured with a set of 10 rain cans set up on the experimental plot.

Results and Discussion

Unsaturated Lateral Flow

In the early stages of the rainfalls, it was observed that lateral flow from the soil face occurred around living and through decayed roots, while the adjacent soil matrix remained dry. This indicated that bypassing flow through macropores was actively contributing to lateral subsurface flow. As time progressed, the lateral face became wet, which showed that the greater part of the soil system was contributing to lateral water movement.

The A&Litter soil horizon contributed first and

ultimately the most volume of lateral subsurface flow while the soil profile remained unsaturated. Unsaturated lateral subsurface flow occurred on 13 out of 17 simulated storms in the upper soil horizon. The relationship between soil water potential at 20 cm of soil depth and lateral subsurface flow showed that lateral discharge took place before the soil horizon was saturated for four storms, except for storm 16 (Figure 1). The relationships between soil water potential at 80 cm and lateral subsurface flow showed that lateral subsurface flow occurred after the soil was saturated (Figure 1). Unsaturated lateral subsurface flow occurred during all 17 storms despite 70 % of the tensiometers showing negative soil water potentials. The rest 30 % of the tensiometers showed positive soil water potentials, although most of these tensiometers were placed at 80 cm and most lateral subsurface flow was initially observed in the upper subsurface flow collectors.

Thomas and Phillips (1979), Jardine et al. (1990), and Andreini and Steenhuis (1990) also reported evidence on the contribution of macropore flow under unsaturated soil conditions. These findings are contradictory with the assumptions of potential flow theory and the suggestions of Beven and Germann (1982) and Germann (1986). They reasoned that local saturation must occur before macropores can contribute to water movement. Local saturation can happen in forested soils by the process of rainfall collection on

matted leaves or stones (Jardine et al., 1990). Local soil saturation can also occur at the entrance of most openings of large macropores, which force soil water to move through soil macropores. The hydraulic conductivity of the soil matrix then becomes critical in this process (Bouma et al. 1979; Smettem and Collis-George, 1985 and Kneale, 1985), although Thomas and Phillips (1979), Mosley (1982) and Germann (1986) ruled out the hydraulic conductivity of the soil matrix as a major control on the macropore flow rate.

The lateral or vertical distance between macropores may also be of critical importance if matrix or micropore flow contributes to bypassing flow (Booltink and Bouma, 1991). The rate of water input also affects the enhancement of bypassing flow through macropores (Ehlers, 1975; Hammermeister et al. 1982; Trudgill et al. 1983 and Edwards et al., 1990).

Tensiometer Response to Rainfall Input. The time of response of tensiometers to rainfall input for all storms provides also evidence of bypassing flow (Table IV). Tensiometers placed at 50 or 80 cm of soil depth responded faster 20 % of the time than tensiometers placed at 20 cm of soil depth. Tensiometers placed at 80 cm of soil depth responded faster 35 % of the time than tensiometer placed 50 cm of soil depth. The faster response of tensiometers located at lower locations demonstrates that vertical bypassing flow occurred.

Observations of rhodamine dye during the excavation of the plot following the experiment showed that the ceramic cups of tensiometer were not stained. Hence, the installation procedure did not create artificial soil openings, and consequently it did not contribute to bypassing flow.

The average time response for tensiometers placed at 20 cm soil depth was similar for all rainfalls, except for the tensiometers located in the middle section of the experimental plot. The mean time response of tensiometers placed at 50 and 80 cm soil depths and located at the lower part of the experimental plot was less than those located at the same soil depths in the middle and upper sections of the experimental plot. These observations provide evidence that water was also moving preferentially downslope.

Development of Perched Water Tables. The average time to saturation for all storms was 24, 31 and 42 minutes with a coefficient of variation of 70, 91, and 88 % for the 20, 50 and 80 cm of soil depths, respectively. Rainfall intensity partially explained the variation of the time to saturation (Figure 2) with the high intensities resulting in short time to saturation. As the regression models show, L20 and L80 saturate simultaneously (Figure 2). This could be explained by rapid bypassing flow through macropores.

For simulated storms smaller than 3 cm h^{-1} , perched water tables developed first at L50 and at U20 ($P=0.0001$).

At the middle of the plot, there is no conclusive evidence about which soil depth saturated first. For storms larger than 3 cm h^{-1} , there is no conclusive evidence about which soil depth saturated first for any of the three locations within the experimental plot. Perched water tables developed simultaneously at all soil depths for all three locations of the experimental plot.

The evidence of unsaturated flow in the vertical and lateral directions, the development of perched water tables in addition to visual observations during simulated rainfalls lead us to reject the concept that lateral subsurface flow occurs only when the soil matrix is saturated.

More Evidence on Bypassing Unsaturated Flow

The average soil water depth needed to bring a specific soil depth to saturation was 1.05, 1.05 and 1.43 cm of water with coefficients of variation of 36, 52, and 38 % for 20, 50 and 80 cm of soil depth, respectively. The lower part of the experimental plot had the smallest means of water depth to saturate the soil profile and in particular the 50 cm soil depth, needed the least water depth to become saturated. The 80 cm depth of the upper section needed the largest amount of rainfall to become saturated ($P=0.0001$).

Rainfall intensity partially explained the variation of the water depth needed to saturate the soil zone of the

upper tensiometers (Figure 3). The relationships for the upper and middle part of the experimental plot are reciprocal unlike the one for the lower part, which is linear. For the first two, the amount of water needed becomes nearly constant after 3 cm of simulated rainfall. The linear relationship of L20 does not attain a nearly constant water depth for the range of rainfall intensities studied. Increasing the rate of rainfall input results in an enhancement of bypassing flow, soil moisture moves preferentially via macropores, with less interaction with the soil matrix, hence more water is needed to bring soil water suction to 0. Therefore the rate of soil sorption is a function of rainfall intensity. Less intense rainfalls would result in an equilibrium with the rate of soil sorption. This logic also rejects the assumption of potential flow theory that micropores serve their water needs first.

Development of Potential Profiles

During Simulated Rainfalls

The time sequence of potential profiles during one simulated rainfall event is presented in Figure 4, although results are discussed generally for all simulated storms. Storm 16 was chosen for graphical presentation because it is typical of rainfall intensities and depths in the region, and because the initial soil moisture conditions were the driest in comparison to all of the other simulations.

Individual wetting zones developed at 20, 50 and 80 cm of soil depth for the upper, middle and lower parts of the experimental plot for most simulated storms. Perched water tables developed from the bottom of the sampled soil depths for most storms, which indicated the occurrence of bypassing flow.

Principles of potential flow theory show that individual water tables or wetting fronts will develop under anisotropic flow conditions, where dramatic hydraulic breaks exist between soil horizons (Hillel, 1980, 1982 and Kung, 1990a, 1990b). This is not the case for this experimental plot. The soils showed a gradual change in physical characteristics between the A&Litter, B1, B2, and B3 horizons. There is an abrupt change at the interface between the B3 and C soil horizons. The soil textural analysis showed a steady increase of clay and decrease of sand content with soil depth. Soil bulk density increased steadily with soil depth (Table I).

A gradual decrease of the hydraulic conductivity with soil depth results in dual wetting fronts when the rate of water input is larger than the lowest K_{sat} (Hillel, 1982). The lateral saturated hydraulic conductivity of the experimental plot decreases steadily with soil depth (Navar, 1992). It is probable that the same trend applies for the vertical saturated hydraulic conductivity of the experimental block.

Early in most storms, when the soil was unsaturated, the slope of the potential profile was less than the equilibrium potential gradient, EPG. For storms with drier than average antecedent soil moisture conditions, the slope of the potential profile between 20-50 cm was less than EPG. As rainfall progressed from 0 to 30 minutes, the soil water potential at 50 cm of soil depth increased at a faster rate than that of the 20 cm. The most plausible mechanism for the faster increase of soil water potential at 50 cm is preferential movement of water into the soil and to that depth. For most storms, a perched water table developed quickly at L50 and M50. This occurred with little or no increase of soil water potential at L20 and M20, indicating bypassing flow occurred through an unsaturated surrounding matrix.

For storms with wetter antecedent conditions and higher rates of rainfall input (Figure 5), the slope of the potential profile between 50-80 cm was less than EPG. The rate of soil water potential at 80 increased faster than at 50 cm. Hammermeister et al. (1982), Abdul and Gillham (1984), and Anderson and Burt (1990) pointed out that the conversion of capillary into phreatic water is greater than it would be expected given the specific yield of the soil and the magnitude of the rainfall input.

The final sorption potential profiles nearly attained the slope of the EPG for most storms. Deviations occurred

for some storms and for some areas within the experimental plot. The deviations were likely caused by: 1) the irregular development of perched water tables, and 2) some soil zones remain open to atmospheric pressures.

Development of Potential Profiles during Desorption of Simulated Rainfalls

The time sequence of vertical potential profiles during soil desorption or drainage following rainfall are shown for three positions within the experimental plot (Figure 6). Although the figure shows storm 15, the discussion is based on three simulated storms: 2, 9 and 15. The potential profiles for these storms showed that early in the desorption process, soil at 80 cm depth drains more rapidly in comparison to soil at 50 and 20 cm. Hence, the potential profiles deviated even more from EPG with time. As time progressed, the 50 and 20 cm soil depths desorpted faster than 80 cm. The slope of the potential profile from 50-80 cm of soil depth decreased, although it did not attain the slope of the EPG.

Individual drying zones developed at three soil depths during desorption. After 60 minutes of desorption, three unsaturated zones were found: 1) in the top 12 cm of soil, 2) between 20-35 cm, and 3) between 45-50 cm of soil depth. The drying zones expanded as time progressed. Perched water tables were dropping because of lateral and vertical

drainage. Germann and Beven (1981) suggested that in soil cores a dual drying zones with a saturated soil zone in between would indicate the presence of macropores. Table II shows eight large macropores observed on the lateral face between 15 and 55 cm of soil depth (Table II). Three other macropores were observed to contribute to lateral drainage at the upper part of the A and one at the B1 soil horizons. The position of these large macropores matches the depth of the drainage fronts, which developed during desorption measurements.

Beven and Germann (1982) suggested that bypassing flow occurs through large soil pores or macropores. Soil macropores, larger than 3 mm in diameter, may be formed by roots or root channels (Gaiser, 1952; Whipkey, 1965; Aubertin, 1971; Mosley, 1979, 1982; McDonnell, 1990; Thomas and Phillips, 1979 and Beven and Germann, 1982), worm burrows (Ehlers, 1975; Edwards et al. 1988, 1989, 1990 and 1992), soil pipes or soil fissures or interpedal spaces (Jones, 1971; Tanaka et al., 1988; Bouma et al. 1979; Bouma, 1990; Booltink and Bouma, 1991). Luxmoore (1981), Watson and Luxmoore (1986), Wilson and Luxmoore (1988), and Jardine et al. (1990) suggested that bypassing flow occurs also through mesopores, between 0.11 to 3 mm in diameter.

Rates of Soil Water Adsorption

The rate of change of soil water potential with time

within the first five minutes after tensiometers showed a response to rainfall input was used to estimate a soil water adsorption rate for all storms. The mean adsorption rate for all tensiometers for all storms was 3.40 cm min^{-1} (C.V. of 93.72 %) (Table V). The large coefficient of variation demonstrates that the experimental plot is heterogeneous with soil zones of quick and slow soil water adsorption. M50, L50 and L80 had the greatest rates of soil water adsorption. Tensiometers U50 and U80 had the least means ($P=0.0001$).

The mean rates of water adsorption of tensiometers M50, L50 and L80 were two times greater than that of the other tensiometers. This indicated that soil water was quickly moving into and storing in these soil places. The efficient mechanism of water delivery was explained by the preferential flow input close to these tensiometers. Booltink and Bouma (1991) also found that tensiometers with highest rates of soil water adsorption were located close to or in areas with a large concentration of stained water passageways in soil columns. Tensiometers with low rates of soil water adsorption may indicate diffusion-type of water movement in accordance with the concept of potential flow theory.

Rates of Soil Water Desorption

An initial rate of soil water desorption was calculated

from the time when tensiometers showed a response to desorption to approximately 40 minutes thereafter for all storms. Most tensiometers, except for U50 and U80, showed that desorption commenced between 1 and 5 minutes after rainfall stopped.

The average soil water desorption rate for all storms for all tensiometers was $0.3761 \text{ cm min}^{-1}$ (C.V = 115 %). Tensiometers L80, L50, and L20 showed the greatest average rate of soil water desorption ($P=0.0001$ Table V). Tensiometers L80 and L50 also had the greatest average rates of soil water adsorption. The mean rate of water desorption for these tensiometers was four times larger than the rest of the other tensiometers. The large variation of the rates of soil water desorption indicates rapid drainage by macropores. Booltink and Bouma (1991) also observed that tensiometers, close to soil zones where bypassing flow was taking place, drained at a faster rate than the bulk of the soil volume.

The irregularity of the sorption and desorption fronts, as well as the large variation in the rates of soil water adsorption and desorption among tensiometers lead us to reject hypothesis 2 that potential flow theory applies to our experimental site. The findings support the alternative of bypassing flow.

Flux Density versus Hydraulic Gradient

The relationships between the lateral hydraulic gradients and lateral flux density for the middle and lower set of tensiometers at three soil depths, A&Litter, B2 and B3, for four simulated storms (1, 5, 10, and 16) are presented in Figure 7. The middle part of the experimental plot was considered the inlet of the hydraulic gradient, $(Th_{\text{middle}} - Th_{\text{lower}})/L$ where $Th = \phi_{\text{pressure}} + \phi_{\text{gravity}}$ and $L = \text{Length}$. The relationships include only positive soil water potentials. The differential rising of perched water tables at the middle and lower part of the experimental plot can be explained by 1) the hysteretic loop of the relationships, and 2) the displacement of the figures from the imaginary vertical line which represents the slope of the experimental plot (0.16). The development of the hydraulic gradient and the displacement of the figures to the left of 0.16 was the result of higher perched water tables at the lower than at the middle part of the experimental plot.

The lateral flux density was independent of the hydraulic gradient since the average amount of soil water potential displayed during desorption was 31 % less than the amount of soil water potential displayed during the rising of the perched water tables for equivalent flux densities. Perched water tables still remained in the experimental plot after lateral discharge stopped.

The lateral saturated hydraulic conductivity and its behavior with soil depth cannot be estimated by plotting

flux density against the hydraulic gradient at different elevations of a perched water table. This approach would have estimated a variable saturated hydraulic conductivity with sorption and desorption processes.

These observations indicate that lateral flux density does not meet the main assumptions of potential flow theory and lead us to reject hypothesis 3 and they probably support the probable alternative that lateral water movement obeys inertial gradients. Germann and Beven (1981) and Beven and Germann (1982), and Germann (1990a, 1990b) suggested that macropore flow is enhanced by gravitational gradients. Macropores do not need to be open to atmospheric pressures to transport water (Thomas and Phillips, 1979). Thomas and Phillips (1979) suggested that positive soil water potentials develop inside the soil which push water into the macropore system.

Because the irregularity of the wetting and drying fronts, the instability of the hydraulic gradients, and the evidence on unsaturated flow, other approaches, in addition to potential flow theory, should be used to predict water movement. Beven and Germann (1981) proposed a dual model based on macropore and micropore flow, with both systems working at a macroscopic scale. The importance of both systems to the overall water movement lies in the relative contribution of macropores and micropores. Although they may not contribute independently to water movement (Beven and

Germann, 1981; Jardine et al. 1991). Germann (1990a, 1990b) proposed another model of water movement in macroporous soils based on kinematic wave theory, which decouples capillary and gravity forces.

Conclusions

This report showed evidence on:

- 1) The wetting and desorpting fronts of the experimental plot were highly irregular.
- 2) The relationship between the lateral hydraulic gradient and lateral flux density was not monotonic.
- 3) Perched water tables raised from the bottom of all sampled soil depths at all places within the experimental plot.
- 4) Lateral unsaturated flow was common at the upper, most responsive, soil horizons.
- 5) The amount of water depth needed to bring a particular soil depth to saturation, the rate of soil water adsorption and desorption were related to rainfall intensity.

These findings and visual observations during the experimental rainfalls demonstrate the importance of bypassing flow in the experimental plot and rejects the hypothesis of potential flow. The relative importance of bypassing flow in comparison to matrix flow or potential flow is of critical importance to water movement.

References

- Abdul, A.S., and Gillham, R.W. 1984. Laboratory studies of the effects of the capillary fringe on streamflow generation. *Water Resources Research* 20:691-698.
- Anderson, M.G., and Burt, T.P. 1978. The role of topography in controlling throughflow generation. *Earth Surface Processes* 3:331-344.
- Anderson, M.G., and Burt, T.P. 1990. Subsurface Runoff processes. *In*: M.G. Anderson and T.P. Burt (Eds). *Process Studies in Hillslope Hydrology*. Chapter 11: 365-400. John Wiley & Sons Ltd. New York.
- Andreini, M.S. and Steenhuis, T.S. 1990. Preferential paths of flow under conventional and conservation tillage. *Geoderma* 46:85-102.
- Aubertin, G.M. 1971. Nature and extent of macropores in forest soils and their influence on subsurface water movement. *Forest Service Paper NE*, 192 PS.
- Beasley, R.S. 1976. Contribution of subsurface flow from the upper slopes of forested watersheds to channel flow. *Soil Science Society of America Journal* 40:955-957.
- Beven, K. and Germann, P. 1981. Water flow in soil macropores. II. A combined flow model. *Journal of Soil Science* 32:15-29.
- Beven, K. and Germann, P. 1982. Macropores and water flow in soils. *Water Resources Research* 18:1311-1325.
- Booltink, H.W.G. and Bouma, J. 1991. Physical and morphological characterization of bypass flow in a well-structured clay soil. *Soil Science Society of America Journal* 55:1249-1254.
- Bouma, J. 1990. Using morphometric expressions for macropores to improve soil physical analyses of field soils. *Geoderma* 46:3-11.
- Bouma, J., Jongerius, A. and Schoonderbeek, D. 1979. Calculation of saturated hydraulic conductivity of some pedal clay soils using micromorphometric data. *Soil Science Society of America Journal* 43:261-264.
- Cassel, D.K., and Klute, A. 1986. Water potential:tensiometry. *In*: A. Klute (Ed) *Methods of Soil Analysis, Part I*. 2nd ed. *Agronomy* 563-596.

- DeVries, J. and Chow, T.L. 1978. Hydrologic behavior of a forested mountain soil in coastal British Columbia. *Water Resources Research* 14:935-942.
- DeWitt, J.N., and Steinbrenner, E.C. 1981. Central Arkansas Soil Survey. Weyerhaeuser Co. Tacoma, WA.
- Edwards, W.M., Norton, L.D. and Redmond, C.E. 1988. Characterizing macropores that affect infiltration into nontilled soil. *Soil Science Society of America Journal* 52:483-487.
- Edwards, W.M., Shipitalo, M.J. Owens, L.B. and Norton, L.D. 1989. Water and nitrate movement in earthworm burrows within long-term no-till cornfield. *Journal of Soil and Water Conservation* 25:240-243.
- Edwards, W.M., Shipitalo, M.J. Owens, L.B. and Norton, L.D. 1990. Effect of Lumbricus terrestris L. burrows on hydrology of continuous no-till corn fields. *Geoderma* 46:73-84.
- Edwards, W.M., Shipitalo, M.J., Dick, W.A. and Owens, L.B. 1992. Rainfall intensity affects transport of water and chemicals through macropores in no-till soil. *Soil Science Society of America Journal* 56:52-58.
- Ehlers, W. 1975. Observations on earthworm channels and infiltration on tilled and untilled loess soil. *Soil Science* 119:242-249.
- Gaiser, R.N. 1952. Root channels and roots in forest soils. *Soil Science Society of America Proceedings* 40:62-65.
- Germann, P.F. 1986. Rapid drainage response to precipitation. *Hydrological Processes* 1:3-13.
- Germann, P.F. 1990a. Macropores and hydrologic hillslope processes. In: *Process Studies in Hillslope Hydrology*. M.G. Anderson and T.P. Burt. (Eds). Chapter 10: 327-363. John Wiley & Sons Ltd. New York.
- Germann, P.F. 1990b. Preferential flow and the generation of runoff. 1. Boundary layer flow theory. *Water Resources Research* 26:3055-3063.
- Germann, P.F. and Beven, K. 1981. Water flow in soil macropores. I. An experimental approach. *Journal of Soil Science* 32:1-13.

- Hammermeister, D.P., Kling, G.F. and Vomocil, J.A. 1982. Perched water tables on hillsides in western Oregon. II. Preferential downslope movement of water and anions. *Soil Science Society of America Journal* 46: 819-826.
- Hillel, D. 1980. *Fundamentals of Soil Physics*. Academic Press, Inc. New York.
- Hillel, D. 1982. *Introduction to Soil Physics*. Academic Press, Inc. New York.
- Jardine, P.M., Wilson, G.V. and Luxmoore, R.J. 1990. Unsaturated transport through a forest soil during rain storm events. *Geoderma* 46:103-118.
- Jones, J.A.A. 1971. Soil piping and stream channel initiation. *Water Resources Research* 7:602-610.
- Kneale, W.R. 1985. Observations of the behaviour of large cores of soil during drainage, and the calculation of hydraulic conductivity. *Journal of Soil Science* 36: 163-171.
- Kung, K-J.S. 1990a. Preferential flow in a sandy vadose zone: 1. Field observation. *Geoderma* 46:51-58.
- Kung, K-J.S. 1990b. Preferential flow in a sandy vadose zone: 2. Mechanisms and implications. *Geoderma* 46:59-71.
- Luxmoore, R.J. 1981. Comments on micro, meso and macroporosity of soil. *Soil Science Society of America Journal* 45:671-672.
- Luxmoore, R.J., Jardine, P.M., Wilson, G.V., Jones, J.R. and Zelazny, L.W. 1990. Physical and chemical controls of preferred path flow through a forested hillslope. *Geoderma* 46:139-154.
- McDonnell, J.J. 1990. A rationale for old water discharge through macropores in a steep humid catchment. *Water Resources Research* 26: 2821-2832.
- Mein, R.G., and Larson, C.L. 1973. Modeling infiltration during a steady rain. *Water Resources Research* 9:384-394.

- Miller, E.L., Beasley, R.S., and Lawson, E.R. 1988. Forest Harvest and site preparation effects on stormflow and peakflow of ephemeral streams in the Ouachita Mountains. *Journal of Environmental Quality* 17:212-218.
- Mosley, M.P. 1979. Streamflow generation in forested watersheds, New Zealand. *Water Resources Research* 15: 795-806.
- Mosley, M.P. 1982. Subsurface flow velocities through selected forest soils, south island, New Zealand. *Journal of Hydrology* 55:65-92.
- Mulholland, P.J., Wilson, G.V. and Jardine, P.M. 1990. Hydrogeochemical response of a forested watershed to storms: effects of preferential flow along shallow and deep pathways. *Water Resources Research* 26:3021-3036.
- Pearce, A.J., Stewart, M.K., and Sklash, M.G. 1986. Storm runoff generation in humid headwater catchments: 1. Where does the water come from. *Water Resources Research* 22:1263-1272.
- Pilgrim, D.H., Huff, D.D., and Steele, T.D. 1978. A field evaluation of surface and subsurface runoff. 2, Runoff processes. *Journal of Hydrology* 38:319-341.
- Richard, T.L. and Steenhuis, T.S. 1988. Tile drain sampling a preferential flow on a field scale. *In*: P.F. Germann (Ed). *Rapid and Far-reaching Hydrologic Processes in the Vadose Zone*. *Journal of Contaminant Hydrology* 3: 307-325.
- Sklash, M.G. 1990. Environmental isotope studies of storm and snowmelt runoff generation. *In*: M.G. Anderson and T.P. Burt (Eds). *Process Studies in Hillslope Hydrology* Chapter 12:401-435. John Wiley & Sons Ltd. New York.
- Sklash, M.G. Stewart, M.K. and Pearce, A.J. 1986. Storm runoff generation in humid headwater catchments. II: A case of study of hillslope and low order stream response. *Water Resources Research* 22:1273-1282.
- Smettem, K.R.J. and Collis-George, N. 1985. Prediction of steady-state ponded infiltration distributions in a soil with vertical macropores. *Journal of Hydrology* 79:115-122.

- Tanaka, T., Yasuhara, M., Sakai, H. and Marui, A. 1988. The Hachioji experimental basin study: storm runoff processes and the mechanism of its generation. In: R.L. Bras, M. Hino, P.K. Kitanidis and K. Takeuchi (Eds), Hydrologic Research: The U.S-Japan Experience. Journal of Hydrology 102:139-164.
- Thomas, G.W. and Phillips, R.E. 1979. Consequences of water movement in macropores. Journal of Environmental Quality 18:149-152.
- Trudgill, S.T., Pickles, A.M. and Smettem, K.R.J. 1983. Soil-water residence time and solute uptake, 2. Dye tracing and preferential flow predictions. Journal of Hydrology 62:279-285.
- Turton, D.J., Haan, T.C. and Miller, E.L. 1992. Subsurface flow responses of a small forested catchment in the Ouachita Mountains. Hydrological Processes 6:111-125.
- U.S.D.A. Forest Service. 1964. Special soil survey report of Alum Creek Experimental Forest Ouachita National Forest, Sabine County, AR.
- Whipkey, R.Z. 1965. Subsurface stormflow from forested watersheds. Bulletin International Association Scientific Hydrology 10:74-85.
- Watson, K.W. and Luxmoore, R.J. 1986. Estimating macroporosity in a forest watershed by use of a tension infiltrometer. Soil Science Society of America Journal 50:578-582.
- Wilson, G.V. and Luxmoore, R.J. 1988. Infiltration and macroporosity distributions on two forested watersheds. Soil Science Society of America Journal 52:329-335.

TABLE I

SOIL DESCRIPTION, TEXTURAL AND SOIL BULK DENSITY ANALYSIS, AND THE LOCATION OF TENSIO-METERS AND SUBSURFACE FLOW COLLECTORS WITHIN THE EXPERIMENTAL PLOT

Soil Pro- file	Soil Depth (cm)	Soil Description	Soil Sand (%)	Texture Clay (%)	Silt (%)	Soil Bulk Density (grcm ⁻³)	Ten- sio- meter	Subsur- face Colle- ctor
01	2.5-3.5	Forest litter						
02	0.0-2.5	Mull layer of partially de- composed organic matter						
A1	0.0-2.5	Pale brown(10YR 6/3) loam						
E	2.5-10	Light yellowish (10YR 6/4)loam						
Bt1	10 -22	Yellowish brown (10YR 5/6)	19.7	34.4	45.9	1.31	20	YES
Bt21	23 -43	Yellowish brown (10YR 5/8)	32.7	24.7	42.8	1.47		YES
Bt22	43 -63	Yellowish brown (10YR 5/8)clay					50	YES
B3	63 -81	Mottled red clay	39.7	17.8	42.5	1.60	80	YES
C	81-102	Moderately weathered shale rock and clay soil material						

The description of soil profiles was carried out by USDA Forest Service (1964). The textural and soil bulk density analysis was carried out by the author.

TABLE II
LARGE SOIL MACROPORES OBSERVED AT THE LATERAL FACE CROSS
SECTIONAL AREA OF THE EXPERIMENTAL PLOT

Coordinates		Diameter	Characteristics
Lateral (cm)	Vertical (cm)	(cm)	
12	48	1.0-0.8	Root channel, some bark lining
26	49	2.6-1.7	Root channel, bark lining decayed
44	47	2.2-1.8	Root channel, decayed lining
43	15	0.8	Root channel, still filled with decayed wood
137	41	1.5-1.3	Root channel, some bark lining
135	23	0.8-0.6	Root channel, bark lined
170	40	2.8-2.2	Root channel, decayed organic inside new root growing inside
114	55	1.1-1.0	Root channel, new root growing inside

TABLE III
SOME CHARACTERISTICS OF SIMULATED RAINFALLS

RUN	DATE	RAIN AMOUNT (cm)	C.V (%)	SIMULATION TIME (hrs)	RAIN INTENSITY (cm/h)	RETURN PERIOD (years)
1	07/17/91	8.26	68	1.22	6.80	20.00
2	07/24/91	5.64		0.90	6.27	4.00
3	07/25/91	6.12	22	0.82	7.49	5.00
4	07/31/91	8.41	22	1.55	5.43	10.00
5	08/01/91	7.63	25	1.67	4.58	6.00
6	08/02/91	6.70	14	1.55	4.32	5.00
7	08/06/91	6.47	27	2.00	3.23	3.00
8	08/07/91	5.79	18	1.75	3.31	3.00
9	08/08/91	5.37	14	1.92	2.80	1.50
10	08/28/91	4.78	17	3.00	1.59	1.00
11	08/29/91	4.46	10	2.75	1.62	1.00
12	08/30/91	4.65	15	2.75	1.69	1.00
13	09/10/91	5.08	29	2.75	1.85	1.00
14	09/11/91	6.26	16	2.33	2.68	2.00
15	09/12/91	5.77	17	2.17	2.66	1.80
16	10/08/91	4.42	12	4.25	1.04	1.00
17	10/09/91	4.04	21	3.08	1.31	1.00

Note the coefficient of variation was estimated from 11 rain cans on the experimental plot.

TABLE VI
THE TIME OF TENSIOMETER RESPONSE TO RAINFALL INPUT
FOR 17 SIMULATED STORMS

RUN #	L20	L50	L80	M20	M50	M80	U20	U50	U80
	(minutes)								
1	11	4	5	10	9	10	6	3	3
2	4	3	7	8	10	15	2	14	4
3	5	5	6	5	9	7	3	3	4
4									
5	8	5	7	8	17	16	8	6	11
6	11	11	10	9	24	17	9	10	17
7	7	8	17	17	20	25	4	6	12
8	6	11	16	12	15	20	11	12	24
9	12	15	17	11	25	16	8	15	31
10	9	5	5	85	85	65	10	35	50
11	10	12	21	22	32	23	12	29	22
12	12	11	21	19	40	30	13	32	27
13	6	13	33	33	36	37	11	38	33
14	10	14	9	11	26	7	5	8	20
15	8	12	14	14	26	4	6	11	14
16	3	3	34	3	4	7	3	60	120
17	7	2	12	8	14	6	8	31	38
Mean	8	8	15	17	25	19	7	20	27
C.V.(%)	34	51	60	110	76	78	45	80	101

TABLE V
 THE AVERAGE MEAN SORPTION AND DESORPTION RATES
 FOR NINE TENSIOMETERS FOR 17 SIMULATED
 RAINFALLS IN THE EXPERIMENTAL
 PLOT IN ARKANSAS

Tensio meter Code	Sorption		Desorption	
	Mean (cmm ⁻¹)	C.V (%)	Mean (cmm ⁻¹)	C.V (%)
U20	3.24 ^{bc}	100	-0.12 ^a	37
U50	1.80 ^{cd}	101	-0.2a ^b	33
U80	0.79 ^d	65	-0.18 ^a	33
M20	2.47 ^{cd}	149	-0.13 ^a	41
M50	5.53 ^{cd}	74	-0.15 ^a	36
M80	2.94 ^c	62	-0.29 ^{ab}	31
L20	2.87 ^c	60	-0.38 ^b	50
L50	5.03 ^a	45	-0.67 ^c	55
L80	5.93 ^a	57	-1.24 ^d	50

Means with the same letter are not significantly different

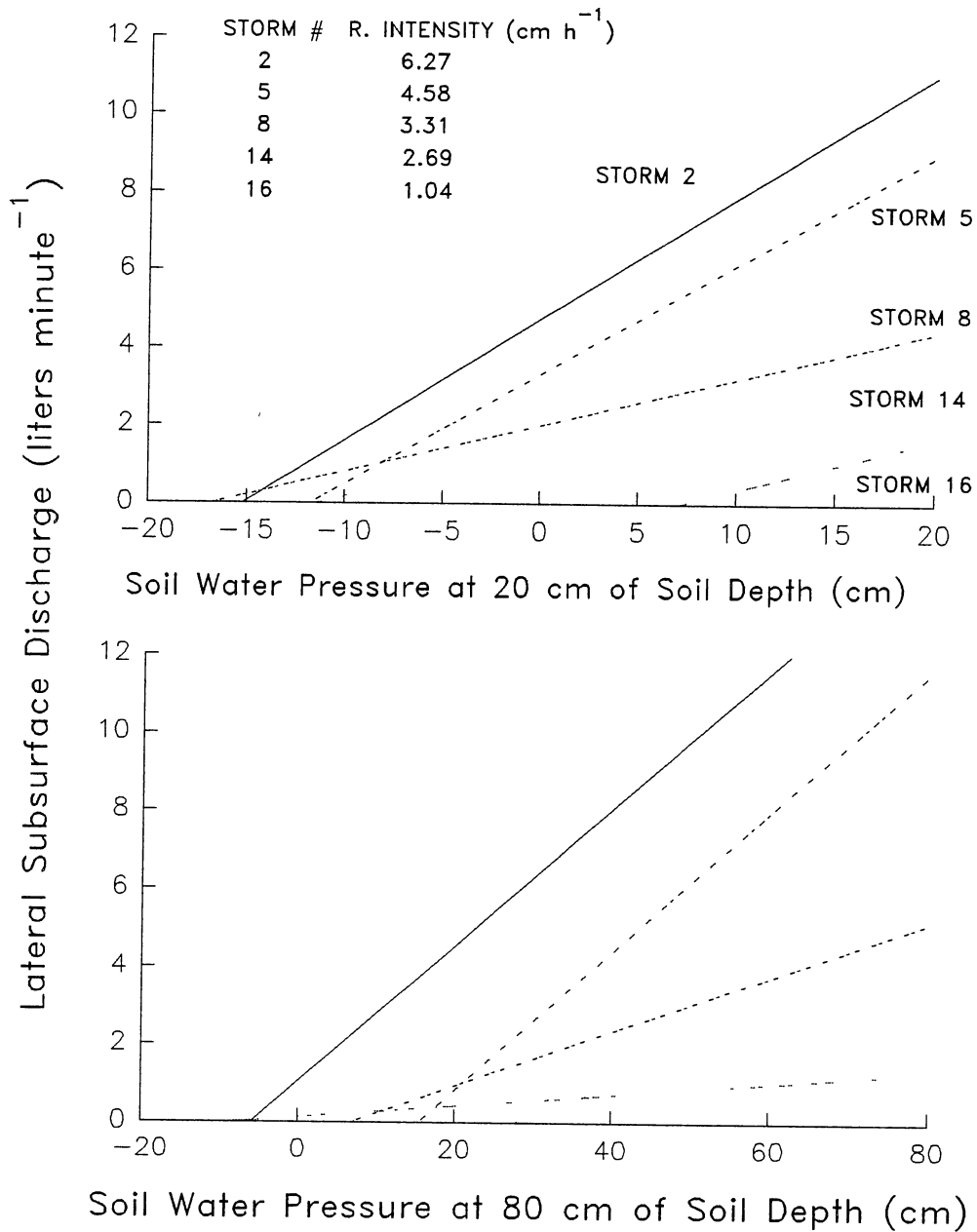


Figure 1. The Linear Relationships between Soil Water Potential and the rate of Lateral Discharge within the Experimental Plot in Arkansas.

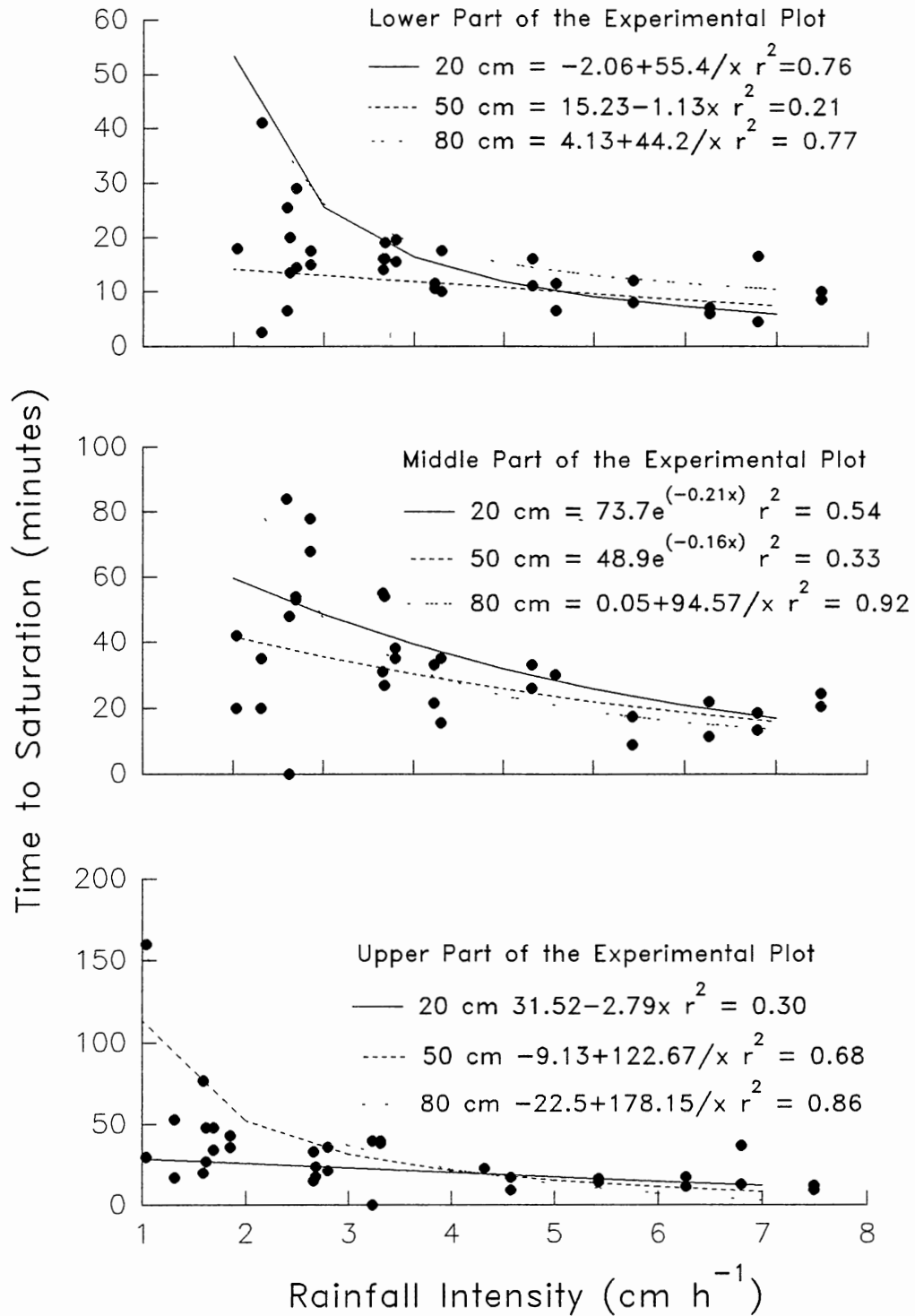


Figure 2. The Regression Models for Rainfall Intensity and the Time to Saturation for three Soil Depths at three Locations within the Experimental Plot.

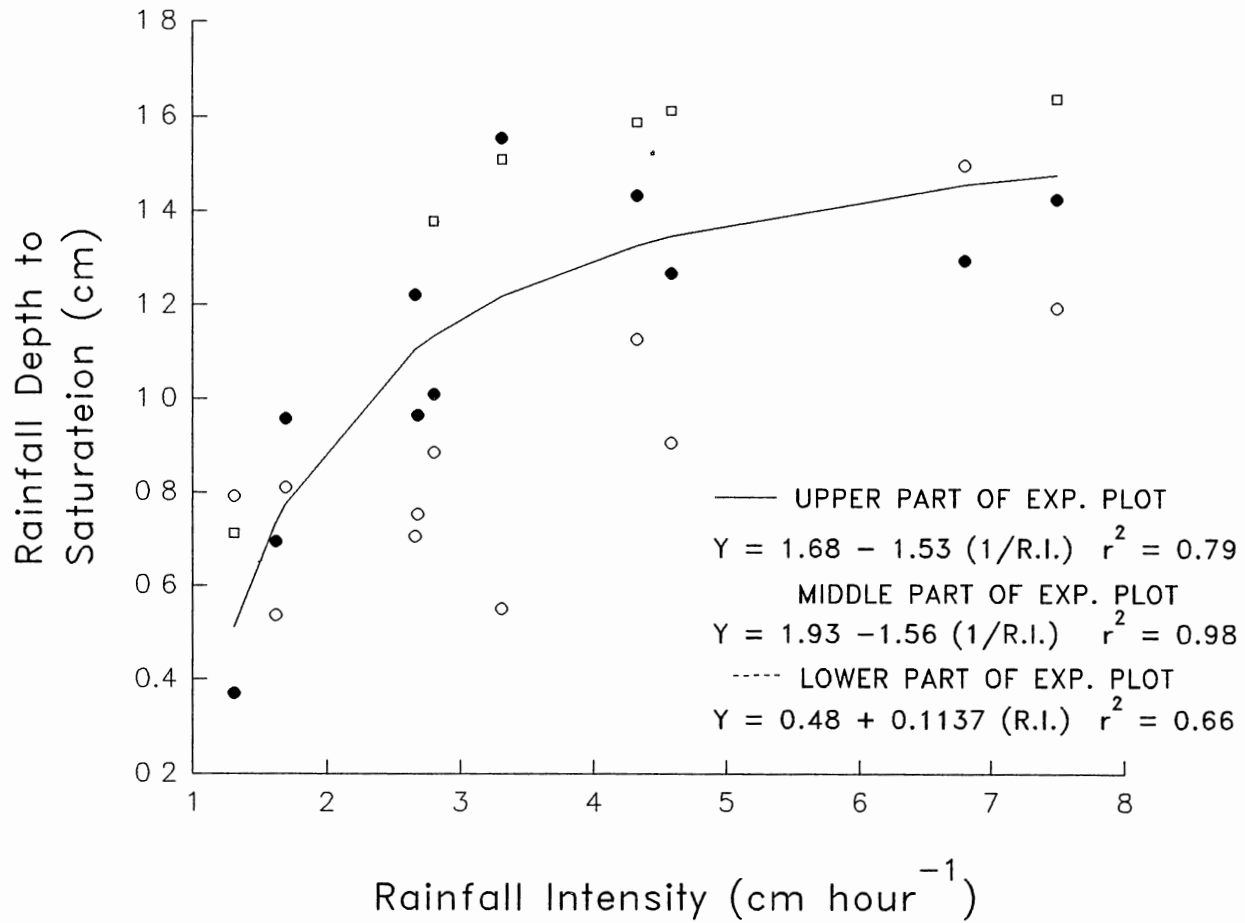


Figure 3. The Dependence of the Rainfall Depth to Saturate a Particular Soil Place on Rainfall Intensity.

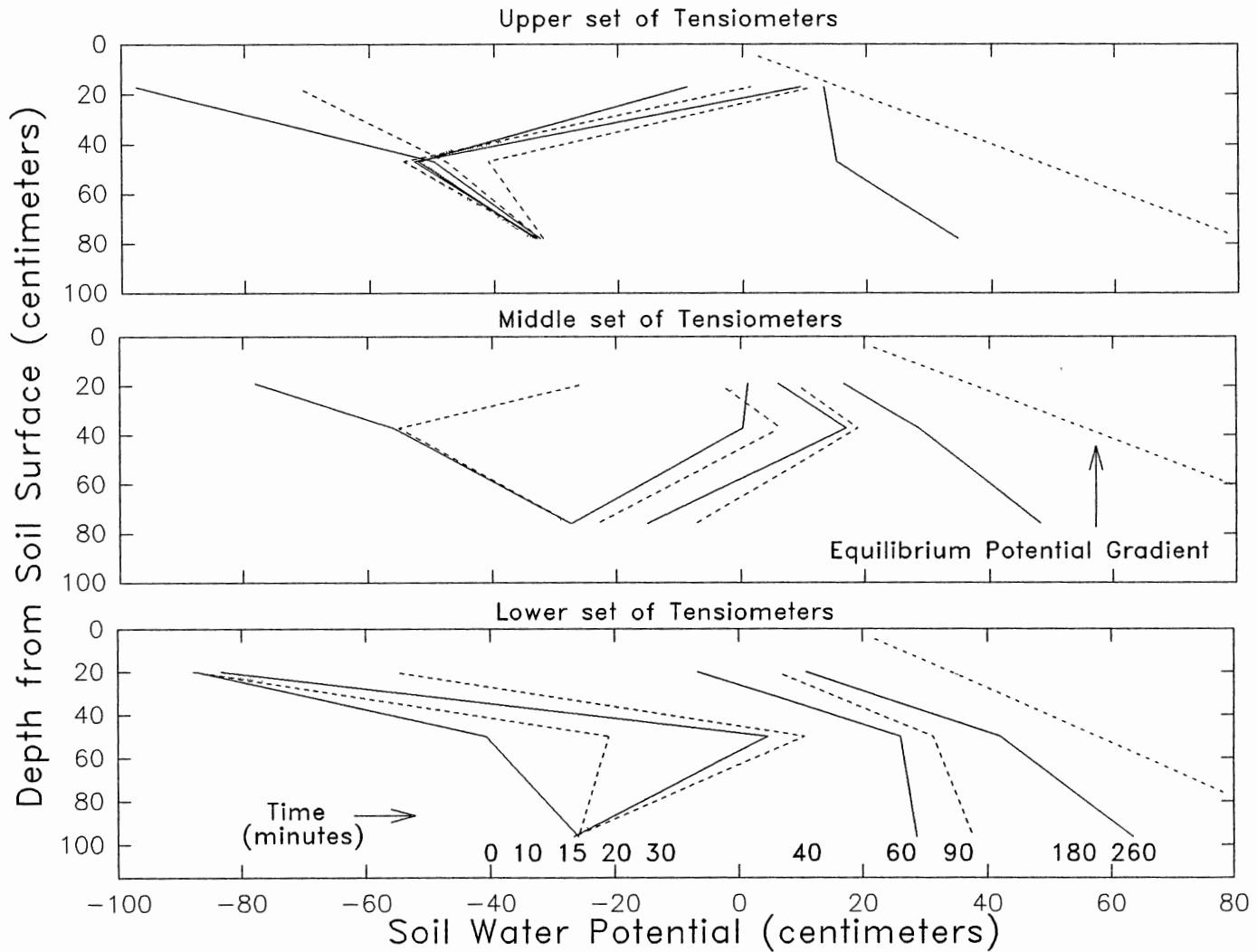


Figure 4. The Development of Vertical Potential Profiles during Sorption Experiments in the Experimental Plot in Arkansas for Rainfall 16.

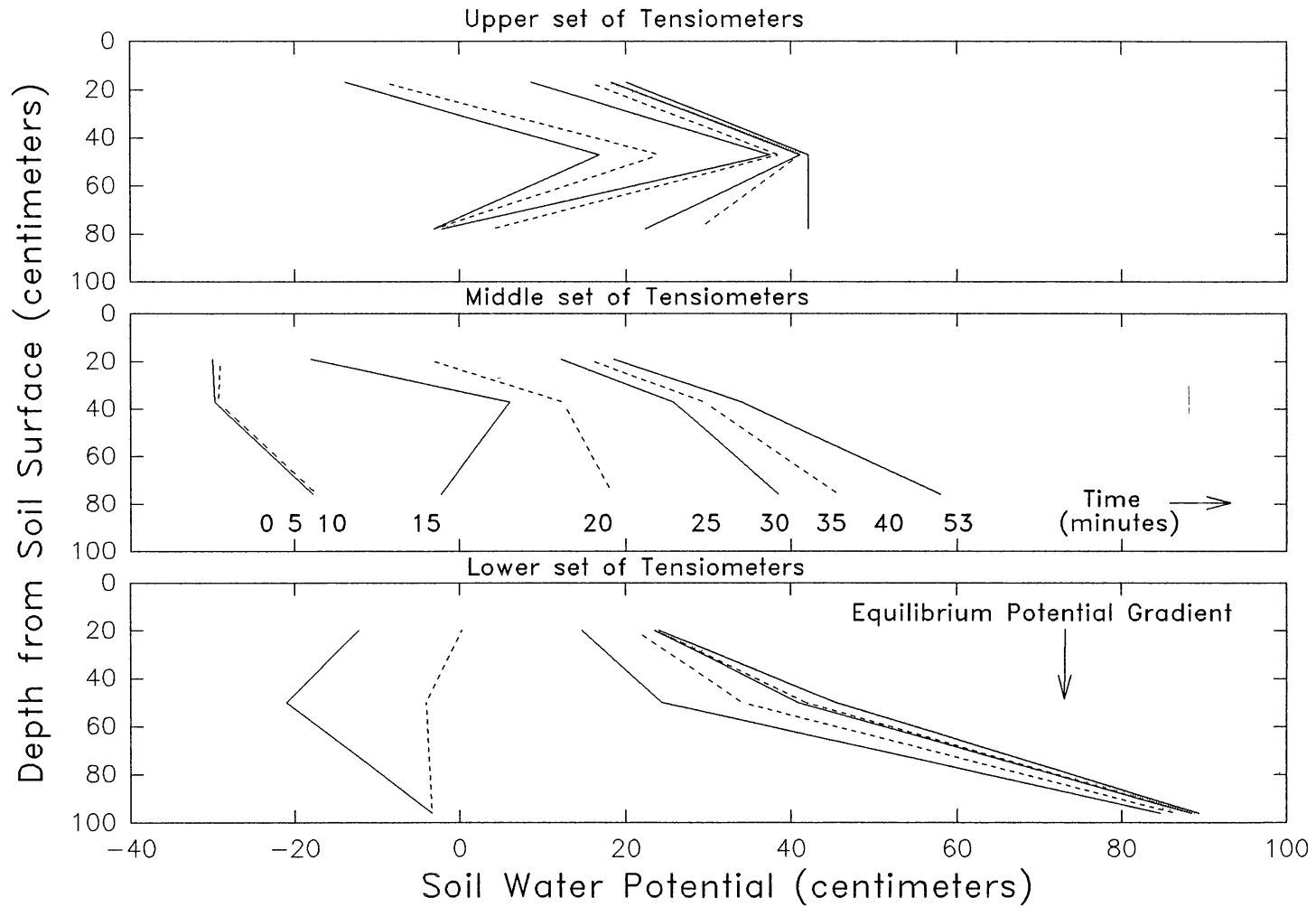


Figure 5. The Development of Vertical Potential Profiles during Sorption Experiments in the Experimental Plot in Arkansas for Rainfall 2.

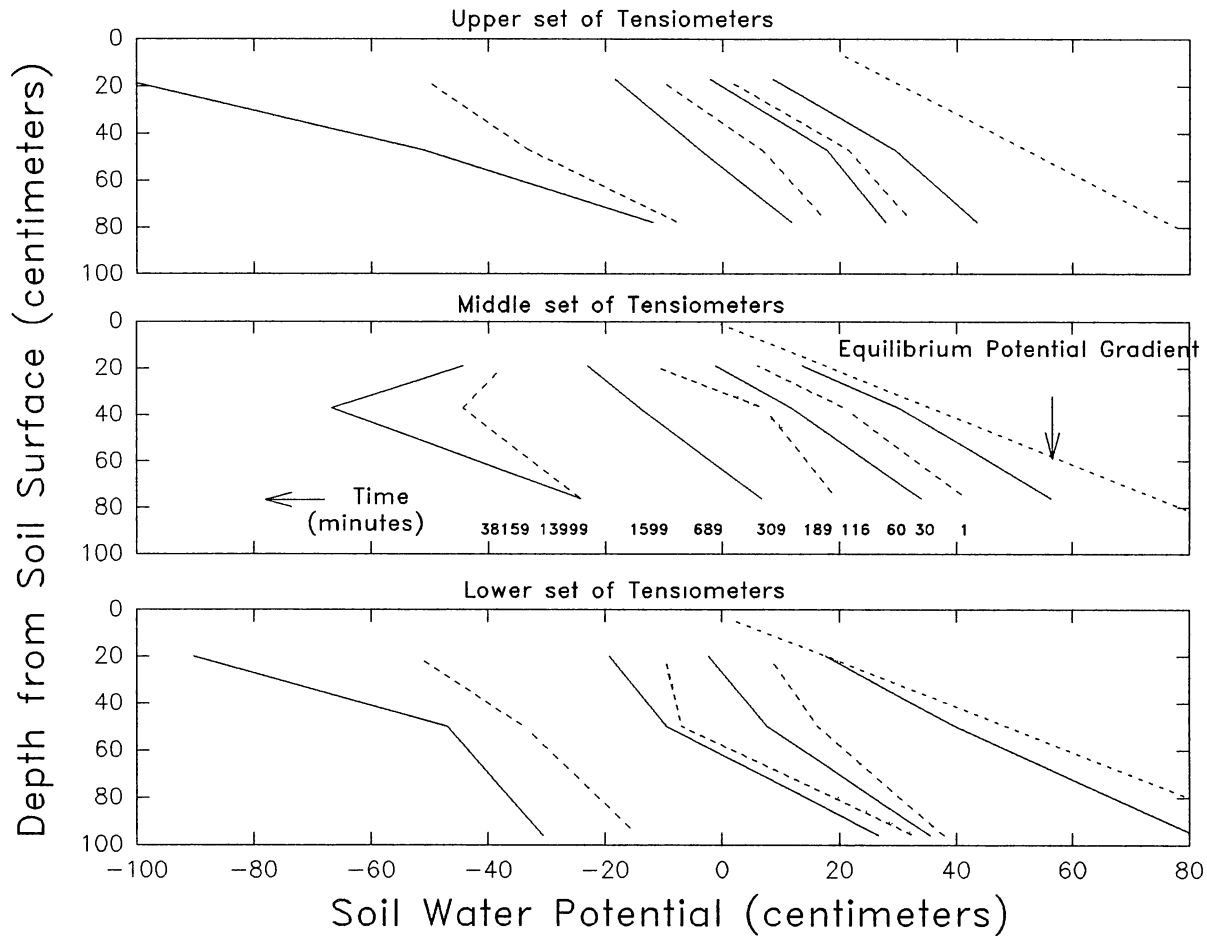


Figure 6. The Development of Vertical Potential Profiles during Desorption Experiments in the Experimental Plot in Arkansa for Rainfall 15.

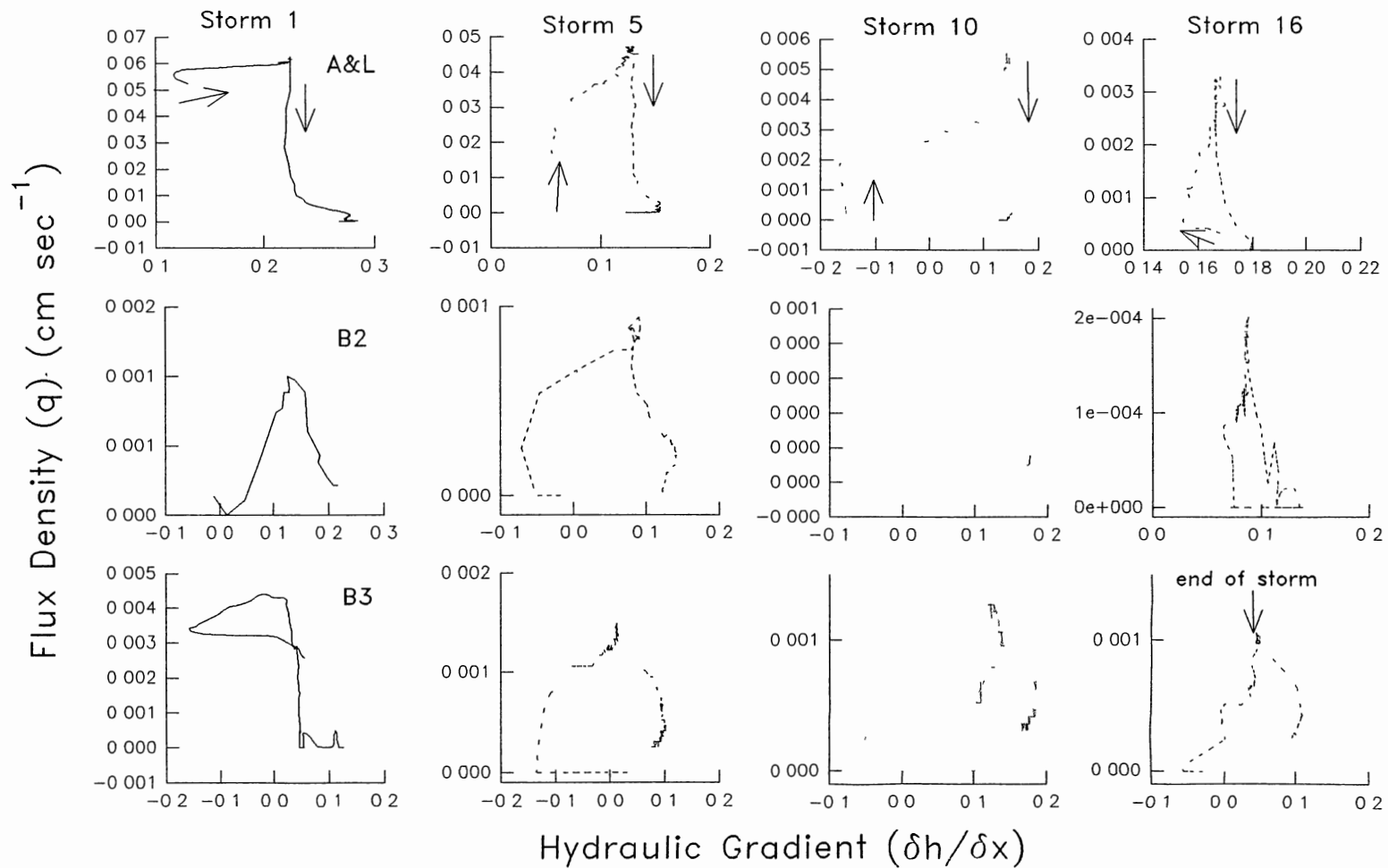


Figure 7. The Relationships between the Hydraulic Gradient and Flux Density for three Soil Horizons for four Simulated Rainfalls of different Durations and Intensities (Arrows indicate the time progression during the storm).

CHAPTER VI

MACROPORE AND MATRIX FLOW IN AN EXPERIMENTAL PLOT IN ARKANSAS

José De Jesús Návar*, Donald J. Turton, and Edwin L. Miller⁶

Abstract

Current approaches to model subsurface flow include a macroscopic flow velocity vector for matrix and macropores. This study was conducted to determine the relative importance of macropore and matrix flow. Lateral water fluxes and soil water potentials, as well as rhodamine dye traces were observed in an isolated experimental plot in the Ouachita Mountains of Central Arkansas during simulated rainfall experiments. Rainfalls were simulated 17 times during the period of July 17 to October 10 of 1991. In all rainfalls, initial soil water potentials were less than 100 cm of water. Lateral macropore space and macropore and matrix flow were estimated from lateral desorption

⁶J. De Jesús Návar, Dept of Ciencias Forestales, Universidad Autónoma de Nuevo León, Apartado Postal # 136, Linares, N.L. 67700 México. E.L. Miller and D.J. Turton, Dept of Forestry, Oklahoma State Univ., Stillwater OK 74078. *Corresponding Author.

measurements. The maximum active lateral macropore space was approximately $0.006 \text{ (cm}^3 \text{ cm}^{-3}\text{)}$. Maximum estimated lateral macropore and matrix flow were 0.041 and $0.00066 \text{ cm sec}^{-1}$, respectively. Active macropore space and macropore flow were not constant among storms. Rainfall intensity and soil water potential explained part of the variation. The relationship between the rate of macropore flow and soil water potential deviated from linearity, which demonstrates that macropores were actively desorpting. Rhodamine dye experiments indicated that water was moving preferentially laterally at the interface of the A&B1 soil horizons through roots and root channels. Several dyed soil traces were along worm and ant burrows and root channels continued vertically into the B2, B3 and C soil horizons.

Key Words: Lateral Subsurface Flow, Lateral Desorption, Macropore Flow, Matrix flow.

Introduction

Increased evidence that macropore flow can produce stormflow in undisturbed forested watersheds (Whipkey, 1965; Beasley, 1976; Mosley, 1979, 1982; McDonnell, 1990; Anderson and Burt, 1990), in addition to its related environmental processes have motivated new trends in forest hydrology research.

Macropore flow, bypassing flow, preferential flow or short circuit flow has been empirically observed in forest

soils and agricultural soils under tillage and zero tillage operations, as well as in soil columns and soil cores (Beven and Germann, 1981; Whipkey, 1965; Jones, 1971; Aubertin, 1971; Beasley, 1976; Pilgrim et al. 1978; Mosley, 1979, 1982; Germann, 1986; Kemper et al. 1987; Andreini and Steenhuis, 1990; McDonnell, 1990; Mulholland et al. 1990; Booltink and Bouma, 1991 and Edwards et al. 1988, 1989, 1990, 1992).

Macropores allow water to quickly bypass the entire soil matrix (Thomas and Phillips, 1979; Beven and Germann, 1982; Germann 1990a, 1990b). Hence, the empirically derived law of Darcy and Richard's model, based on potential flow theory, do not apply to macroporous soils (Germann, 1990a, 1990b).

Germann (1990a, 1990b) predicted lateral subsurface flow in macroporous soils using kinematic wave theory. Other approaches to model subsurface flow through macropores require information on the number, diameter and length of macropores. The measurement of these parameters involves intensive and detailed experiments. Omoti and Wild (1979), Bouma et al. (1979), Bouma (1990), and Booltink and Bouma, 1991) used solute markers to determine macropore morphology in soil cores. Germann and Beven (1981) and Kluitenberg and Horton (1990) estimated macropore space in soil cores by using potential flow theory. One weakness of these approaches is the small size of the soil cores used.

Macropore flow has been observed in root channels (Aubertin, 1971; DeVries and Chow, 1978 and Mosley, 1979, 1982) and worm burrows (Ehlers, 1975; Edwards et al. 1988, 1989; 1990; 1992). Watson and Luxmoore (1986) and Wilson and Luxmoore (1988) used a tension infiltrometer to measure macropore flow. However, estimations of macropore space and macropore flow from larger soil blocks in the field are lacking.

The objectives of this report were: 1) to estimate macropore space and macropore flow, and 2) to estimate matrix flow from the desorption phase of the experiment on an experimental soil block in the Ouachita Mountains of Arkansas.

Materials and Methods

The Study Area

An experimental plot was established 35 miles north of Hot Springs, Arkansas, on the U.S Forest Service Alum Creek Experimental Forest in the Ouachita Mountains of Arkansas. The mountains were formed as a result of the Ouachita Orogeny, in the Late Paleozoic Era. Sedimentary rocks (sandstones, shales, limestones and conglomerates) were folded and faulted in the east-west orientation, due to northerly compressive forces (US Forest Service, 1964). The soils on the Alum Creek experimental watersheds are classified by the USDA Forest Service as the Alemance

associations (Typic Hapludults). DeWit and Steinbrenner (1981) classified the soil as the Sandlick Series. The slope of the experimental plot was 16 %. The soil description of the area, textural and bulk density analyses and the location of tensiometers and subsurface flow collectors are reported in Table I.

The vegetation of the Alum Creek Watersheds is classified as an association of Loblolly- Shortleaf pine, Pinus taeda-Pinus echinata and hardwoods, Quercus alba, Quercus rubra, Cornus florida, Acer rubrum, Carya spp and Nyssa silvatica.

The climate of the area is temperate-humid with an annual average temperature of 74.3° F; ranging from 52.7° F in January and 93.2° F in August. The mean annual precipitation is 1250 mm of which 33 % occurs during April through June. The wettest month of the year is April with 153 mm and the driest is October with 90 mm. There is no well defined dry season, however summer precipitation is highly variable and high rates of summer evapotranspiration cause frequent soil moisture deficits.

The Experimental Plot

An experimental plot 6.3 m in length by 2.05 m in width, with a 0.5 m buffer strip zone on each side, was hydrologically isolated by digging a trench down to the C soil horizon (0.90 to 1.1 meters). The side and upslope

walls were sealed with polyethylene sheets, while the lower wall was left uncovered for sample collection and observations during the storms. Perforated pipes were layed at the bottom of the upper and two side trenches and covered with 35 cm of gravel to allow drainage around the experimental plot. The remainder of the trench was filled with the original soil to provide support to the experimental block. The site was cleared of all shrubby and large trees to eliminate transpiration.

The experimental plot was instrumented with three sets of tensiometers and four subsurface flow collectors. A rainfall simulator was constructed to supply rainfall to the plot and the buffer area. A tarp was also set up at approximately 1.80 m height to prevent direct throughfall into the experimental plot.

Subsurface Flow Collectors

The system to measure subsurface flow at the lower open cross sectional area, 13630 cm^3 , of the experimental plot was constructed as described by Turton et al. (1992). The subsurface collection system consisted of four troughs placed at 14, 26, 44 and 67 cm of soil depth. The first trough collected water from the Litter, A and E soil horizons, 2680 cm^2 , the second and third troughs from the B1, 2375 cm^2 and B2, 3870 cm^2 , soil horizons, and the last one from the interface between the B and C soil horizons,

4710 cm². To avoid soil crumbling from the open lateral face, galvanized wire screen was used. Before the installation of the subsurface flow collection system, the largest lateral soil macropores were mapped (Table II).

Troughs were constructed by cutting 0.11 X 2.1 m PVC drain pipe in half lengthwise. Polyethylene sheeting was inserted horizontally into the soil to approximately 5 cm to direct collected subsurface flow from soil horizons into the troughs. Flow collected from each through was drained into a recording individual tipping bucket. A data logger (Campbell Scientific 21X) recorded the number and time of tips for each tipping bucket.

Soil Water Potentials

Soil water potential was measured with pressure transducers and mercury-water manometers connected to custom-made tensiometers. The tensiometers were constructed following the design of Cassel and Klute (1986). Eighteen tensiometers were installed in the fall of 1990 on the experimental plot: one year in advance of the experiments to allow the soil to settle from any disturbance caused by the installation procedure. Tensiometers were installed at three soil depths, 20, 50 and 80 cm, in the upper, middle and lower part of the experimental plot. Nine tensiometers were fitted with pressure transducers, which were coded as follows: U20, U50, U80; M20, M50, M80; and L20, L50, and L80

for the upper, middle and lower part of the experimental block at 20, 50 and 80 cm of soil depth, respectively. Tensiometers without pressure transducers were installed to insure having at least one operational unit at each location. Calibration and performance of the pressure transducers and mercury-water manometers are reported elsewhere (Navar, 1992).

Rainfall Simulator

A rainfall simulator, similar in size to the experimental plot, was built to generate water movement within the experimental plot. It consisted of a rectangular frame made of (1.905 cm diameter schedule 40) PVC pipe with spraying nozzles placed underneath. The spraying nozzles were of the industrial type (Lechler from Jackson and Associates⁷) having a full cone axial spray pattern. The number and type of nozzles varied according to rainfall intensity. The rainfall simulator was suspended by ropes and swung back and forth to insure even distribution of rainfall. A 5000 liter plastic tank was located upslope from the simulator to provide gravity feed of water. The system was capable of delivering water through a 3.81 cm diameter PVC pipe at a pressure of approximately 700 cm of water. A

⁷ P.O. Box 551585, Dallas, TX 75355-1585. Note: use of trade names does not imply endorsement of the product by the authors.

pressure gauge was installed between the supply pipe and the rainfall simulator to ensure a constant rainfall rate.

Field Procedure

Simulated rainfall was applied to the experimental plot for 17 storms ranging in depth and duration from 8.26 to 4.04 cm and 0.82 to 4.25 hours, respectively (Table III). Rainfall was simulated until changes on the rates of outflow and soil water potentials become negligible. Soil water potentials from pressure transducers and the number of tips from the tipping buckets were recorded at one minute intervals during simulated rain and for a 2-hour period after simulated rain was stopped. After 2-hours, data were recorded at 10 minute intervals. Mercury-water manometers were read every two to three minutes during simulated rainfall. Rainfall input was measured with a set of 10 rain cans set up on the experimental plot.

During rainfall 11, rhodamine dye was applied in lines 5 cm width across the experimental plot at three discrete locations: 1.5, 3.0 and 4.5 m upslope of the subsurface flow collectors at three different times during equilibrium conditions of the lateral subsurface flow. The time of dye appearance at the subsurface flow collectors was recorded. Forty-five liters of water were mixed with 50 grams of rhodamine dye, which was also applied to the entire experimental plot before and during rainfall 17. A month

latter, the entire experimental plot was excavated and pictures were taken of the dyed traces in the soil.

Determining Macropore Space

According to the capillary equation, the amount of water drained from desorption process is a function of pore diameter (Hillel, 1980, 1982). The large pores drain first and smaller macropores latter. Germann and Beven (1981) proposed a dual drainage process, where rapid drainage of macroporous soils is followed by a slow nearly constant rate of drainage. The rapid initial drainage has been attributed to flow from macropores (Germann and Beven, 1981 and Kluitenberg and Horton, 1990). The slow constant and extended drainage has been attributed to the water held in micropores or matrix flow. Macropore space was logically determined by the measurement of the volume of water drained during the initial rapid stages of desorption or drainage of a saturated soil block.

The number of macropores actively contributing to subsurface flow is a function of rainfall intensity (Edwards et al. 1992). Active macropore space can be estimated by the integration of the total lateral water desorbed from time $t=0$, when the soil is saturated and rainfall input ceases, until lateral desorption attains a constant desorption rate. Lateral active macropore space, ϵ_m (vol vol⁻¹), is:

$$\epsilon_m = \frac{Q_{ft}}{A_t L_t} \quad (1)$$

where

$$\begin{aligned} Q_{ft} &= \text{Total volume of lateral discharge (cm}^3\text{)}. \\ A_t &= \text{Cross sectional area (cm}^2\text{)}. \\ L_t &= \text{Length of the soil block (cm)}. \end{aligned}$$

Determining Macropore Flow Rates

Lateral subsurface flow in the experimental plot did not follow potential energy gradients when the soil water potential was less than 100 cm of water (Navar, 1992). Hence gravity, $\delta\phi_g/\delta x$, dominates lateral discharge. Lateral macropore flow rates, ϵ_{qm} (cm sec⁻¹), are estimated as follows:

$$\epsilon_{qm} = \frac{Q_{fr}}{A_c \delta h} \quad (2)$$

where

$$\begin{aligned} Q_{fr} &= \text{Lateral flow rate (cm}^3 \text{ sec}^{-1}\text{)}. \\ A_c &= \text{Cross sectional area (cm}^2\text{)}. \\ \delta h &= \text{Hydraulic gradient (cm cm}^{-1}\text{)}. \end{aligned}$$

Note that Q_{fr} is now given as a lateral flow rate, rather than as total lateral flow. Because lateral discharge was independent of the hydraulic gradient (Navar, 1992), it was assumed that the hydraulic gradient for the desorption process is equal to the slope of the experimental plot. When the water table is parallel to the soil surface, the initial lateral macropore flow rate approaches the value of the lateral saturated hydraulic conductivity.

Determining Matrix Flow

Smaller soil pores or micropores also contribute to lateral discharge during desorption processes because the slope of the experimental plot is the driving force and soil water potential, $\phi_p, \geq 0$ when a perched water table develops with height = z. Macropore flow decays with time and micropore or matrix flow continues contributing to lateral desorption. Hence lateral desorption attains a nearly constant final rate. This lateral desorption rate represents the contribution of the soil matrix to lateral desorption. This approach is in agreement with the dual flow mode proposed by Germann and Beven (1981), as well as with the functional relationship between $K(\theta)$ and θ for macroporous soils.

Results and Discussion

The rates of water desorption after the simulation of 17 rainfalls are highly variable (Figure 1). After having stopped rainfall, the hydrographs started to decline at about 2, 4, 6, and 7 minutes for the A&Litter, B1, B2, and B3 soil horizons respectively. Lateral desorption ended after 65, 14, 343, and 798 minutes for the A&Litter, B1, B2, and B3 soil horizons, respectively.

The two modes of water movement proposed by Germann and Beven (1981) are obvious early in the desorption process (Figure 1). The early stages of desorption are dominated by

macropore flow. The latter stages of desorption are dominated by matrix flow. Most discharge rates converge statistically at 120 minutes of desorption (Table IV). Time $t=_{120 \text{ min}}$ is, hence, the boundary between macropore and matrix flow. Matrix flow does start at $t=_{120 \text{ min}}$, but its total contribution to initial lateral desorption is small.

Lateral Macropore Space

Lateral macropore space was estimated using equation 1. Q_{fr} was estimated by integrating the volume of drainage from time $t=_{0 \text{ min}}$ to time $t=_{120 \text{ min}}$. Germann and Beven (1981) measured macropore space by desorpting soil cores for 4 hours. Kluitenberg and Horton (1990) assumed that desorption for 12 hours would be a good estimate of macropore flow. Because desorption rates fitted reciprocal regression models well, the integration was carried out on the reciprocal equations (Table V). The estimates of macropore space (vol^{-1}) from equation 1 for the 17 simulated rainfalls were normally distributed. The mean macropore space was 0.0053 with a coefficient of variation of 46 %.

The rate of rainfall input and the height of the perched water table at 20 cm explained part of the variation of total active macropore space (Figure 2). Rainfall intensity explained most of the variation of total active macropore space. The likely physical explanation for this statistical relationship is that desorption after intense

rainfalls involves more macropores and light rainfalls involve less macropores. Therefore rainfall intensity is critical to determine the active macropore space. This finding is consistent with the estimation of the unsaturated hydraulic conductivity by the sprinkling infiltration method (Hillel, 1980). Edwards et al. (1992) also found evidence in agricultural soil that the number of macropores contributing to percolation of soil columns changed with rainfall intensity.

The soil water potential at 20 cm of soil depth also explained part of the variation of active macropore space. The data fitted better a power model. The physical explanation of this relationship is that most macropore space is found close to the soil surface. Gaiser (1952) and Aubertin (1971) observed in forest soils that most roots and root channels were located in the upper soil horizons. Edwards et al (1988, 1990) also observed that the volume of worm burrows decreased with soil depth.

Maximum macropore space was approximately $0.0060 \text{ (cm}^3 \text{ cm}^{-3}\text{)}$ when the perched water table was close to the soil surface. It is the equivalent to a water depth of 0.36 cm in the experimental plot. Maximum macropore space is approximately 3.55 % of the total porosity of the upper 20 cm of soil depth and 1.01 % of the total porosity of 67 cm of soil depth. In contrast to the mapped macropore space (Table II), which was approximately 0.25 % of the cross

sectional area of the experimental plot. This indicates that there were other macropores present and contributing to lateral discharge.

Total lateral macroporosity is in good agreement with the findings of other researchers. Bouma et al. (1979) found < 1 % of active, stained, voids. Using the tension infiltrometer, Watson and Luxmoore (1986) estimated 0.32 % and Wilson and Luxmoore (1988) estimated 0.00025 m³ m⁻³ of the soil volume. Using the drainage method, Kluitenberg and Horton (1990) estimated 7.9, 5.8 and 3.1 % of the total porosity of several soil cores at three soil depths and Germann and Beven (1981) estimated 0.01 and 0.045 (cm³ cm⁻³) in two soil cores.

Lateral Macropore Flow

Lateral macropore flow decayed in approximately 10 minutes after stopping rainfall. The large variation of lateral macropore flow rates early in the desorption process were partially explained by the rate of rainfall input (Figure 3). Rainfall intensity was driving lateral discharge. This finding supports the concept of macropore funneling. That is, macropores can accommodate and discharge the maximum rainfall intensity simulated in this experiment. Macropore funneling interacts little if at all with the soil matrix. This is consistent with the bromide observations carried out in the experimental plot during the same

simulated rainfalls by Barnes (1992). Edwards et al. (1990) also found a positive relationship between the rate of rainfall and macropore flow in worm burrows in Ohio.

The slopes and coefficients of determination of the regression models between rainfall intensity and macropore flow decayed with time of desorption. This means that the effect of rainfall on lateral macropore flow became negligible with time of desorption. Eventually, the soil system became memoryless of what happened with the initial rainfall input. The largest soil pores had desorbed and the soil matrix controlled the rate of water movement.

The large variation of macropore flow was also explained in part by the soil water potential at 20 cm of soil depth (Figure 4). An increase in the elevation of the water table caused an increase in macropore flow. However, macropore flow was independent of the average soil water potential at 20 cm. Rainfall intensity explained the differential rate of macropore flow. This finding supports the concept of active macropore space.

Macropore flow is not constant with soil depth because macropore space is also a function of soil depth. This is reflected by the initial rates of macropore flow during the desorption process, which were a power function of rainfall intensity. However, macropore flow was not constant with macropore space, because macropore flow was also a power function of macropore space (Figure 5). Darcy's and

Poiseuille's laws predict that outflow is a linear function of pressure. The non-linear relationships observed herein are consistent with macropore funneling and the initiation of turbulent flow through macropores.

The increase of lateral macropore flow with an increase of the water table from 20 cm of soil depth and rainfall intensity shows that positive soil water potential forces water into the active macropore system determined by rainfall intensity. When macropore velocity remains constant, the effect of soil water potential on macropore flow is in agreement with potential flow theory as well as with the observations and suggestions of Beven and Germann (1982) and Booltink and Bouma (1991). Hence, after rapid macropore drainage, additional flow into the macropore system is slow and controlled by matrix flow (Bouma et al. 1979; Smettem and Collis-George, 1985; and Kneale, 1985). Therefore the relationship between pressure and macropore flow becomes linear. In contrast, Thomas and Phillips (1979) and Mosley (1979, 1982) rejected the hydraulic conductivity of the soil matrix as a major control of macropore flow. Macropore flow or bypassing flow was also observed under unsaturated soil moisture conditions in the experimental plot (Navar, 1992), in agreement with the findings of Thomas and Phillips (1979) and Jardine et al. (1990).

The application of the power equation at $t=0_{\min}$ for an elevation of the perched water table of 18 cm estimates the

maximum macropore flow. It is approximately $0.042 \text{ cm sec}^{-1}$. This estimate of macropore flow is 20 times larger than those of Ehlers (1975) and Edwards et al. (1989) for earthworm burrows (> than 5 mm in diameter), as well as those of Aubertin (1971) for root channels. The observations made by Mosley (1979, 1982) are astonishing and surpass our measurements by 240 and 7.3 times, respectively.

Lateral Matrix Flow

The lateral discharge at 120 minutes for all storms, where the desorption curves converged was considered to be soil matrix flow. The average matrix flow rate was $0.086 \text{ liters min}^{-1}$ or $0.00066 \text{ cm sec}^{-1}$. This estimate is also in good agreement with $0.001 \text{ cm sec}^{-1}$ reported by Mosley (1979), as well as, with and 0.002 and $0.003 \text{ cm sec}^{-1}$ measured by Wilson and Luxmoore (1988) and Watson and Luxmoore (1986). Bouma (1990) reported a matrix flow of $0.00035 \text{ cm sec}^{-1}$ for the B soil horizon of a Glossaqualf soil.

The concept of matrix flow applies here for saturated conditions at several places in the experimental plot. Soil water potentials at the end of lateral desorption were approximately 2, +8, and +25 cm of water for the 20, 50, and 80 cm of soil depth. Germann and Beven (1981) pointed out that soil water potentials of the order of -40 cm of water mark the boundary between macropore and micropore flow.

Watson and Luxmoore (1986) and Wilson and Luxmoore (1988) estimated from capillary theory that -15 cm of soil water potential represents water movement through soil micropores or matrix flow.

From potential flow theory our definition of matrix flow may also include small macropores and mesopores (Luxmoore, 1981; Watson and Luxmoore, 1986; and Wilson and Luxmoore, 1988). The contribution of smaller macropores or mesopores to lateral flow discharge are probably controlled by the rate of micropore flow, in agreement with the solute flux observations made by Jardine et al. (1990).

Comparisons between the estimates of macropore and matrix flows with the bromide observations carried out by Barnes (1992) are important to determine the performance of the separation technique of macropore and matrix flow. Considering maximum lateral macropore flow, 98 % of the initial maximum macropore flow was new water, whereas for storm 16, the percentage decreased to 90 %. Barnes (1992) observed for intense rainfalls that 97 % of the lateral discharge flow was new water, whereas for storm 16, 74 % of the lateral subsurface flow was old water.

Rhodamine Dye Experiments

During the excavation of the experimental plot, it was observed that decayed roots and living roots were the most stained water passageways. The major portion of stained

roots was found between 10 and 15 cm of soil depth, at the interface of the A&B1 soil horizons. This is in agreement with the observations of largest macropore space and macropore flow close to the soil surface. McDonnell et al (1991) also found evidence of water moving freely at the interface of these horizons in an experimental watershed in New Zealand. The depth of most stained roots are also in agreement with the observations of Aubertin (1971). The sampling procedure did not allow a better estimation of the dimensions of root channels because of the large rhodamine concentrations at the interface of the A and B soil horizons and the one directional soil slicing procedure.

Worm and ant burrows were stained immediately below most large stones close to the soil surface. Stone area at the soil surface was measured as 7 % of the experimental plot. One stained ant burrow with several branches went into the C horizon. Stained worm burrows indicated they were actively contributing though for vertical distances; between 15-30 cm from the soil surface. These holes are tubular in shape and range from 1 mm to over 15 mm in diameter.

The rhodamine dye applications at discrete places within the experimental plot showed that the first application at 1.50 m upslope of the lateral face appeared 2.4, 3.5, and 10.0 minutes at the A&Litter, B1 and B3 soil horizons, respectively. Because most rhodamine dye appeared at discrete places at the upper soil horizon and at one

particular place at the B1 soil horizon, water fluxes are larger for rhodamine applications than general average flux densities for the upper soil horizons. Further discrete applications of rhodamine dye farther upslope showed faint dye traces in lateral subsurface flow and it could not be exactly determined the initial time of rhodamine dye appearance.

Conclusions

This report showed that desorption experiments can give information on the active lateral macropore space, and the rates of macropore and matrix flow. Maximum active macropore space was $0.006 \text{ (cm cm}^{-1}\text{)}$ and maximum macropore flow when the soil block was close to saturation was $0.041 \text{ cm sec}^{-1}$. Maximum matrix flow was $0.00066 \text{ cm sec}^{-1}$. Active macropore space and macropore flow were dependent on the rate of rainfall input and the relative position of the water table. Both parameters seem to operate independently on macropore flow. Velocity in the macropore space was not constant, which is consistent with desorption process through large soil pores.

References

- Abdul, A.S., and Gillham, R.W. 1984. Laboratory studies of the effects of the capillary fringe on streamflow generation. *Water Resources Research* 20:691-698.

- Anderson, M.G., and Burt, T.P. 1990. Subsurface Runoff processes. In: Process Studies in Hillslope Hydrology. M.G. Anderson and T.P. (Eds.). Burt. Chapter 11: 365-400. John Wiley & Sons Ltd. New York.
- Andreini, M.S. and Steenhuis, T.S. 1990. Preferential paths of flow under conventional and conservation tillage. *Geoderma* 46:85-102.
- Aubertin, G.M. 1971. Nature and extent of macropores in forest soils and their influence on subsurface water movement. Forest Service Paper NE, 192 PS.
- Barnes, D. 1992. Release of old and new water from an undisturbed forest pedon in the Ouachita National Forest. M. Sc. thesis. Oklahoma State University.
- Beasley, R.S. 1976. Contribution of subsurface flow from the upper slopes of forested watersheds to channel flow. *Soil Science American Journal* 40:955-957.
- Beven, K. and Germann, P. 1981. Water flow in soil macropores. II. A combined flow model. *Journal of Soil Science*. 32:15-29.
- Beven, K. and Germann, P. 1982. Macropores and water flow in soils. *Water Resources Research* 18:1311-1325.
- Booltink, H.W.G. and Bouma, J. 1991. Physical and morphological characterization of bypass flow in a well-structured clay soil. *Soil Science Society of America Journal* 55:1249-1254.
- Bouma, J. 1990. Using morphometric expressions for macropores to improve soil physical analyses of field soils. *Geoderma* 46:3-11.
- Bouma, J., Jongerius, A. and Schoonderbeek, D. 1979. Calculation of saturated hydraulic conductivity of some pedal clay soils using micromorphometric data. *Soil Science Society American Journal* 43:261-264.
- Cassel, D.K., and Klute, A. 1986. Water potential:tensiometry. In: Klute, A. (Ed.) *Methods of Soil Analysis*. Part I. 2nd ed. Agronomy. 563-596.
- DeVries, J. and Chow, T.L. 1978. Hydrologic behavior of a forested mountain soil in coastal British Columbia. *Water Resources Research* 14:935-942.
- DeWitt, J.N., and Steinbrenner, E.C. 1981. Central Arkansas Soil Survey. Weyerhaeuser Co. Tacoma, WA.

- Edwards, W.M., Norton, L.D. and Redmond, C.E. 1988. Characterizing macropores that affect infiltration into nontilled soil. *Soil Science Society American Journal* 52:483-487.
- Edwards, W.M., Shipitalo, M.J. Owens, L.B. and Norton, L.D. 1989. Water and nitrate movement in earthworm burrows within long-term no-till cornfield. *Journal of Soil and Water Conservation* 15:240-243.
- Edwards, W.M., Shipitalo, M.J. Owens, L.B. and Norton, L.D. 1990. Effect of Lumbricus terrestris L. burrows on hydrology of continuous no-till corn fields. *Geoderma* 46:73-84.
- Edwards, W.M., Shipitalo, M.J., Dick, W.A. and Owens, L.B. 1992. Rainfall intensity affects transport of water and chemicals through macropores in no-till soil. *Soil Science Society American Journal* 56:52-58.
- Ehlers, W. 1975. Observations on earthworm channels and infiltration on tilled and untilled loess soil. *Soil Science* 119:242-249.
- Gaiser, R.N. 1952. Root channels and roots in forest soils. *Soil Science Society American Proceedings* 40:62-65.
- Germann, P.F. 1986. Rapid drainage response to precipitation. *Hydrological Processes* 1:3-13.
- Germann, P.F. 1990a. Macropores and hydrologic hillslope processes. In: *Process Studies in Hillslope Hydrology*. M.G. Anderson and T.P. Burt. (Eds.). Chapter 10:327-363. John Wiley & Sons Ltd. New York.
- Germann, P.F. 1990b. Preferential flow and the generation of runoff. 1. Boundary layer flow theory. *Water Resources Research* 26:3055-3063.
- Germann, P. and Beven, K. 1981. Water flow in soil macropores. I. An experimental approach. *Journal of Soil Science* 32:1-13.
- Hammermeister, D.P., Kling, G.F. and Vomocil, J.A. 1982. Perched water tables on hillsides in western Oregon. II. Preferential downslope movement of water and anions. *Soil Science Society American Journal* 46:819-826.
- Hillel, D. 1980. *Fundamentals of Soil Physics*. Academic Press, Inc. New York.

- Hillel, D. 1982. Introduction to Soil Physics. Academic Press, Inc. New York.
- Jardine, P.M., Wilson, G.V. and Luxmoore, R.J. 1990. Unsaturated transport through a forest soil during rain storm events. *Geoderma* 46:103-118.
- Jones, J.A.A. 1971. Soil piping and stream channel initiation. *Water Resources Research* 7:602-610.
- Kemper, W.D., Trout, T.J., Segeren, A. and Bullock, M. 1987. Worms and water. *Journal of Soil and Water Conservation* 42:401-404.
- Kluitenberg, G.J. and Horton, R. 1990. Effect of solute application method on preferential transport of solute in soil. *Geoderma* 46:283-297.
- Luxmoore, R.J. 1981. Comments on micro, meso and macroporosity of soil. *Soil Science Society American Journal* 45:671-672.
- Luxmoore, R.J., Jardine, P.M., Wilson, G.V., Jones, J.R. and Zelazny, L.W. 1990. Physical and chemical controls of preferred path flow through a forested hillslope. *Geoderma* 46:139-154.
- McDonnell, J.J. 1990. A rationale for old water discharge through macropores in a steep humid catchment. *Water Resources Research* 26:2821-2832.
- McDonnell, J.J., Owens, F.I., and Stewart, M.K. 1991. A case of shallow flow paths in a steep zero-order basin. *Water Resources Bulletin* 27:679-685.
- Mosley, M.P. 1979. Streamflow generation in forested watersheds, New Zealand. *Water Resources Research* 15:795-806.
- Mosley, M.P. 1982. Subsurface flow velocities through selected forest soils, south island, New Zealand. *Journal of Hydrology* 55:65-92.
- Mulholland, P.J., Wilson, G.V. and Jardine, P.M. 1990. Hydrogeochemical response of a forested watershed to storms: effects of preferential flow along shallow and deep pathways. *Water Resources Research* 26:3021-3036.
- Navar, J.J., 1992. Water movement in an experimental plot in the Ouachita Mountains of Arkansas: the effect of soil macropores. Ph.D. diss. Oklahoma State University.

- Omoti, U. and Wild, A. 1979. Use of fluorescent dyes to mark the pathways of solute movement through soils under leaching conditions. 2. Filed experiments. Soil Science 128:98-104.
- Pearce, A.J., Stewart, M.K., and Sklash, M.G. 1986. Storm runoff generation in humid headwater catchments: 1. Where does the water come from. Water Resources Research 22:1263-1272.
- Pilgrim, D.H., Huff, D.D., and Steele, T.D. 1978. A field evaluation of surface and subsurface runoff. 2, Runoff processes. Journal of Hydrology 38:319-341.
- Sklash, M.G. 1990. Environmental isotope studies of storm and snowmelt runoff generation. In: M.G. Anderson and T.P. Burt (Eds.). Process Studies in Hillslope Hydrology. Chapter 12:401-435. John Wiley & Sons Ltd. New York.
- Sklash, M.G. Stewart, M.K. and Pearce, A.J. 1986. Storm runoff generation in humid headwater catchments.II: A case of study of hillslope and low order stream response. Water Resources Research 22:1273-1282.
- Thomas, G.W. and Phillips, R.E. 1979. Consequences of water movement in macropores. Journal of Environmental Quality 18:149-152.
- Turner, J.V., Macpherson, D.K. and Stokes, R.A. 1987. The mechanisms of catchment flow processes using natural variations in deuterium and oxygen-18. In: A.J. Peck and D.R. Williamson (Eds.). Hydrology and Salinity in the Collie River Basin, Western Australia. Journal of Hydrology 94:143-162.
- Turton, D.J., Haan, T.C. and Miller, E.L. 1992. Subsurface flow responses of a small forested catchment in the Ouachita Mountains. Hydrological Processes 6:111-125.
- Whipkey, R.Z. 1965. Subsurface stormflow from forested watersheds. Bulletin International Association Scientific Hydrology 10:74-85.
- Watson, K.W. and Luxmoore, R.J. 1986. Estimating macroporosity in a forest watershed by use of a tension infiltrometer. Soil Science Society American Journal 50:578-582.

Wilson, G.V. and Luxmoore, R.J. 1988. Infiltration and macroporosity distributions on two forested watersheds. Soil Science Society American Journal 52:329-335.

TABLE I
SOIL DESCRIPTION, TEXTURAL AND SOIL BULK DENSITY ANALYSIS, AND THE LOCATION
OF TENSIOMETERS AND SUBSURFACE FLOW COLLECTORS WITHIN
THE EXPERIMENTAL PLOT

Soil Pro- file	Soil Depth (cm)	Soil Description	Soil Sand (%)	Texture Clay (%)	Silt (%)	Soil Bulk Density (g/cm ³)	Ten- sio- meter	Subsur- face Collec- tor
01	2.5-3.5	Forest litter						
02	0.0-2.5	Mull layer of partially de- composed organic matter						
A1	0.0-2.5	Pale brown(10YR 6/3) loam						
E	2.5-10	Light yellowish (10YR 6/4) loam						
Bt1	10 -22	Yellowish brown (10YR 5/6)	19.7	34.4	45.9	1.31	20	YES
Bt21	23 -43	Yellowish brown (10YR 5/8)	32.7	24.7	42.8	1.47		YES
Bt22	43 -63	Yellowish brown (10YR 5/8) clay					50	YES
B3	63 -81	Mottled red clay	39.7	17.8	42.5	1.60	80	YES
C	81-102	Moderately weathered shale rock and clay soil material						

The description of soil profiles was carried out by USDA Forest Service (1964).
The textural and soil bulk density analysis was carried out by the author.

TABLE II
LARGE SOIL MACROPORES OBSERVED AT THE LATERAL FACE CROSS
SECTIONAL AREA OF THE EXPERIMENTAL PLOT

Coordinates		Diameter	Characteristics
Lateral (cm)	Vertical (cm)	(cm)	
12	48	1.0-0.8	Root channel, some bark lining
26	49	2.6-1.7	Root channel, bark lining decayed
44	47	2.2-1.8	Root channel, decayed lining
43	15	0.8	Root channel, still filled with decayed wood
137	41	1.5-1.3	Root channel, some bark lining
135	23	0.8-0.6	Root channel, bark lined
170	40	2.8-2.2	Root channel, decayed organic inside new root growing inside
114	55	1.1-1.0	Root channel, new root growing inside

TABLE III
SOME CHARACTERISTICS OF SIMULATED RAINFALLS

RUN	DATE	RAIN AMOUNT (cm)	C.V (%)	SIMULATION TIME (hrs)	RAIN INTENSITY (cm/h)	RETURN PERIOD (years)
1	07/17/91	8.26	68	1.22	6.80	20.00
2	07/24/91	5.64		0.90	6.27	4.00
3	07/25/91	6.12	22	0.82	7.49	5.00
4	07/31/91	8.41	22	1.55	5.43	10.00
5	08/01/91	7.63	25	1.67	4.58	6.00
6	08/02/91	6.70	14	1.55	4.32	5.00
7	08/06/91	6.47	27	2.00	3.23	3.00
8	08/07/91	5.79	18	1.75	3.31	3.00
9	08/08/91	5.37	14	1.92	2.80	1.50
10	08/28/91	4.78	17	3.00	1.59	1.00
11	08/29/91	4.46	10	2.75	1.62	1.00
12	08/30/91	4.65	15	2.75	1.69	1.00
13	09/10/91	5.08	29	2.75	1.85	1.00
14	09/11/91	6.26	16	2.33	2.68	2.00
15	09/12/91	5.77	17	2.17	2.66	1.80
16	10/08/91	4.42	12	4.25	1.04	1.00
17	10/09/91	4.04	21	3.08	1.31	1.00

Note the coefficient of variation was estimated from 11 rain cans on the experimental plot.

TABLE IV

THE PARAMETERS OF A COVARIANCE ANALYSIS PROCEDURE FOR
TESTING THE HOMOGENEITY OF SLOPES AND INTERCEPTS
FOR THE DESORPTION RATES WITH TIME

Time (min)	Intercept			Slope			Model
	F	P>F	n	F	P>F	n	
0-300	56	0.0001	10	48	0.0001	7	Reciprocal
20-300	43	0.0001	8	43	0.0001	8	Exponential
40-300	40	0.0001	8	20	0.0001	7	Exponential
60-300	27	0.0001	7	8	0.0001	7	Linear
80-300	21	0.0001	7	7	0.0001	6	Linear
100-300	15	0.0001	7	4	0.0001	4	Linear
120-300	5	0.0001	4	2.6	0.0580	1	Linear

Note n is the number of either slopes or intercepts significantly different.

TABLE V
 THE RECIPROCAL REGRESSION EQUATIONS FOR LATERAL
 DESORPTION WITH TIME AND MACROPORE SPACE
 IN AN EXPERIMENTAL PLOT IN ARKANSAS

Run #	r^2	P>F	Intercept (l)	Slope ($l\text{min}^{-1}$)	(vol vol ⁻¹)
1	0.82	0.0001	0.029	15.30	0.008869
2	0.88	0.0001	0.075	14.51	0.009069
3	0.80	0.0001	0.010	17.35	0.009742
4	0.86	0.0001	0.119	10.97	0.007720
5	0.87	0.0001	0.098	11.01	0.007453
6	0.83	0.0001	0.129	10.05	0.007350
7	0.79	0.0001	0.142	5.70	0.005120
8	0.75	0.0001	0.189	5.17	0.005485
9	0.75	0.0001	0.119	5.20	0.004528
10	0.73	0.0001	0.140	1.84	0.002963
11	0.69	0.0001	0.098	2.47	0.002730
12	0.72	0.0001	0.119	2.82	0.003212
13	0.73	0.0001	0.128	2.88	0.003371
14	0.76	0.0001	0.095	4.74	0.003944
15	0.76	0.0001	0.127	5.14	0.004606
16	0.57	0.0001	0.080	1.46	0.001921
17	0.61	0.0001	0.095	2.60	0.002761

Note Macropore space (vol vol⁻¹) results from $(\int i*s/t)/v$; where i =intercept, s =slope and t =time. The integration was carried out from $t=0$ to $t=120$ min.

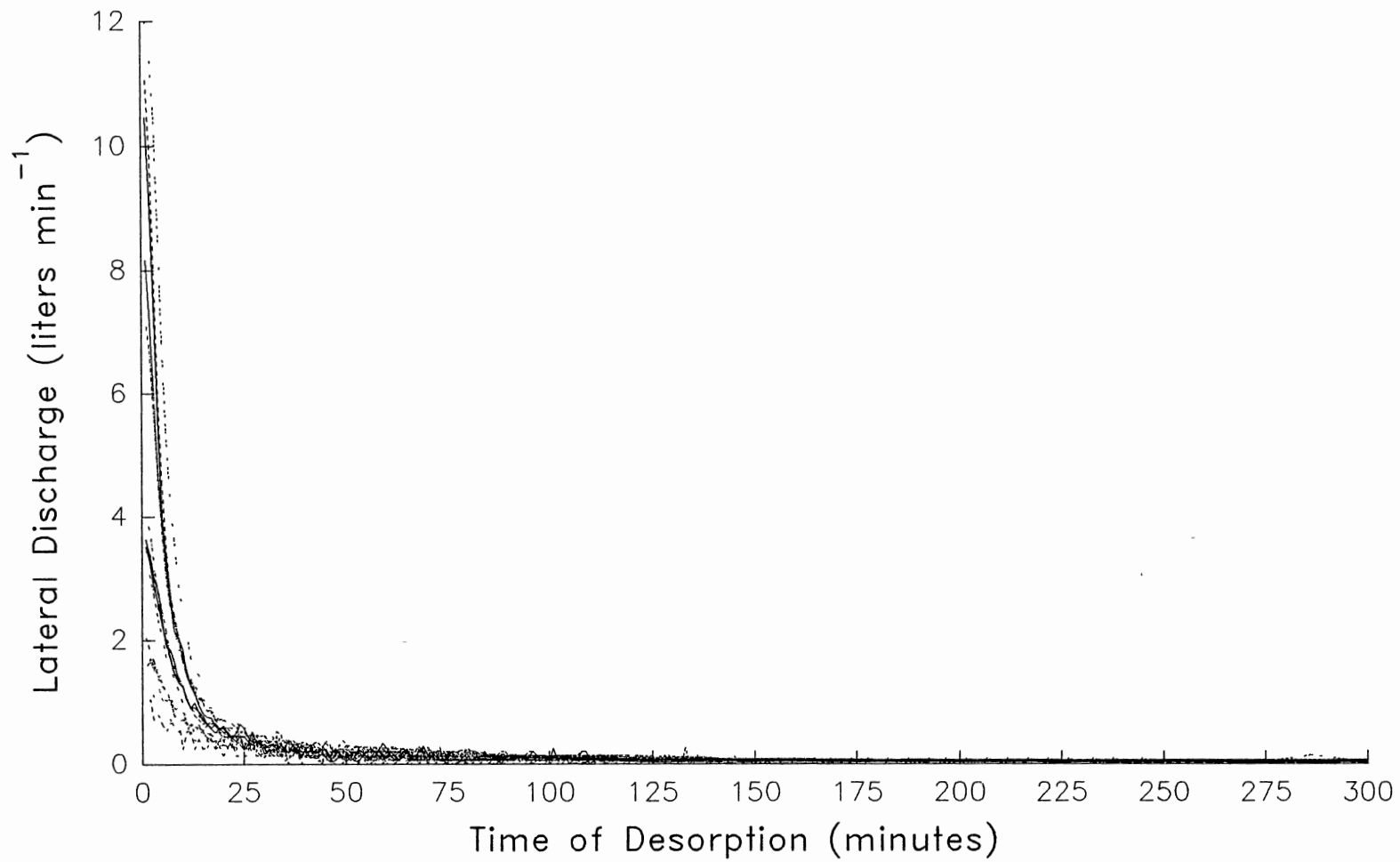


Figure 1. Lateral Desorption Rates of an Experimental Plot in Arkansas after the Simulation of 17 Rainfalls of Different Durations and Intensities.

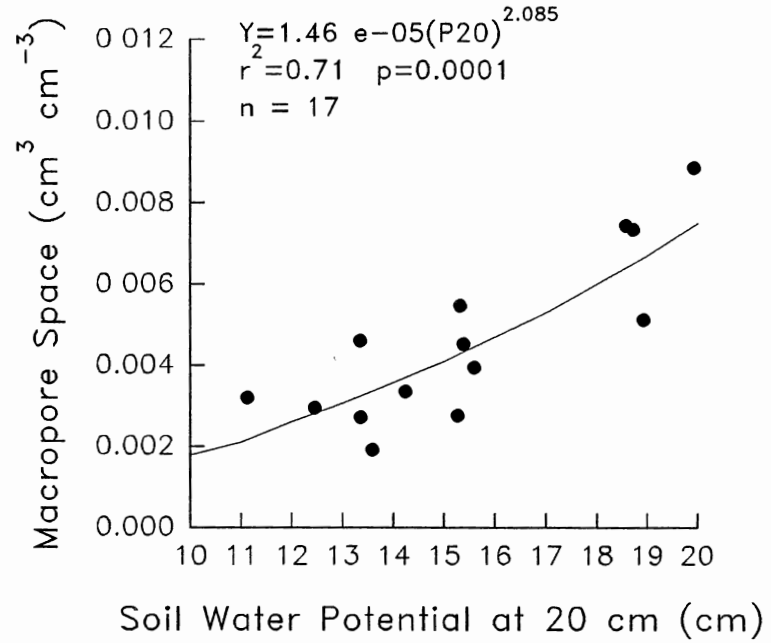
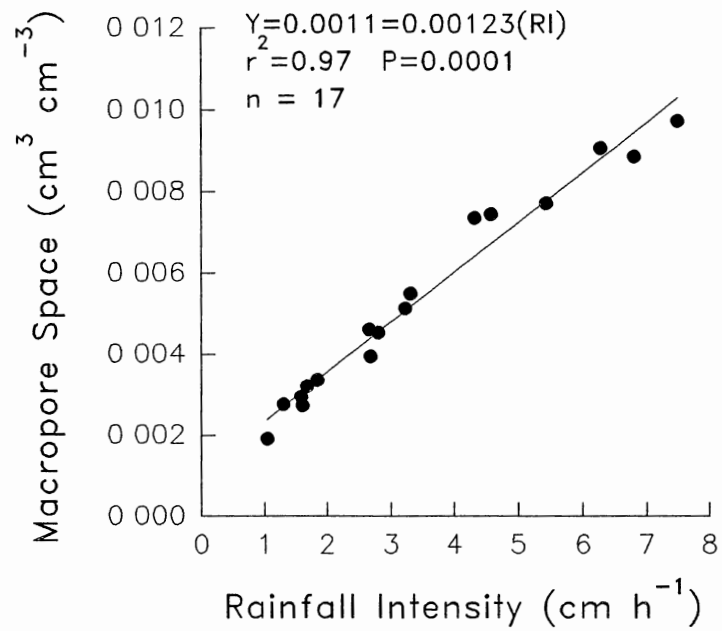


Figure 2. The Dependence of the Lateral Macropore Space on Rainfall Intensity and Soil Water Potential in an Experimental Plot in Arkansas.

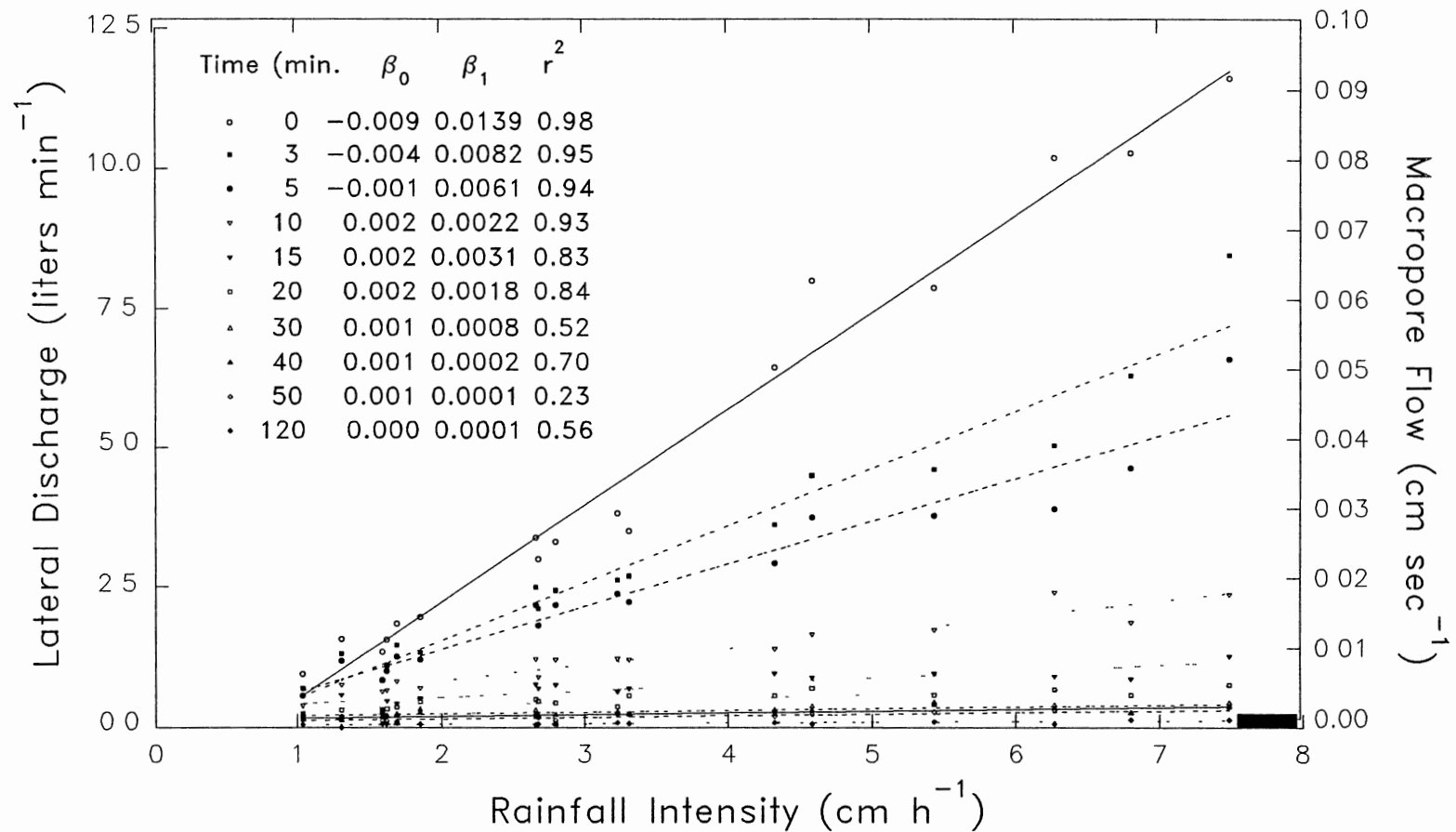


Figure 3. The Relationships between Rainfall Intensity and Macropore Flux Density for 17 Simulated Storms in an Experimental Plot in Arkansas.

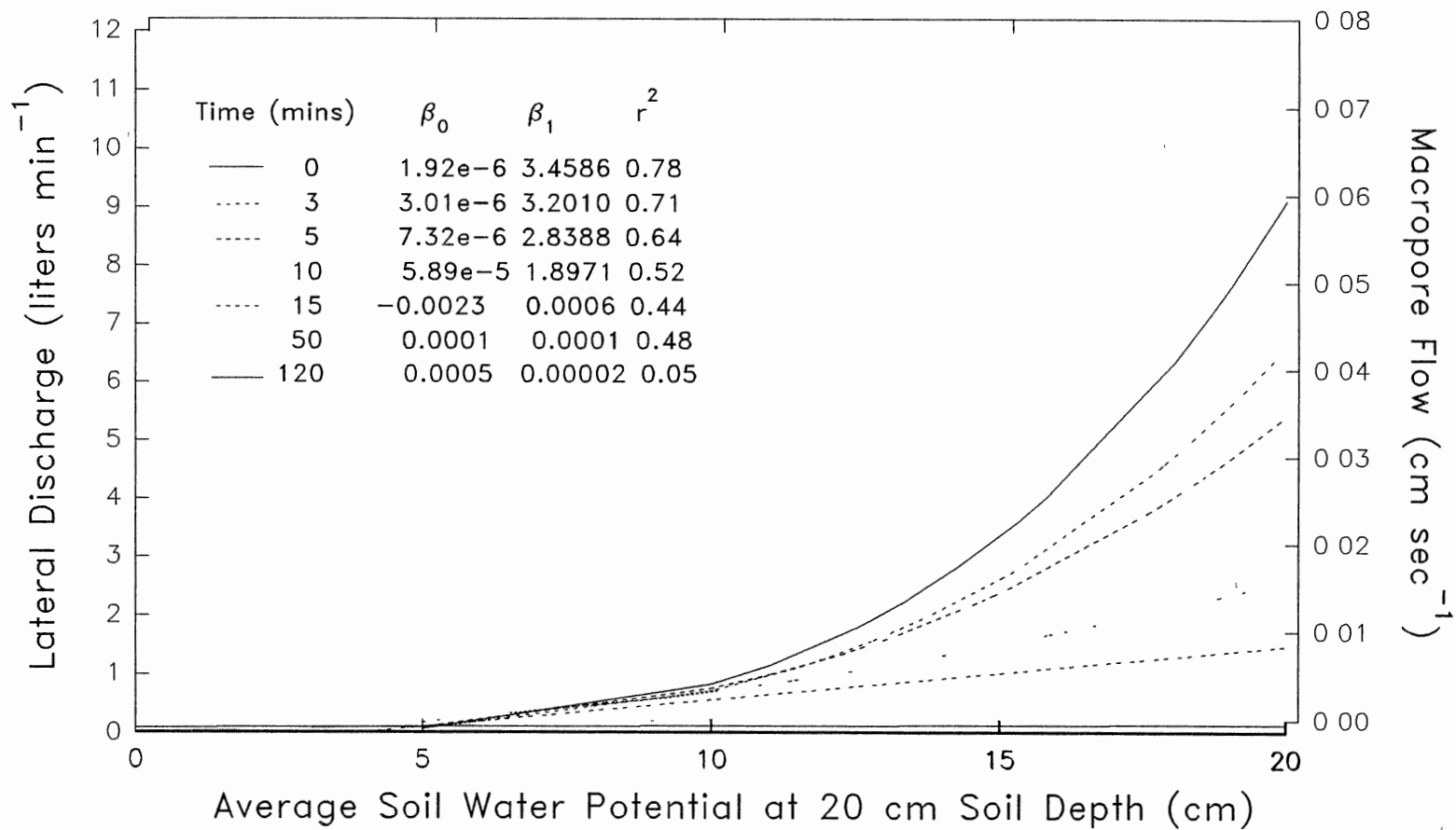


Figure 4. The Relationships between Average Soil Water Potential and Macropore Flux Density Desorption Experiments for 17 Simulated Storms in an Experimental Plot in Arkansas.

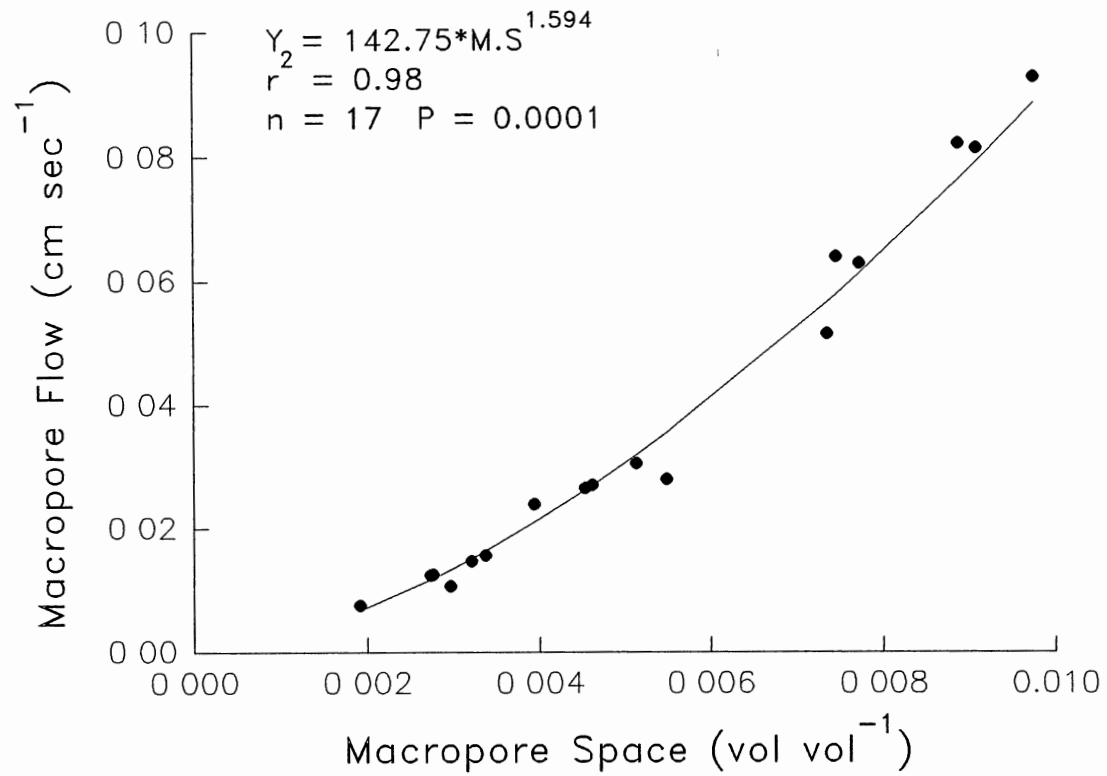


Figure 5. The Non-linear Dependence of Macropore Flow with Macropore Space.

LITERATURE CITED

- Abdul, A.S., and Gillham, R.W. 1984. Laboratory studies of the effects of the capillary fringe on streamflow generation. *Water Resources Research* 20:691-698.
- Amoozegar, A. and Warrick, A.W. 1986. Hydraulic Conductivity of saturated soils: Field Methods. *In*: A. Klute (Ed) *Methods of Soil Analysis, Part I*. 2nd ed. Agronomy 735-768.
- Anderson, M.G., and Burt, T.P. 1978. The role of topography in controlling throughflow generation. *Earth Surface Processes* 3:331-344.
- Anderson, M.G., and Burt, T.P. 1990. Subsurface Runoff processes. *In*: M.G. Anderson and T.P. Burt (Eds). *Process Studies in Hillslope Hydrology*. Chapter 11:365-400. John Wiley & Sons Ltd. New York.
- Andreini, M.S. and Steenhuis, T.S. 1990. Preferential paths of flow under conventional and conservation tillage. *Geoderma* 46:85-102.
- Aubertin, G.M. 1971. Nature and extent of macropores in forest soils and their influence on subsurface water movement. *Forest Service Paper NE*, 192 PS.
- Barnes, R.D. 1992. Release of old and new water from an undisturbed forest pedon in the Ouachita National Forest. M.Sc. thesis. Oklahoma State University.
- Beasley, R.S. 1976. Contribution of subsurface flow from the upper slopes of forested watersheds to channel flow. *Soil Science Society of America Journal* 40:955-957.
- Betson, R.P. and Marius, J.B. 1969. Source areas of storm runoff. *Water Resources Research* 5:574-582.
- Beven, K. 1981. Kinematic subsurface stormflow. *Water Resources Research* 17:1419-1424.
- Beven, K. 1982. On subsurface stormflow: predictions with simple kinematic theory for saturated and unsaturated flows. *Water Resources Research* 18:1627-1633.

- Beven, K. and Germann, P. 1981. Water flow in soil macropores. II. A combined flow model. *Journal of Soil Science* 32:15-29.
- Beven, K. and Young, P.C. 1988. An aggregated mixing zone model of solute transport through porous media. *Journal of Contaminant Hydrology* 3:129-143.
- Beven, K. and Germann, P. 1982. Macropores and water flow in soils. *Water Resources Research* 18:1311-1325.
- Binley, A., Beven, K. and Elgy, J. 1989. A physically based model of heterogeneous hillslopes. 2. Effective hydraulic conductivities. *Water Resources Research* 25: 1227-1233.
- Blake, G.R. and Hartge, K.H. 1986. Bulk density. *In*: A. Klute (Ed) *Methods of Soil Analysis, Part I*. 2nd ed. *Agronomy* 363-375.
- Booltink, H.W.G. and Bouma, J. 1991. Physical and morphological characterization of bypass flow in a well-structured clay soil. *Soil Science Society of America Journal* 55:1249-1254.
- Bouma, J. 1990. Using morphometric expressions for macropores to improve soil physical analyses of field soils *Geoderma* 46:3-11.
- Bouma, J., Jongerius, A. and Schoonderbeek, D. 1979. Calculation of saturated hydraulic conductivity of some pedal clay soils using micromorphometric data. *Soil Science Society of America Journal* 43:261-264.
- Bren, L.J. and Turner, A.K. 1985. Hydrologic behaviour of a small forested catchment. *Journal of Hydrology* 76:333-350.
- Cassel, D.K., and Klute, A. 1986. Water potential:tensiometry. *In*: A. Klute (Ed) *Methods of Soil Analysis, Part I*. 2nd ed. *Agronomy* 563-596.
- DeVries, J. and Chow, T.L. 1978. Hydrologic behavior of a forested mountain soil in coastal British Columbia. *Water Resources Research* 14:935-942.
- DeWitt, J.N., and Steinbrenner, E.C. 1981. *Central Arkansas Soil Survey*. Weyerhaeuser Co. Tacoma, WA.
- Dowd, J.F., and Williams, A.G. 1989. Calibration and use of pressure transducers in soil hydrology. *Hydrological Processes* 3:43-49.

- Dunne, T. and Black, R.D. 1970a. An experimental investigation of runoff production in permeable soils. *Water Resources Research* 6:478-490.
- Dunne, T. and Black, R.D. 1970b. Partial area contributions to storm runoff in a small New England watershed. *Water Resources Research* 6:1296-1311.
- Dunne, T. and Leopold, L.B. 1978. *Water in Environmental Planning*. W.H. Freeman Company. San Francisco, CA.
- Edwards, W.M., Norton, L.D. and Redmond, C.E. 1988. Characterizing macropores that affect infiltration into nontilled soil. *Soil Science Society of America Journal* 52:483-487.
- Edwards, W.M., Shipitalo, M.J. Owens, L.B. and Norton, L.D. 1989. Water and nitrate movement in earthworm burrows within long-term no-till cornfield. *Journal of Soil and Water Conservation* 25:240-243.
- Edwards, W.M., Shipitalo, M.J. Owens, L.B. and Norton, L.D. 1990. Effect of Lumbricus terrestris L. burrows on hydrology of continuous no-till corn fields. *Geoderma* 46:73-84.
- Edwards, W.M., Shipitalo, M.J., Dick, W.A. and Owens, L.B. 1992. Rainfall intensity affects transport of water and chemicals through macropores in no-till soil. *Soil Science Society of America Journal* 56:52-58.
- Ehlers, W. 1975. Observations on earthworm channels and infiltration on tilled and untilled loess soil. *Soil Science* 119:242-249.
- Everts, C.J., Kanwar, R.S., Alexander, E.C. and Alexander, S.C. 1989. Comparison of tracer mobilities under laboratory and field conditions. *Journal of Environmental Quality* 18:491-498.
- Gaiser, R.N. 1952. Root channels and roots in forest soils. *Soil Science Society of America Proceedings* 40:62-65.
- Germann, P.F. 1986. Rapid drainage response to precipitation. *Hydrological Processes* 1:3-13.
- Germann, P.F. 1990a. Macropores and hydrologic hillslope processes. In: *Process Studies in Hillslope Hydrology*. M.G. Anderson and T.P. Burt. (Eds). Chapter 10: 327-363. John Wiley & Sons Ltd. New York.

- Germann, P.F. 1990b. Preferential flow and the generation of runoff. 1. Boundary layer flow theory. Water Resources Research 26:3055-3063.
- Germann, P.F. and Beven, K. 1981. Water flow in soil macropores. I. An experimental approach. Journal of Soil Science 32:1-13.
- Green, R. E., Ahuja, L.R. and Chong, S.K. 1986. Hydraulic Conductivity, Diffusivity, and Sorptivity of Unsaturated Soils: Field Methods. In: A. Klute (Ed) Methods of Soil Analysis, Part I. 2nd ed. Agronomy 771-796.
- Hammermeister, D.P., Kling, G.F. and Vomocil, J.A. 1982. Perched water tables on hillsides in western Oregon. II. Preferential downslope movement of water and anions. Soil Science Society of America Journal 46:819-826.
- Haan, C.T. 1986. Statistical Methods in Hydrology. Fourth Printing. The Iowa State University Press. Ames IO.
- Hewlett, J.D. 1961. Soil moisture as a source of baseflow from steep mountain watersheds. U.S. Forest Service, Asheville, N.C. South Forest Experimental Station Paper No. 132.
- Hewlett, J.D. and Hibbert, A.R. 1963. Moisture and energy conditions within a sloping soil mass during drainage. Journal of Geophysical Research 68:1081-1087.
- Hewlett, J.D. and Hibbert, A.R. 1967. Factors affecting the response of small watersheds to precipitation in humid areas. In: Sopper, W.E. and Lull, H.W. (Eds). International Symposium on Forest Hydrology. 275-290. Pergamon Press, New York.
- Hillel, D. 1980. Fundamentals of Soil Physics. Academic Press, Inc. New York.
- Hillel, D. 1982. Introduction to Soil Physics. Academic Press, Inc. New York.
- Horton, R.E. 1933. The role of infiltration in the hydrologic cycle. Transactions American Geophysical Union 14:446-460.
- Horton, R.E. 1940. An approach toward a physical interpretation of infiltration capacity. Soil Science Proceedings 4:399-417.

- Hursh, C.R. 1944. Report of the subcommittee on subsurface flow. Transactions American Geophysical Union 25:743-746.
- Jardine, P.M., Wilson, G.V. and Luxmoore, R.J. 1990. Unsaturated transport through a forest soil during rain storm events. Geoderma 46:103-118.
- Jones, J.A.A. 1971. Soil piping and stream channel initiation. Water Resources Research 7:602-610.
- Kennedy, V.C., Kendall, C., Zellweger, G.W., Weyerman, T.A. and Avanzino, R.J. 1986. Determination of the components of stormflow using water chemistry and environmental isotopes, Mattole River Basin, California. Journal of Hydrology 84:107-140.
- Kneale, W.R. 1985. Observations of the behaviour of large cores of soil during drainage, and the calculation of hydraulic conductivity. Journal of Soil Science 36:163-171.
- Klute, A., and Gardner, W.R. 1962. Tensiometer response time. Soil Science 93:204-207.
- Klute, A. and Dirksen, C. 1986. Hydraulic Conductivity and Diffusivity: Laboratory Methods. In: A. Klute (Ed) Methods of Soil Analysis, Part I. 2nd ed. Agronomy 687-732.
- Kung, K-J.S. 1990a. Preferential flow in a sandy vadose zone: 1. Field observation. Geoderma 46:51-58.
- Kung, K-J.S. 1990b. Preferential flow in a sandy vadose zone: 2. Mechanisms and implications. Geoderma 46:59-71.
- Kuyane, I. and Kaihotsu, I. 1988. Some experimental results concerning rapid water table response to surface phenomena. In: R.L Bras, M. Hino, P.K. Kitanidis and K. Takeuchi (Eds), Hydrologic Research: The U.S-Japan Experience. Journal of Hydrology 102:165-178.
- Lowery, B., Datairi, B.C., and Andraski, B.J. 1986. An electrical readout system for tensiometers. Soil Science Society American Journal 50:494-496.
- Long, F.L. 1982. A new solid state device for reading tensiometer. Soil Science 133:131-132.

- Luxmoore, R.J. 1981. Comments on micro, meso and macroporosity of soil. *Soil Science Society of America Journal* 45:671-672.
- Luxmoore, R.J., Jardine, P.M., Wilson, G.V., Jones, J.R. and Zelazny, L.W. 1990. Physical and chemical controls of preferred path flow through a forested hillslope. *Geoderma* 46:139-154.
- McDonnell, J.J. 1990. A rationale for old water discharge through macropores in a steep humid catchment. *Water Resources Research*. 26:2821-2832.
- McDonnell, J.J., Owens, F.I., and Stewart, M.K. 1991. A case of shallow flow paths in a steep zero-order basin. *Water Resources Bulletin* 27:679-685.
- Mein, R.G. and Larson, C.L. 1973. Modeling infiltration during a steady rain. *Water Resources Research* 9:384-394.
- Miller, E.L., Beasley, R.S., and Lawson, E.R. 1988. Forest Harvest and site preparation effects on stormflow and peakflow of ephemeral streams in the Ouachita Mountains. *Journal of Environmental Quality* 17:212-218.
- Mosley, M.P. 1979. Streamflow generation in forested watersheds, New Zealand. *Water Resources Research*. 15: 795-806.
- Mosley, M.P. 1982. Subsurface flow velocities through selected forest soils, south island, New Zealand. *Journal of Hydrology* 55:65-92.
- Mulholland, P.J., Wilson, G.V. and Jardine, P.M. 1990. Hydrogeochemical response of a forested watershed to storms: effects of preferential flow along shallow and deep pathways. *Water Resources Research* 26:3021-3036.
- Pearce, A.J., Stewart, M.K., and Sklash, M.G. 1986. Storm runoff generation in humid headwater catchments: 1. Where does the water come from. *Water Resources Research* 22:1263-1272.
- Philip, J.R. 1957. The theory of infiltration: 1. The infiltration equation and its solution. *Soil Science* 83:345-357.
- Pilgrim, D.H., Huff, D.D., and Steele, T.D. 1978. A field evaluation of surface and subsurface runoff. 2, Runoff processes. *Journal of Hydrology* 38:319-341.

- Rawlins, S.L., and Campbell, G.S. A. 1986. Water potential:thermocouple psychrometry. In: A. Klute. (Ed) Methods of Soil Analysis. Part I, 2nd ed. Agronomy 597-618.
- Richard, T.L. and Steenhuis, T.S. 1988. Tile drain sampling a preferential flow on a field scale. In: P.F. Germann (Ed). Rapid and Far-reaching Hydrologic Processes in the Vadose Zone. Journal of Contaminant Hydrology. 3: 307-325.
- SAS/STAT Guide for Personal Computers. 1987. Version 6 Edition. SAS Institute Inc. Cary, N.C.
- SENSYM: Solid-State Sensor Handbook. 1991. Sunnyvale, CA.
- Schoeneberger, P. and Amoozegar, A. 1990. Directional saturated hydraulic conductivity and macropore morphology of a soil-saprolite sequence. Geoderma 46: 31-49.
- Sklash, M.G. 1990. Environmental isotope studies of storm and snowmelt runoff generation. In: M.G. Anderson and T.P. Burt (Eds). Process Studies in Hillslope Hydrology. Chapter 12: 401-435. John Wiley & Sons Ltd. New York.
- Sklash, M.G. and Farvolden, R.N. 1979. The role of groundwater in storm runoff. Journal of Hydrology 43:45-65.
- Sklash, M.G. Stewart, M.K. and Pearce, A.J. 1986. Storm runoff generation in humid headwater catchments. II: A case of study of hillslope and low order stream response. Water Resources Research 22:1273-1282.
- Smettem, K.R.J. and Collis-George, N. 1985. Prediction of steady-state ponded infiltration distributions in a soil with vertical macropores. Journal of Hydrology 79:115-122.
- Steel, R.G.D., and Torrie, J.H. 1980. Principles and Procedures of Statistics: A Biometrical Approach. 2nd ed. McGraw-Hill. New York.
- Steenhuis, T.S. and Muck, R.E. 1988. Preferred movement of nonadsorbed chemicals on wet shallow, sloping soils. Journal of Environmental Quality 17:370-384.

- Tanaka, T., Yasuhara, M., Sakai, H. and Marui, A. 1988. The Hachioji experimental basin study: storm runoff processes and the mechanism of its generation. In: R.L. Bras, M. Hino, P.K. Kitanidis and K. Takeuchi (Eds), Hydrologic Research: The U.S-Japan Experience. Journal of Hydrology 102:139-164.
- Thomas, G.W. and Phillips, R.E. 1979. Consequences of water movement in macropores. Journal of Environmental Quality. 18:149-152.
- Trotter, C.M. 1984. Errors in reading tensiometer vacuum with pressure transducers. Soil Science American Journal 50:494-496.
- Troendle, C.A. 1985. Variable source area models. In M.G. Anderson and T.P. Burt (Eds). Hydrological Forecasting. John Wiley, Chichester. 347-403.
- Trudgill, S.T., Pickles, A.M. and Smettem, K.R.J. 1983. Soil-water residence time and solute uptake, 2. Dye tracing and preferential flow predictions. Journal of Hydrology 62:279-285.
- Tsukamoto, Y. and Ohta, T. 1988. Runoff process on a steep forested slope. In: R.L. Bras, M. Hino, P.K. Kitanidis and K. Takeuchi (Eds), Hydrologic Research: The U.S -Japan Experience. Journal of Hydrology 102:165-178.
- Turner, J.V., Macpherson, D.K. and Stokes, R.A. 1987. The mechanisms of catchment flow processes using natural variations in deuterium and oxygen-18. In: A.J. Peck and D.R. Williamson (Eds). Hydrology and Salinity in the Collie River Basin, Western Australia. Journal of Hydrology 94:143-162.
- Turton, D.J., Haan, T.C. and Miller, E.L. 1992. Subsurface flow responses of a small forested catchment in the Ouachita Mountains. Hydrological Processes 6:111-125.
- U.S.D.A. Forest Service. 1964. Special soil survey report of Alum Creek Experimental Forest Ouachita National Forest, Sabine County, AR.
- Ward, R.C. 1984. On the response to precipitation of headwater streams in humid areas. Journal of Hydrology 74:171-189.
- Whipkey, R.Z. 1965. Subsurface stormflow from forested watersheds. Bulletin International Association Scientific Hydrology 10:74-85.

- Watson, K.W. and Luxmoore, R.J. 1986. Estimating macroporosity in a forest watershed by use of a tension infiltrometer. Soil Science Society of America Journal 50:578-582.
- Weyman, D.R. 1973. Measurements of the downslope flow of water in a soil. Journal of Hydrology 20:267-288.
- Whitelaw, A. 1988. Hydrological modelling using variable source areas. In: M.G. Anderson and T.P. Burt (Eds). Process Studies in Hillslope Hydrology. John Wiley & Sons Ltd. New York.
- Williams, T.H.L. 1978. An automatic scanning and recording tensiometer system. Journal of Hydrology 39:175-183.
- Wilkinson, L. SYSTAT: The System for Statistics. 1989. Evanston, IL: SYSTAT, Inc.
- Wilson, G.V. and Luxmoore, R.J. 1988. Infiltration and macroporosity distributions on two forested watersheds. Soil Science Society of America Journal 52:329-335.
- Woodruff, J.E. and Hewlett, J.D. 1970. Predicting and mapping the average hydrologic response for the eastern United States. Water Resources Research 6:1312-1326.

APPENDIX A

DESCRIPTION OF DATA COLLECTED

The data collected in the field for 17 simulated storms during July 13th to October 12th include: Soil Water Pressure Potentials with Mercury-Water Manometers and Pressure Transducers, Lateral discharge at four Soil Depths, Soil Moisture Contents with 6 Neutron Probes and 6 Sentry 200 Probes. Most of these data was recorded at 1 minute time intervals during simulated rainfalls and 10 minutes during dry periods. Because of the amount of data collected would need approximately 100 pages, the data are available in 17 Diskets 3½ in Lotus format at the Watershed Laboratory of Department of Forestry, Oklahoma State University.

VITAE

José de Jesús Návar Cháidez

Candidate for the Degree of

Doctor of Philosophy

Thesis: WATER MOVEMENT IN AN EXPERIMENTAL PLOT IN THE
OUACHITA MOUNTAINS OF ARKANSAS: THE EFFECT OF SOIL
MACROPORES

Major Field: Environmental Science

Biographical:

Personal Data: Born in Tepehuanes, Durango, México, May
15, 1959, the son of Gilberto Návar Gallarzo and
María Cháidez Garibay.

Education: Graduate from Centro de Estudios
Tecnológicos Forestales, El Salto, P.N. Durango,
México in 1979; received a Forestry Degree with
honors from Instituto Tecnológico Forestal No. 1.
Durango, Durango, México in June, 1986; received
Master of Science degree with a major in Forestry
from University of Toronto in March, 1989;
completed the requirements for Doctor of
Philosophy at Oklahoma State University in July,
1992.

Professional Experience: Worked for Productos
Forestales Mexicanos as a Forest Manager, 1983
-1984; Research Assistant at Departamento de
Ciencias Forestales de la Universidad Autónoma de
Nuevo León, 1984-1986.